UNIVERSITÀ DEGLI STUDI DI MILANO

FACOLTÀ DI MEDICINA E CHIRURGIA

Corso di Dottorato in SCIENZE ODONTOSTOMATOLOGICHE

CICLO XXXI

Tesi di Dottorato di Ricerca

DETECTION OF HUMAN POLYOMAVIRUSES AND PAPILLOMAVIRUSES IN ORAL SPECIMENS OF IMMUNOCOMPETENT AND HIV POSITIVE SUBJECTS

Tesi di Dottorato di:
Sonia **VILLANI**
Matricola: R11193

TUTORE: Dott.ssa Serena **DELBUE**

CO-TUTORE: Prof. Massimo **DEL FABBRO**

Anno Accademico 2017/2018

Alla mia famiglia

INDEX

ABSTRACT

The oral cavity of healthy subjects is colonized by several and different microorganisms, such as viruses, bacteria, fungi and protozoa. Many of these are commensal species, which are essential to maintain a health status when in equilibrium with the environment, but can became pathogenic and capable to eliciting disease when occur environmental changes or shifts in the composition of the oral microbiota. Despite there are numerous studies concerning the bacterial communities inhabiting the oral cavity, there are very few studies defining the oral viral community and their role, if any, in the development of oral diseases. To date, the Human herpesviruses (HHVs) have been often associated with the development of periodontitis, while the Human Papillomaviruses (HPVs) have been studied as possible risk factor for the development of oropharyngeal cancer. Additionally, the Human Polyomaviruses (HPyVs) seems to be an excellent candidates as possible factors involved in the pathogenesis of oral diseases.

Given the increasing incidence of oral diseases and the very limited study of viral involvement in these disorders, our study was aimed to give new insights on the possible presence of HPyVs and HPVs genomes in the oral mucosa of both 105 healthy subjects, without or with periodontitis (9) and 20 HIV positive patients. Nucleic acids isolation from saliva, buccal swab and paper points and subsequent Real Time PCR were the employed techniques.

We could observe that the prevalence of HPyVs was significantly higher in the group of HIV positive subjects (60.0%) compared to the control group (25.7%), and among the HPyVs, the most prevalent were MCPyV: MCPyV genome was detected at the highest percentage (20.8%) and with high viral load (mean: 3.15*E+07) in all types of the oral specimens. Regarding the presence of HPVs, three high risk-HPV genotypes were detected in 2/20 (10.0%) HIV positive subjects, only in the saliva samples.

To our knowledge, this is the first study to examine and compare the presence of HPyVs and HPVs in a broad range of oral sample types. Based on our results, we could conclude that MCPyV may be part of the normal viroma of the oral cavity. Nonetheless, its well-known association with the Merkel Cell carcinoma leads to state the its presence should be monitored, in order to verify whether an association between MCPyV and oral diseases can be rule out.

RIASSUNTO

Il cavo orale dei soggetti sani è colonizzato da numerosi e differenti microorganismi, quali virus, batteri, funghi e protozoi. Molti di questi sono specie commensali, che essendo in equilibrio con il microambiente circostante sono essenziali per mantenere uno stato di salute, ma possono diventare patogene e capaci di causare malattie quando si verificano cambiamenti nel microambiente o nella composizione del microbioma orale. Sebbene vi siano numerosi studi riguardanti le comunità batteriche che abitano la cavità orale, pochissimi sono gli studi che definiscono la comunità virale orale e il suo ruolo, se esiste, nello sviluppo di patologie orali. Ad oggi, gli Herpesvirus umani (HHV) sono stati spesso associati allo sviluppo della parodontite, mentre i Papillomavirus umani (HPV) sono stati valutati come possibili fattori di rischio per lo sviluppo dei tumori orofaringei. In aggiunta, i Polyomavirus umani (HPyV) sono stati recentemente considerati candidati eccellenti come possibili fattori coinvolti nella patogenesi delle malattie orali.

Data la crescente incidenza delle malattie orali e lo studio molto limitato riguardo al coinvolgimento virale in esse, il presente studio è stato volto a fornire nuove informazioni sulla presenza di HPyV e HPV nella mucosa orale di 105 soggetti sani, senza o con parodontite (9 soggetti) e 20 pazienti HIV positivi. Le tecniche impiegate sono state l'isolamento degli acidi nucleici da saliva, tampone buccale e paper points e successiva analisi tramite Real Time PCR.

I risultati ottenuti mostrano che la prevalenza dei HPyV è risultata significativamente più alta nel gruppo di soggetti HIV positivi (60,0%) rispetto al gruppo di controllo (25,7%), e tra gli HPyV, il prevalente è stato MCPyV: il genoma di MCPyV è stato rilevato con la più alta percentuale (20,8%) e con la più alta carica virale (media: 3,15*E+07) in tutti i tipi di campioni orali. Per quanto riguarda la presenza di HPV, sono stati rilevati tre genotipi ad alto rischio in 2/20 soggetti HIV positivi (10,0%), solo nei campioni di saliva. A nostra conoscenza, questo è il primo studio condotto per valutare e confrontare la presenza di HPyV e HPV in un'ampia gamma di differenti campioni orali. Sulla base dei nostri risultati, potremmo concludere che MCPyV potrebbe far parte del normale viroma della cavità orale. Tuttavia, la sua ben nota associazione con il carcinoma a cellule di Merkel porta a suggerire che la sua presenza deve essere monitorata, al fine di verificare se è possibile escludere un'associazione tra MCPyV e patologie orali.

INTRODUCTION

1.1 MICROBIOMA OF ORAL CAVITY

Each human body contains a personalized microbiome, consisting of a complex community of foreign inhabitants, essential to maintain heath, but capable of eliciting disease (Zarco et al., 2012; Parahitiyawa et al., 2010). The human microbiome can be divided into: core microbiome and variable microbiome (Turnbaugh et al., 2007). The core microbiome is common to all individuals and consists of the predominant species, which are present in health conditions in different body districts (Turnbaugh et al., 2007; Zaura et al; 2009; Sonnenburg et al., 2011). However, there are several differences in species and strains (Dethlefsen et al.; 2007). The variable microbiome is characteristic of the single person and comes in response to unique lifestyle, phenotypic and genotypic elements (Figure 1).

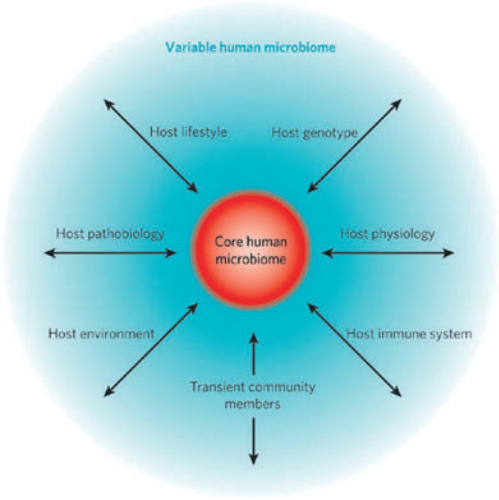

Figure 1. Human microbiome consists of a core microbiome, common to all individuals, and a variable microbiome, unique to individuals depending on lifestyle and physiological differences (Turnbaugh et al, 2007).

Each person harbors a unique microbiome that plays an important role in the etiology of some diseases, which can then manifest and progress differently between different individuals (Sonnenburg et al., 2011). It is therefore necessary to deepen the effect that these microorganisms have on the health of the host and to characterize the microbiome patterns involved in the diseases. This would allow faster diagnosis and establish personalized therapeutic strategies.

The oral cavity of healthy persons is strongly colonized by microorganisms, including viruses, bacteria, fungi, and protozoa. Many of these are responsible for the formation of biolfilms, which are resistant to mechanical stress and antibiotic treatments; many others are commensal species, which maintains health when in equilibrium. They can become pathogenic in response to certain ecological shifts in the microbiome, such as poor oral hygiene, immunological disorders and specific genetic compositions (Avila et al., 2015) (Figure 2).

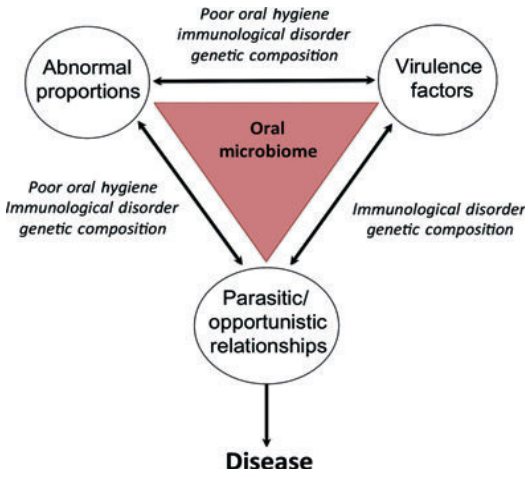

Figure 2. Cycle of ecological shifts in the oral microbiome that cause disease (Turnbaugh et al, 2007).

The normal microbiota of the mouth is responsible for the two most common oral diseases of man: dental caries and periodontal diseases.

The oral-pharyngeal cavity is composed of sophisticated anatomical structures. Various microorganisms colonize the environment provided by those structures, therefore a mucosal membrane and inherent mucosal immune system are indispensable for the protection of the integrity of the internal environment (Wu et al., 2014). Dysregulation of these innate and adaptive immune systems may play an important role in the etiology of infections, which are the basis of the periodontal disease, a highly prevalent complex infectious disease with several etiologic and contributory factors, resulting from inflammation of the supporting structures of the teeth (Ebersole et al., 2017; Slots 2017). Periodontitis affects the majority of adult subjects worldwide, but relatively few patients receive adequate treatment for the disease. Current periodontal therapy is successful in fighting initial and moderate types of periodontitis, but may show limited efficacy in resolving late-stage disease (Albandar et al., 2005). A greater understanding of the etiopathogenetic process of periodontal disease seems to be a prerequisite for the development of preventive and therapeutic strategies, that are more efficient and less burdensome for patients.

Microbiological culture-dependent and culture-independent molecular studies have identified more than 1,200 bacterial species and 19,000 phylotypes in the oral cavity. At least 400 bacterial species inhabit subgengival sites, but despite the long list of different bacteria in periodontitis, fewer than 20 species are considered to be major periodontal pathogens (Paster et al., 2006). Till now, there have been numerous studies about bacterial communities inhabiting the oral cavity, but fewer studies of the viral communities. Different types of viruses are frequent inhabitants of periodontitis lesions, but their role, if any, in the pathogenesis of the disease is still unknown. Research during the past 15 years has implied that Human Herpesviruses (HHV) are involved in the etiopathogenesis of destructive periodontal disease. It appears that a high periodontal load of active Epstein–Barr virus (EBV) and/or Human Cytomegalovirus (HCMV) is statistically associated with aggressive periodontitis, and latent HHVs infections are preferentially found in chronic periodontitis and gingivitis sites. Co-infection with EBV and HCMV shows a particularly close link with progressive periodontitis (Jakovljevic et al., 2014). Also, specific genotypes of herpesvirus species may exhibit increased periodontopathic potential. Because of the high copy-counts of EBV and HCMV in aggressive periodontitis, it is unlikely that these pathogenic viruses are acting merely as innocuous bystanders present in proportion to the severity of the underlying periodontal pathogenesis. Probably due to the difficulties of detection, the differences in sampling and the samples used, the studies on the presence of viruses in the oral cavity have a great variability. The studies on the healthy periodontium have showed few herpesvirus genomes, with a median genome detection rate of 8% for both EBV and HCMV. However, among the different studies there is a wide variation in the virus detection frequencies, that oscillate from 0% to 20% for Herpes Simplex Virus (HSV), from 0% to 23 % for EBV and from 0% to 57% for HCMV (Slots et al., 2010) (Table 1).

Table 1. Prevalence of Human Herpesviruses (HHVs) in periodontal health and gengivitis (Slots et al., 2010)

Virus	Healthy periodontium % positive sample	Gengivitis % positive sample	Reference
Herpes simplex 1 (HSV)	0%	0%	Granier et al., 2009
	20%	53%	Imbronito et al., 2008
	0%	-	Nishisyama et al., 2008
	0%	-	Sayagun et al., 2004
	0%	-	Contreas et al., 2000
Epstein-Barr Virus (EBV)	9%	-	Dawson et al., 2009
	23%	0%	Grenier et al., 2009
	0%	20%	Imbronito et al., 2008
	7%	-	Chalabi et al., 2008
	8%	-	Rotola et al., 2008
	-	13%	Sayagun et al., 2008
	7%	-	Sunde et al., 2008
	3%	-	Moghim et al., 2007
	21%	20%	Wu et al., 2008
	-	30%	Watanabe et al., 2007
	0%	-	Klemenc et al., 2005
	9%	-	Konstantinidis et al.,2005
	6%	-	Sayagun et al., 2004
	18%	-	Contreas et al., 2000
MEDIAN	**8%**	**20%**	
Human Cytomegalovirus (HCMV)	0%	-	Dawson et al., 2009
	8%	25%	Grenier et al., 2009
	57%	40%	Imbronito 2008
	0%	-	Combs et al., 2008
	0%	-	Chalabi et al., 2008
	8%	-	Rotola et al., 2008
	13%	-	Ding et al., 2008
	0%	-	Sunde et al., 2008
	42%	49%	Wu et al., 2008
	18%	-	Botero et al.,2007
	0%	-	Klemenc et al., 2005
	3%	-	Tantivanich et al., 2004
	32%	-	Chen et al., 2006
	0%	-	Sayagun et al., 2004
	9%	-	Contreas et al., 2000
MEDIAN	**8%**	**33%**	Sayagun et al., 2008

Even among numerous studies on aggressive/chronic periodontitis, there is a considerable variability regarding the presence of HHVs. The prevalence of HSVs ranges from 13 to 100% with a total value of 52%, from 3 to 89% with an overall value of 52% for EBV, and finally from 0.3 to 89% with an overall value of 47% for HCMV (Slots et al., 2010) (Table 2).

Table 2. Prevalence of Human Herpesviruses (HHVs) in aggressive and chronic periodontitis (Slots et al., 2010)

Virus	Aggressive Periodontitis % positive sample	Chronic Periodontitis % positive sample	Reference
Herpes simplex 1 (HSV)	-	13%	Granier et al., 2009
	57%	100%	Bilichodmath et al., 2009
	87%	40%	Imbronito et al., 2008
	-	16%	Grande et al., 2008
	-	26%	Nishiyama et al., 2008
	-	31%	Ling et al., 2004
	78%	-	Sayagun et al., 2004
	-	21%	Contreas et al., 2000
MEDIAN	**78%**	**26%**	
Epstein-Barr Virus (EBV)	-	28%	Dawson et al., 2009
	-	3%	Grenier et al., 2009
	29%	79%	Bilichodmath et al., 2009
	33%	47%	Imbronito et al., 2008
	-	48%	Grande et al., 2008
	-	79%	Chalabi et al., 2008
	55%	46%	Rotola et al., 2008
	60%	-	Sayagun et al., 2004
	-	40%	Sunde et al., 2008
	-	45%	Imbronito et al., 2008
	-	61%	Moghim et al., 2007
	-	38%	Wu et al., 2008
	57%	-	Klemenc et al., 2005
	-	55%	Konstantinidis et al.,2005
	89%	46%	Kubar et al.,2005
	58%	23%	Li et al., 2004
	-	4%	Ling et al., 2004
	72%	-	Sayagun et al., 2004
	-	81%	Contreas et al., 2000
MEDIAN	**58%**	**46%**	
Human Cytomegalovirus (HCMV)	-	0.3%	Dawson et al., 2009
	-	35%	Grenier et al., 2009
	7%	26%	Bilichodmath et al., 2009
	47%	50%	Imbronito et al., 2008
	-	59%	Chalabi et al., 2008
	-	80%	Grande et al., 2008
	44%	-	Ding et al., 2008
	-	80%	Botero et al., 2007
	53%	-	Sayagun et al., 2004
	-	12%	Sunde et al., 2008
	-	83%	Imbronito et al., 2008
	-	63%	Wu et al., 2008
	40%	60%	Botero et al., 2007

	7%	-	Wayanabe et al., 2007
	-	59%	Chen et al., 2006
	-	3%	Klemenc et al., 2005
	78%	27%	Kubar et al.,2005
	-	34%	Tantivanich et al., 2004
	-	52%	Ling et al., 2004
	72%	-	Sayagun et al., 2004
	-	64%	Contreas et al., 2000
MEDIAN	**42%**	**52%**	

Furthermore, oral diseases associated with Human Immunodeficiency Virus (HIV) / Acquired Immune Deficiency Syndrome (AIDS) status includes mucosal diseases and destructive periodontal conditions (Ryder et al., 2012). Oral mucosal infections, especially candidiasis, are features of HIV disease, suggesting that compromised mucosal immunity within the oral cavity is a consequence of the viral infection. Despite HIV oral disease prevention has been partially advanced by improving patients access to highly active antiretroviral therapy (HAART), further preventive strategies are needed for minimizing the occurrence or recurrence of specific oral conditions (Patton et al., 2013). However, how this mucosal immunity is compromised is still unclear. Investigators have then realized that to fully understand human health and disease, we need to understand not just the few suspected pathogens, but rather all the microbial members of the oral environment. Moreover, the increased accessibility of sequencing technology and the improvement of the analytical capabilities can provide a newly approach to investigate in greater detail the oral microbial communities (Zhou et al., 2013). In immunocompromised patients, such as HIV-infected subjects, HSV, EBV and HCMV are found more frequently in the saliva samples and have been related to periodontitis and oral cancer (Fons, et al., 1994; Grande et al., 2008; Slots et al., 2009). The most commonly HHV identified in HIV-positive patients was HCMV, that was found in 81% periodontitis lesion, while EBV was detected in 57% of periodontitis biopsies (Contreas et al., 2001). However, HHV are probably not stand-alone periodontopathic agents, but cooperate with specific bacteria in periodontal tissue breakdown. A co-infection of active herpesviruses and periodontopathic bacteria may constitute a major cause of periodontitis and explain a number of the clinical characteristics of the disease (Saygun et al., 2004).

Additionally, another family of viruses, called Human Papillomaviruses (HPV), that are strictly related to different oropharyngeal cancers, could be implicated in periodontal disorders. This viral family consist of a group of epitheliotropic viruses associated with cell

proliferative processes and may be benign (warts and condylomas) and pre-malign or malign (leukoplakia and carcinomas) in the stratified epithelia of the skin and mucosa. (Sanders et al., 2015). The prevalence of HPV in the oral cavity has not yet been studied in a deep way as it for the vaginal tract. While the prevalence of these viruses in oropharyngeal cancers has increased, with estimates of 72% in America and in Europe (Mehanna, et al., 2013), prevalence of their oral infection in heathy subjects, natural history and risk factors remain largely unexplored. The detection rate of HPV in the oral mucosa presents a great variability (from 0% to 80%) in the different studies, and this can probably be explained by the difference in sensitivity of the techniques, by the limited size of the sample analyzed and depending on the type and site of oral specimens (Tominga et al., 1996; Kellokoski et al., 1992; Terai et al., 1999).

Among the more than 100 identified genotypes of human papillomaviruses, 25 of them were detected in the oral cavity. In 2010, *Kreimer and colleagues* have conducted a systematic review of the literature concerning the data published on the prevalence of HPV in healthy subjects, showing that 4.5% of the healthy subjects analyzed was positive for any HPV. Moreover, HPV16 accounted for 28% of all HPV detected in the oral region and 3.5% of the healthy subjects analyzed was positive for high risk HPV (Kreimer et al., 2010). Several studies suggest there may be a synergy between periodontitis, oral human papillomavirus infection and oropharyngeal cancers (Pullos et al., 2015; Psyrri et al., 2008). One of the most reliable hypotheses for the association between periodontitis and human papillomavirus infection supports that specific pathogens cause a state of chronic inflammation that results in periodontitis (Horewicz et al., 2010). The constant state of inflammation of the periodontium and the consequent formation of periodontal pockets create a perfect microenvironment for the persistence of the virus (Tezal et al, 2012). Furthermore, periodontal pockets can be specifically a reservoir for HPV and more generally also for other viruses/bacteria (Hormia et al., 2005). The replication of the virus also contributes to the maintenance of the chronic inflammatory state, with the possibility of finding high viral loads in patients' saliva (Hubbers et al., 2015). On the other hand, the relationship is bidirectional, the infection of the oral epithelium by the human papillomaviruses leads to its hyperproliferation, which in turn causes pathological changes in the periodontium, supports the inflammation and progression of periodontitis (Tommasino et al., 2014; de Paula et al., 2000; Kim et al., 2006). As known, an important immunosuppressive state can lead to an increased susceptibility to viral infection or/and an increase in viral replication. In the study of *Adamopulous and colleagues*, it has

reported that the prevalence of HPV is significantly higher in the saliva of HIV-positive patients than those from oral cancer patients (35.3% and 10.3% respectively) (Adamopulous et al., 2008). Also in another study on saliva of HIV-positive patients has been reported an elevate frequency of HPV (about 33%) (Cameron et al., 2005). Indeed, among oral complications in HIV-positive patients, there are two diseases determined by HPV, which are oral warts associated with HPV-32 and oral tumors associated with HPV-16 (Cameron et al.,2008).

Another viral family may be implicated into the periodontitis pathogenesis is the *Polyomaviridae* family, small DNA viruses that can establish latency in the human host. To date, at least thirteen members of this family have been identified, some of them playing an etiological role in malignancies in immunosuppressed patients. In particular, very recently, Merkel cell polyomavirus was isolated from the skin of a patient affected by Merkel Cell carcinoma (MCC) showing its ability to cause most of the Merkel skin cancers (Feng et al., 2008). Infection with Human Polyomaviruses has been recently categorized by the International Agency for Research in Cancer as "probable carcinogen". Infections with BK and JC polyomaviruses have been classified as "possible carcinogens" with studies in humans showing inconsistent evidence for an association with cancers at various sites (Http://monographs.iarc.fr/ENG/Monographs/vol104/mono104). In particular, the newly discovered viruses, such as Human Polyomaviruses 6, 7, and 9, that are commonly part of the skin viroma of the human host, are probably also involved in numerous, various, and unknown, as well, disorders. Additionally, already in the 1960s, it had been shown that Polyomavirus infection was able to develop periodontal disease in experimental animals (Shklar et al., 1963, Cohen et al., 1964). *Fleming and colleagues* have described severe periodontal disease in mice infected by Polyomavirus. The animals showed periodontal alterations of varying degrees of importance, from gingival recession, deep periodontal pockets formation to wide bone resorption. Furthermore, some Human Polyomaviruses have been already found in the saliva of both transplanted patients and healthy subjects. Indeed, *Robaina and colleagues,* who have conducted a study on the saliva of immunocompetent subjects, have detected in the 24.3% of the saliva samples analyzed the presence of at least one of the Human Polyomaviruses screened (Robaina et al., 2013). In another study, they have reported a higher frequency of Human Polyomaviruses infection in the HIV-positive children than among the healthy controls (28.3% *versus* 10.0%) (Robaina et al., 2013). Instead, *Freze Baez and colleagues* have conducted a study on the saliva and oral biopsy of

both immunocompetent subject and renal transplant recipients. Among the viruses for which the samples were screened, including several HHV, Merkel Cell Polyomavirus was the one that showed a predominant prevalence. Moreover, its genome was detected predominantly in the saliva of subjects with oral lesion (33.3%), such as gingivitis or periodontitis, of both healthy and transplant groups, and in the saliva samples of immunosuppressed patients (36.7%) (Freze Baez et al., 2013). Also *Loyo et al*. have described high titers of Merkel Cell Polyomavirus in the saliva samples (Loyo et al., 2010). Another study has described the presence of BK Polyomavirus in the saliva collected from HIV-positive and negative subjects (Jeffers et al., 2009). Only few studies are available providing evidence that head and neck cancers (HNSCCs), a heterogeneous groups of tumors including oral cavity cancers, might be associated with Human Polyomaviruses (Kutsuna et al., 2008; Polz et al., 2015; Polz-Gruszka et al., 2015; Poluschkin et al., 2018). Unfortunately, the number of studies concerning Human Polyomaviruses and the oral cavity is extremely limited (Table 3). Whether they are simple bystanders or are involved in the pathogenesis of some oral cavity diseases is completely unknown.

Table 3. Prevalence of Human Polyomaviruses (HPyVs) in healthy and immunocompromised subjects

Virus	Control group % positive sample	Case group % positive sample	HPyV	Sourse	Reference
Human Polyomavirus (HPyV)	15%	37%	MCPyV	Saliva	Freze Baez et al., 2013
	12%	14%	JCPyV	Saliva	Martelli et al., 2018
	3%	4%	BKPyV	Saliva	Martelli et al., 2018
	8%	0%	MCPyV	Saliva	Martelli et al., 2018
	7%	-	BKPyV	Saliva	Robaina et al., 2013
	0.3%	-	JCPyV	Saliva	Robaina et al., 2013
	13%	-	WUV	Saliva	Robaina et al., 2013
	2%	-	KIPyV	Saliva	Robaina et al., 2013
	-	0%	JCPyV	Oral	Matos et al., 2012
	0%	5%	BKPyV	Saliva	Robaina et al., 2013
	7%	3%	JCPyV	Saliva	Robaina et al., 2013
	2%	2%	WUPyV	Saliva	Robaina et al., 2013
	0%	13%	KIPyV	Saliva	Robaina et al., 2013
	28%	10%	HPyVs	Saliva	Robaina et al., 2013
	0%	0%	JCPyV	Saliva	Berger et al., 2006
	0%	0%	JCPyV	Saliva	Sundsfjord et al., 1994
	0%	0%	BKPyV	Saliva	Sundsfjord et al., 1994
	50%	50%	BKPyV	Saliva	Castro et al., 2017
	0%	8%	JCPyV	Saliva	Castro et al., 2017
MEDIAN	**3%**	**4%**			

2.1 HUMAN POLYOMAVIRUSES

Initially, according to taxonomy, Polyomaviruses (PyVs) were classified as a genus of the *Papovaviridae* family together with Papillomaviruses; afterwards in 2000, in-depth studies have shown that the two groups have few similar sequences and have been recognized by the International Committee on Virus Taxonomy that has formally divided this family into two new separate families: *Polyomaviridae* and *Papillomaviridae*.

PyVs are small, naked viruses able to infect a large number of vertebrates. Viruses belonging to this family have many common characteristics: the absence of envelope, a capsid with icosahedral symmetry with a diameter of about 45 nm and a genome consisting of a double stranded circular DNA molecule of approximately 5 Kb.

The first identified PyVs was the murine polyomavirus (MPyV), ubiquitous in the mouse, capable of inducing tumors in newborn or immunosuppressed mice (Stewart et al., 1958). Indeed, the name of the family derives from this particular characteristic, and is formed by the Greek root "poly-" which means "many" and the ending "-oma" which means "tumors". The next one that was identified, in 1960, was the simian virus 40 (SV40), isolated for the first time from monkey kidney cells. Similarly, to MPyV, SV40 proved capable of inducing tumors in mice and rodents (Sweet et al., 1960). In the following years, following an increased interest in these viruses, PyVs have been isolated from many other guests, such as birds, cats, rabbits and humans. Until 2007, the only PyVs known able to infect the humans were JC virus (JCPyV) and BK virus (BKPyV). Due to improvements in molecular diagnostic techniques, many other Human Polyomaviruses (HPyVs) were discovered. So far, at least 13 HPyVs have been identified and most of them are still orphan of any disease associations (Feltkamp et al., 2013; Mishra et al., 2014).

JCPyV and BKPyV were isolated for the first time in 1971: the first one was found in the brain of a patient with Hodgkin's lymphoma and progressive multifocal leukoencephalopathy (PML) (Padgett BL et al., 1971), while the latter in the urine of a kidney transplant patient (Gardner et al., 1971). Karolinska Institute Polyomavirus (KIPyV) and Washington University Polyomavirus (WUPyV) were isolated from nasopharyngeal aspirates of children with respiratory tract infection (Allander et al., 2007; Gaynor et al., 2007); while Merkel Cell Polyomavirus (MCPyV) was identified in skin lesions of a rare carcinoma of Merkel cells (Feng et al., 2008). In 2010, other three HPyVs were discovered, Human Polyomavirus 6 (HPyV6) and -7 (HPyV7) identified in skin samples of healthy subjects (Schowalter et al.,

2010), and Trichodysplasia Spinulosa-Associated Polyomavirus (TSPyV) recognized as the etiologic agent of a rare skin disease called trichodispasia spinulosa (van der Meijden et al., 2010). Human Polyomavirus 9 (HPyV9) was detected in both serum and skin (Scuda et al., 2011), Malawi Polyomavirus (MWPyV), also known as HPyV10 according to its order of discovery, was isolated from stool and skin samples of a Malawi patient affected by Warts, Hypogammaglobulinemia, Immunodeficiency, and Myelokathexis syndrome (WHIM) (Siebrasse et al., 2012; Buck et al., 2012) and also Saint Louis Polyomavirus (SLPyV) was isolated from stool but from a healthy patient (Lim et al., 2013). The last two discovered polyomaviruses, the Human Polyomavirus 12 (HPyV12) and New Jersey Polyomavirus (NJPyV), were isolated respectively from the gastrointestinal tract tissues and muscle tissue of a pancreastransplanted patient (Korup et al., 2013; Mishra et al., 2014) (Table 4).

Table 4. The list of the human polyomaviruses (HPyVs), their abbreviation, the year of discovery, NCBI RefSeq number, the sample from which they were isolated for the first time, the associated pathology and the reference of their discovery.

Human Polyomavirus						
Name	**Abbreviation***	**Year of discovery**	**NCBI RefSeq**	**Source**	**Association Disease**	**Reference**
Polyomavirus BK	BKPyV	1971	NC_001538.1	Kidney Transplant Recipient	Polyomavirus-associated nephropathy (PVAN), hemorrhagic cystitis	Gardner et al.
Polyomavirus JC	JCPyV	1971	NC_001699.1	PML patient	Progressive multifocal leukoencephalopathy (PML)	Padgett et al.
Karolinska Institute polyomavirus	KIPyV	2007	NC_009238.1	Nasopharyngeal tissue	None	Allander et al.
Washington University polyomavirus	WUPyV	2007	NC_009539.1	Nasopharyngeal tissue	None	Gaynor et al.
Merkel cell polyomavirus	MCPyV	2008	NC_010277.1	Lesion	Merkel cell carcinoma	Feng et al.
Human polyomavirus 6	HPyV6	2010	NC_014406.1	Normal Skin	None	Schowalter et al.
Human polyomavirus 7	HPyV7	2010	NC_014407.1	Normal Skin	None	Schowalter et al.
Trichodysplasia spinulosa-associated polyomavirus	TSPyV (HPyV8)	2010	NC_014361.1	Lesion	Trichodysplasia spinulosa, pilomatrix dysplasia	Van der Meijden et al.
Human polyomavirus 9	HPyV9	2011	NC_015150.1	Kidney Transplant recipient	None	Scuda et al.
Malawi polyomavirus	MWPyV (HPyV10)	2012	NC_018102.1	Healthy Stool from Malawi WHIM patient	None	Siebrasse et al.; Buck et al.
St Louis polyomavirus	STLPyV	2012	NC_020106.1	Healthly Stool	None	Lim et al.
Human polyomavirus 12	HPyV12	2013	NC_020890.1	Gastrointestinal Organs	None	Korup et al.
New Jersey polyomavirus	NJPyV	2014	NC_024118.1	Pancreatic transplant recipient	None	Mishra et al.

*ICTV-designated abbreviation

2.1.1 Virion structure

HPyVs have a small icosahedral capsid with a diameter ranging between 40-50 nm. The structural viral proteins that compose it are called: viral protein 1 (VP1), the major capsid protein; VP2 and VP3, the two minor capsid proteins. Indeed, the viral capsid consists of 360 molecules of VP1 and 30-60 molecules of both minor structural proteins. The capsid is organized into 72 pentameric capsomers, each containing 5 molecules of VP1 and a molecule of VP2 or VP3 (Liddington et al., 1991; Griffith et al., 1992). Nevertheless, VP1 is the only protein exposed on the surface of the capsid and therefore it is responsible for virus attachment to host cell receptor, and this determines the receptor specificity (Figure 3).

Figure 3. Structure of the icosahedral capsid of Human Polyomavirus

2.1.2 Genome organization

Within the capsid, the viral DNA is organized into a double-stranded, circular and super-coiled molecule and has a length of about 5,000 pairs of bases. The genomic organization of the HPyVs is designed to enclose the maximum information (made up of 6 genes) in the smallest possible space (5 Kb). This is allowed by using both strands of the DNA molecule and overlapping genes. The nucleic acid is complexed with the histones H2A, H2B, H3 and H4 to give a chromatin complex (Louieet al., 1975; Keller et al., 1978). The viral genome contains two transcriptionally divergent units: a region called early, which encodes multifunctional regulatory proteins expressed in the early stage of infection, and a region called late, which encodes the three capsid proteins (VP1, VP2, VP3) expressed in permissive cells during the late phase of infection, and for a protein called agnoprotein. Furthermore,

there is a non-coding hypervariable regulatory region called non-coding control region (NCCR), located between the early and late transcription units (Cole et al, 2001; Moens et al., 2001) (Figure 4).

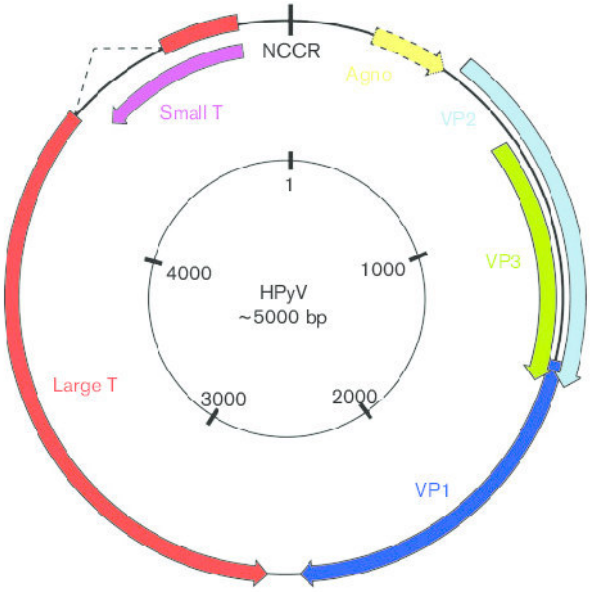

Figure 4. Schematic organization of the Human Polyomavirus genome

The Early region is the first part of the genome to be transcribed and translated during the life cycle of the virus. It includes the genes coding two proteins called Large Tumor Antigen (T-Ag) and Small Tumor Antigen (sT-Ag), which have the ability to reprogram the host cell to allow viral replication (Brodsky et al., 1998). These proteins are produced by alternative splicing of a common pre-mRNA. LT-Ag is a polyfunctional phosphoprotein, which during the productive infection determines the beginning of viral DNA synthesis, binding itself to the origin of replication. Furthermore, this protein determines the repression of early transcription and the stimulation of late transcription. The ability of LT-Ag to interfere in many different biological processes during the replicative cycle of the virus can be explained by the presence of different structural domains with distinct biochemical activities. Most of the information about the structure and the activity of LT-Ag, in particular regarding its transforming capacities, has been obtained from the SV40 studies (An P et al., 2012; Van Ghelue et al., 2012). Through genetic and protein analysis, it has been demonstrated that all HPyVs' LT-Ag have four conserved domains: DnaJ domain, origin-binding domain (OBD), zinc (Zn)-binding domain, and helicase/ATPase (adenosine triphosphatase) domain (An P et al., 2012; Van Ghelue et al., 2012; Topalis et al., 2013; 34. Kwun et al., 2009) (Fig 5).

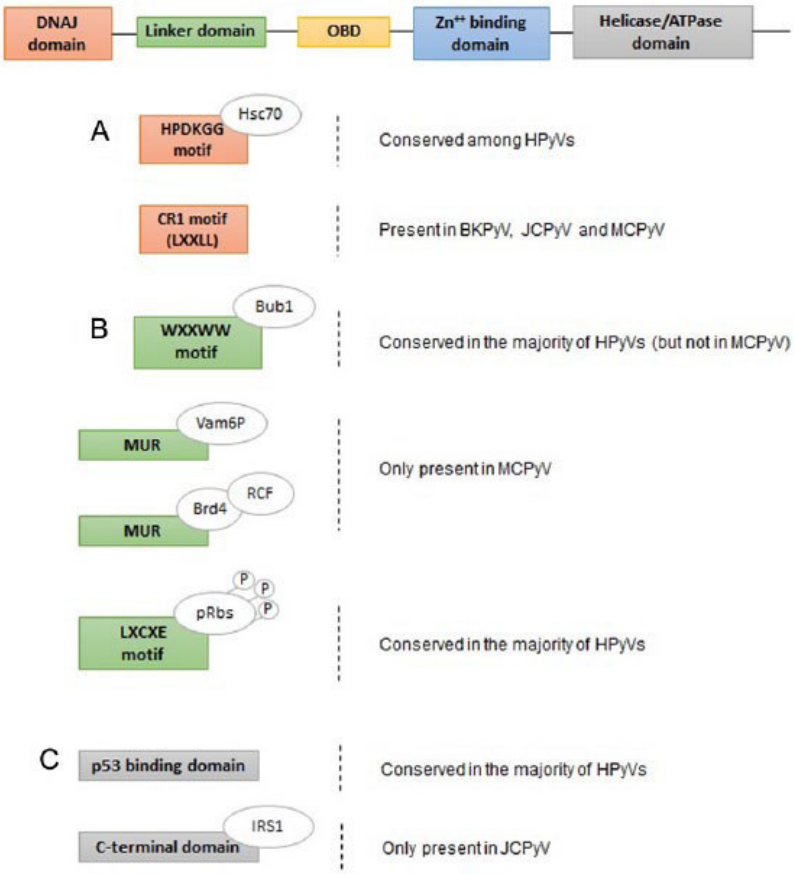

Figure 5. Schematic organization of the functional domains of the HPyVs' large tumor antigen (LT-Ag) and their main interactions with cellular factors (Baez CF et al.,2017)

The DnaJ domain is located at the N-terminal of the LT-Ag, contains a HPDKGG motif which is able to bind to the Heat shock cognate 70 kDa protein (Hsc70), a cellular chaperone and transcriptional repressor; and a CR1 motif (LXXLL) is present only in BKPyV, JCPyV, and MCPyV (Whalen et al., 2005; Berjanskii et al., 2000; Chromy et L., 2003; Sheng et al., 1997). The OBD domain is able to recognize GAGGC sequences and is an essential element for the beginning of viral replication; instead, the Zn-binding domain mediates the oligomerization of LT-Ag. The helicase/ATPase domain provides the energy for the helicase activity and in most of the HPyVs there is a conserved domain called p53-binding domain, responsible for the interaction of LT-Ag with the tumor-suppressor p53 (Lane et al., 1979; Meinke et al., 2016).

The role of sT-Ag is different, which probably acts as an aid to the activity of T-Ag. However, the role of this protein has not been fully clarified, since there is experimental

evidence that has shown that viral replication is successful even in its absence (Eash S. et al., 2007; White et al., 2015). sT-Ag has DnaJ domain, followed by a unique domain, that is eliminated from LT-Ag during the splicing process (Srinivasan et al., 1997; Whalen et al., 1999; Kolzau et al., 1999) (Fig 6).

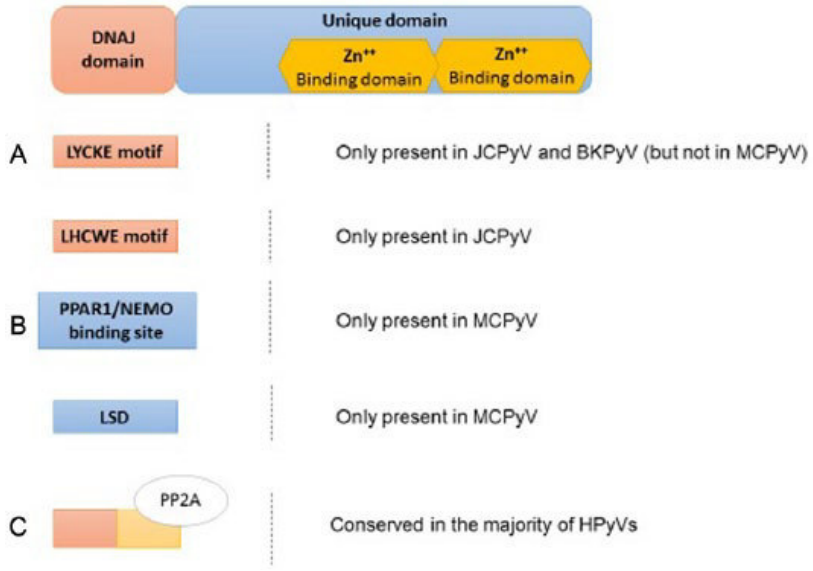

Figure 6. Schematic organization of the functional domains of the HPyVs' small tumor antigen (sT-Ag) and their main interactions with cellular factors (Baez CF et al.,2017)

The Late region, on the other hand, contains genetic information for the synthesis of capsid structural proteins: the major VP1 protein and the two minor VP2 and VP3 proteins, which contain specific functional domains that facilitate the packaging of complete viral particles (Erickson et al., 2012). They derive from the same pre-mRNA by an alternative splicing process. The late region of the viral genome also encodes for the agnoprotein, whose role in the replicative cycle of human polyomaviruses remains to be clarified (Gerits et al., 2012).

Finally, the NCCR is characterized by the presence of the origin of viral DNA replication, of both early and late promoters, of the enhancer regions, of the binding sites for the cellular transcription factors and of the LT-Ag binding sites (Lynch et al., 1990; Sock et al., 1993).

2.1.3 Lifecycle (attachment, entry and trafficking)

Despite having a well-conserved structural organization, HPyVs have a narrow host variety and a particular cellular specificity; this seems to be due to the presence of characteristic receptors on the cell surface and the presence of specific cellular factors of the host, which allow the expression of viral genes and the completion of the viral life cycle.

To start their life cycle, require the binding of their specific VP1 receptor to sialic acid, contained in glycoproteins or gangliosides present on the cell surface (Neu et al., 2012; Assetta et al., 2013; Schowalter et al., 2011). For example, for BKPyV the binding that allows the entry of the virus into the host cell has been identified: the studies conducted have suggested that the binding of the virus to the α (2,3) residues of sialic acid contained within the N-glycoproteins is sufficient to allow entry of the virus into the host cell (Dugan et al., 2005).

Following the adsorption of the virus to the membrane of the host cell, the virus is transported internally by endocytosis. In the case of BKPyV, the virus enters the cell rather slowly through a process of caveo-mediated endocytosis, lasting about four hours, and subsequently, anchoring itself to the microtubules and through the cytoskeletal transport system, reaches the nucleus (Eash et al., 2005). In contrast, it was demonstrated that JCPyV enters the host cell via a clathrin-dependent endocytosis mechanism (Querbeset al., 2006).

At this point, the infection can proceed through two alternative routes:

- Productive infection in permissive cells, with production of viral progeny and cell lysis;
- Non-productive infection in non-permissive cells, which leads to the arrest of the replication cycle of the virus, preventing the replication of the viral genome and the expression of late genes. The arrest of DNA replication that occurs during non-permissive infection may lead to either abortive infection or cell transformation.

After entering the cytoplasm of the host cell, the virus goes to the nucleus. The passage inside the nucleus, instead, takes place through the nuclear pores of the nuclear membrane. In the nucleus, the process of scapsidation or uncoating takes place, which determines the exposure of the viral genome, followed by the expression and replication of the viral genome. In the case of most HPyVs, viral DNA does not integrate into the genome of the host cell, but

remains in an episomic form. The transcription process takes place by transcription apparatus of the host cell and follows a very precise order, defined by the organization of coding sequences: first the early genes are expressed, which through an alternative splicing process give rise to the two different mRNAs for the LT-Ag and st-Ag; subsequently LT-Ag promotes viral replication of DNA, thanks to its ability to bind to specific genomic sequences and to recruit the cellular proteins involved in the DNA synthesis process. Finally, the late genes are expressed, leading to the synthesis of capsid proteins. The resulting proteins return to the nucleus, where the new virions are assembled, they are observable as early as 24 hours after infection. The accumulation of viral particles determines the break of the nuclear membrane and the consequent release of the neo-assembled viral particles in the cytosol. The lysis of the cell membrane releases the infecting virions into the extracellular environment, where they can engage in a new replicative cycle.

2.1.4 Molecular mechanism of transformation

The oncogenic transformation is mediated by the early protein LT-Ag, through which the virus can bypass the cell cycle controls in order to replicate efficiently. Surely, one of the most important LT-Ag interactions is that with members of the pRB family (Van Ghelue et al., 2012; An P et al., 2012)

The pRB protein product, encoded by the RB1 tumor suppressor gene, controls the G1 / S transition of the cell cycle (Di Fiore et al., 2013; Chinnam et al., 2011). The hypo-phosphorylated state of pRB is its active form capable to bind EF2, thus preventing cellular progression. Since this complex recalls a deacetylase, which, by increasing the state of compaction of chromatin, prevents the cellular transcription. The phosphorylated and inactive form of pRB, generated by the cyclin-dependent kinases (CDKs) - cyclin D complexes, on the other hand, is unable to bind EF2 and to inhibit cell cycle progression. E2F is therefore able to act as a transcription activation factor (Bertoli et al., 2013) (Figure 7, panel A). The interaction between LT-Ag and pRB proteins results in the activation of the transcription factors of the E2F family, which induce the expression of cellular genes essential for S-phase entry and DNA synthesis (Stubdal et al., 1997; Brown et al., 2002; Sullivan et al., 200; Lin et al., 2003)

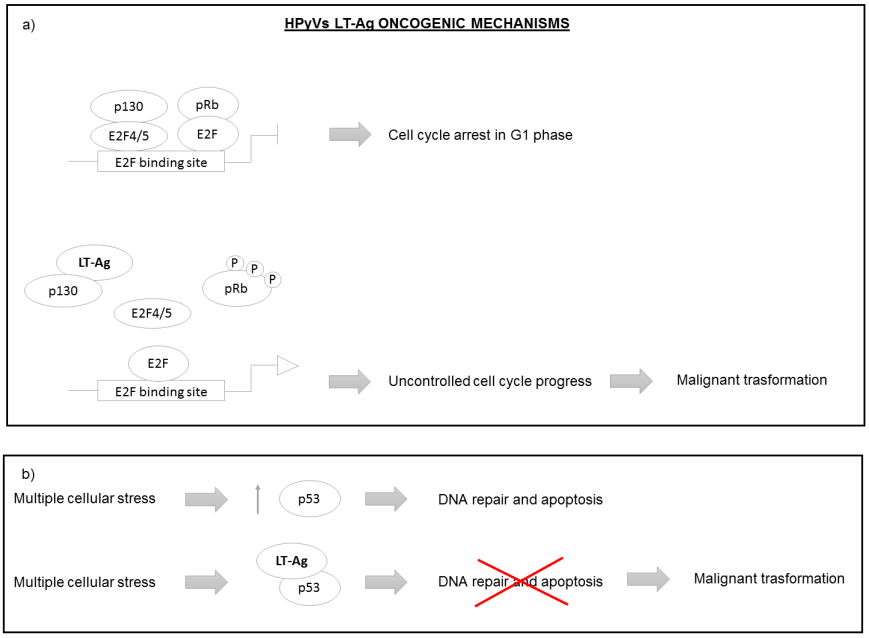

Figure 7. HPyVs' large tumor antigen (LT-Ag) oncogenic mechanisms. (A) In physiological conditions, the retinoblastoma proteins (pRbs) are in a hypophosphorylated state, which allows them to bind and inhibit the E2F transcription factors, preventing the E2F-mediated gene expression and consequently the transition from G1 to S phase. HPyVs' LT-Ag is able to bind the pRbs promoting their hyperphosphorylation, thus pRb is unable to bind E2F, leading to its transcriptional activity; at the same time, the hyperphosphorylation of p130 disrupts the transcriptional repressor complex (p130- E2F4/5), leading to uncontrolled cell cycle progression and sometimes to malignant transformation. (B) Multiple cellular stress, normally, raises the levels of p53, which promotes the DNA repair and cell cycle arrest. HPyVs' LT-Ag is able to bind and block the activity of p53 protein, preventing apoptosis and cell cycle arrest induced by DNA damage.

Moreover, LT-Ag can also inactivate the tumor suppressor p53, promoting the transition of the cell from the G1 phase to the S phase and preventing the apoptotic phenomenon (Liu et al., 2015) (Figure 7, panel B). In a permissive host, this allows the production of viral progeny, followed by lysis and death of the host cell. In a non-permissive host, however, this may be a possible oncogenic factor, since the LT-Ag are expressed continuously without the viral cycle being completed. The p53 tumor suppressor plays a crucial role in cell cycle control. As a transcription factor, it mediates the expression of genes involved in cell growth, differentiation and proliferation processes (Harris et al., 2005). One of the main functions of p53 is the stimulation of p21 expression, which can promote cellular quiescence and induction of apoptosis, both intrinsically and extrinsically. The choice between quiescence and apoptosis is influenced by the extent of DNA damage and is mediated by proteins such as MYC, which can inhibit the expression of p21 favoring that of pro-apoptotic proteins.

Furthermore, p53 can also repress gene transcription by acting on E2F indirectly by p21 (cyclin dependent kinase inhibitor), which inhibits the CDK-cyclin complexes, favoring the action of pRB (Xiong Y et al., 1993). The regulation of p53 is carried out above all at the level of its half-life through the action of the MDM2 protein, induced by p53 itself. It promotes the degradation of p53 by ubiquitination. MDM2 is inhibited by p14ARF induced by E2F (Lahav et al., 2004; Brown et al., 2009). The most reliable hypothesis concerning the interaction between p53 and LT-Ag supports that LT-Ag is able to associate itself with p53 by sequestering and inactivating it. The expression of LT-Ag and the consequent inactivation of p53 mimics, therefore, the same phenotypic effect that is caused by mutations affecting this tumor suppressor (Das et al., 2007). It is interesting to note that some viral oncoproteins, such as E6 of HPV, act on p53 degrading it, while LT-Ag leads to the accumulation of p53, stabilizing it as a p53-T-Ag complex (Russo et al., 2008; Das et al., 2007).

3.1 HUMAN PAPILLOMAVIRUSES (HPV)

Papillomaviruses represent a diverse and large group of species-specific and tissue-specific viruses, which are widespread among mammals but are also capable of infecting reptiles and birds (Bernard et al., 1994). As already described above, until the early 80s, Papillomaviruses were classified together with PyVs in the *Papoviridae* family; however, later studies showed that the initial similarities found were small compared to their differences. Thus two distinct families were defined: *Polyomaviridae*, to which the PyVs belong, and *Papillomaviridae*, to which the Papillomavirus belong. Based on the study of the entire genome, the International Agency for Cancer Research (IARC) described 189 genotypes of Papillomavirus. Of these, 120 are human tropicviruses, called Human Papillomavirus (HPV), 64 infecting non-human mammals (rabbits, dogs, cats, horses), 3 birds and 2 reptiles (de Villiers et al., 2004). Moreover, the use of phylogenetic algorithms, able to compare multiple genomic sequences, has allowed to divide Papillomavirus types into 29 genera (from the genus Alpha Papillomavirus to the genus Dyoiota Papillomavirus) based on the percentage of similarity at the nucleotide sequence of the Open Reading Frame (ORF) of the capsid major protein (L1) (Bernard et al., 2010). HPVs belong to 5 of these genera: α, β, γ, μ and ν. Each genus is subdivided into different species, which include viruses with a sequence homology in L1 between 60% and 70%; within each species there are genotypes (or types) with a sequence similarity between 71% and 89%. Viruses with a homology greater than 90% but less than 98% are defined subtypes; while those with a homology of 98% - 99% are called variants.

Based on the tropism of the virus, HPVs are divided into two broad categories: skin HPV and mucosal HPV. The former infects the keratinized epithelium causing skin lesions such as common warts frequently found at the level of the hands and feet. The latter infect the mucosal epithelium of the ano-genital tract, of the urinary tract, of the oral cavity and of the respiratory tract. Lesions of the mucosa are mainly represented by benign neoformations called condylomas. In addition, mucosal HPVs are also associated with squamous intraepithelial lesions that may progress to invasive squamous carcinoma (Murray PR and RH et al., 2003). Mucosal-genital HPVs are also classified, based on their ability to develop cancerous lesions in humans, in high (high-risk, HR) and low (low-risk, LR) oncogenic risk genotypes.

3.1.1 Virion structure

HPVs are naked viruses, lacking of lipoprotein coating (pericapsid), have an icosahedral capsid with a diameter of 45-55 nm, within is contained the viral genome, which consists of a circular closed molecule of DNA of about 8000 base pairs. The capsid is formed by the repetition of two proteins, L1 and L2: organized in 72 capsomers, for a total size of about 55 nanometers (Modis et al., 2002).

3.1.2 Genome organization

The structure and genomic organization of HPVs is highly conserved among the different genotypes. The viral genome consists of a single double stranded circular DNA molecule of about 8 kb. It is divided into 3 coding regions: an early region, consisting of 6 genes (E1, E2, E4, E5, E6 and E7); a late region, codifying for structural proteins (L1, L2); and finally a non-coding regulatory region called “long control region” (LCR) or also "upstream regulatory region (URR), containing the origin of replication and the binding sites of the different transcription factors (Figure 8) (Narisawa-Saito et al., 2007; Munoz et al., 2006).

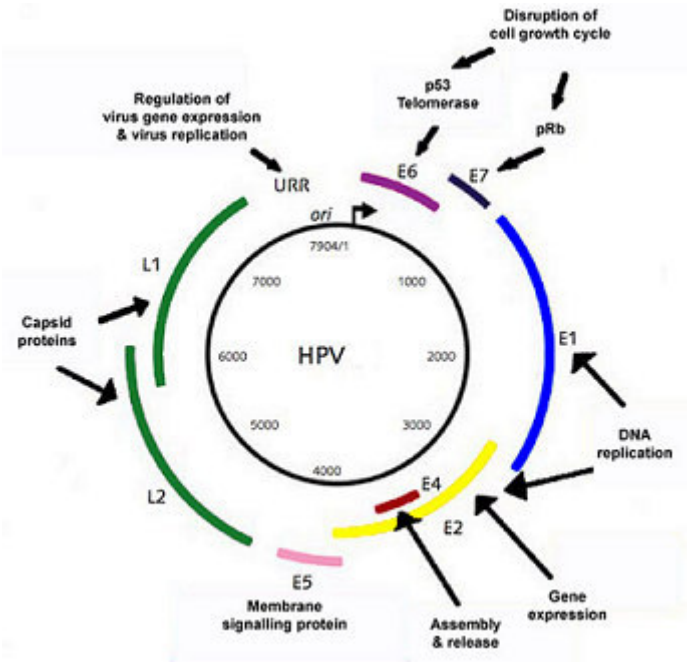

Figure 8. Schematic organization of the Human Papillomavirus genome

The 6 early genes encode for as many regulatory proteins, each of them with a specific function during the replicative cycle of the virus. E1 and E2 proteins are involved in viral replication and transcription (Hughes FJ et al., 1993). E1 is a phosphoprotein, which has ATP-asic and helicase activity necessary to recognize and bind the origin of viral replication. Instead, E2 is a dimeric protein, which is able to positively or negatively regulate the expression of early genes. In fact, when the E2 protein is expressed at low levels it is able to activate the early promoters and thus favour the expression of early proteins; however, if expressed at high levels, it represses their expression (Spalholz et al, 1987; Mohr et al., 1990; Wilson et al., 2002).

The E4 protein is expressed in the late stages of viral infection, it is indeed involved in the release phase of the mature virions. It seems to interact with the cytoskeleton of the host cell, affecting its structural integrity, and thus favouring the release of the neo-formed virions in the extracellular environment (Doorbar et al., 1991; Wilson et al., 2005). The activity of the E5 is a hydrophobic protein that is localized on the Golgi membrane and on the cell membrane. It would seem able to stimulate cell proliferation at different levels: inducing activation of the epidermal growth factor's receptor, promoting mitotic signal transduction through interaction with transcription factors, and contributing to the inactivation of the apoptotic process (Ashrafi et al., 2005). The proteins E6 and E7 are called oncogene proteins, in fact they are responsible for the transformation of the host cell. These oncogene proteins

act by inactivating two important tumor suppressor proteins: p53 and pRb. Thus leading to deregulation of the cell cycle and transformation of the host cell.

On the other hand, the late proteins are structural proteins, which form the viral capsid. The L1 protein is the major capsidic protein, has a molecular weight of about 55 kDa; while L2 is the minor capsid protein and has a molecular weight of about 70 kDa. The L1 proteins self-assemble into 72 pentamers, in which L2 proteins are intercalated, leading to the formation of complete virion.

3.1.3 Lifecycle (attachment, entry and trafficking)

The lifecycle of HPVs is strictly dependent on the state of differentiation in which is present its target cell, that is the epithelial cells of the skin or mucosa depending on the specific tropism of the considered genotype (Longworth et al., 2004; Stanley et al., 2007). The entry of the virus into the host is via micro-lesions of the skin or mucosa. The initial infection occurs in the cells of the basal layer. HPV adhesion on the surface of the host cell occurs through the interaction of the L1 capsid protein with specific cell receptors. Controversy exists as to the nature of the cell surface receptor that allows initial attachment of the virus to the cell, although most studies have suggested a dependence on the presence of heparin sulphate (Giroglou et al., 2001; Joyce et al., 1999). Following the adsorption of the virus to the membrane of the host cell, the virus is transported internally by the endocytosis of clathrin coated vesicles (Culp et al., 2004; Day et al., 2003; Selinka et al., 2007).

Once HPV has entered the host cell, the uncoating phase takes place, by breaking the intracapsidic disulphide bonds, allowing viral DNA to be transported into the nucleus.

In the initial stages of infection in the basal cells of the epithelium, the pattern of viral gene expression consists of the E1 and E2 proteins, which allow a high replication of the viral genome (up to 100 copies per cell) (Wilson et al., 2002) and facilitates the correct segregation of genomes during cell division (You et al., 2004). When the infected cell divides, one of the two daughter cells escapes from the basal layer and begins the differentiation process, while the other one remains in the basal layer and allows the maintenance of the latent and persistent infection.

When the infected epithelial cell reaches the spinous layer of the epithelium the expression of the other early genes also begins (E4, E5, E6, E7) and the late promoter is activated (L1, L2) (Figure 9).

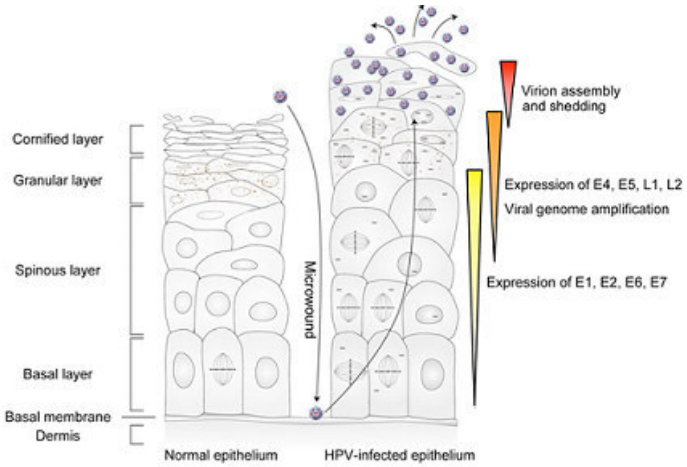

Figure 9. Schematic representation of the expression of HPV genes while the infected cell migrates to the epithelial surface.

Then, in the granular layer begins the productive phase of the viral cycle, leading to a massive replication of the viral genome in spite of a clear reduction in cellular DNA synthesis and an increase of the expression of late genes. The formation of mature viral particles occurs only in the most superficial layers of the epithelium, in completely differentiated cells, within which the genomes of the viral progeny are encapsulated and then released externally exploiting the physiological cellular turnover (Doorbar et al., 2004, Stanley et al., 2007).

3.1.4 Molecular mechanism of transformation

In several papers, both in *vitro* and in *vivo* experiments, have been shown that the co-expression of E6 and E7 proteins of high-risk HPV genotypes shows transforming capacities (Durst et al., 1987). E6 is able to alter numerous cellular functions. One of the main mechanisms by which E6 is able to promote cell transformation is the binding of the tumor suppressor p53. The binding of E6 to p53 is mediated by an ubiquitin cellular ligase called E3-associated E6 protein (E6-AP E3). In particular, while the binding of low-risk HPV E6 protein has no effect on the stability of p53, the binding of high-risk HPV E6 accelerates the degradation of p53. This leads to the inhibition of p53 functions, such as G1 cycle arrest, repair of damaged DNA, and the induction of irreparably damaged cell apoptosis (Scheffner et al., 1990). E6 of high-risk genotypes may negatively regulate p53 also indirectly, inhibiting gene transcription through interaction with transcription factors, like p300 and CREB-binding protein (CBP) (Patel et al., 1999). Another pathway through which E6 is able to inhibit the apoptosis of the host cell is by induction of the degradation of c-Myc and Bak, which are pro-apoptotic proteins belonging to the Bcl-2 family. Normally, c-Myc induces the cell apoptosis

through the activation of p14ARF, which binds mdm2 that increases the half-life of p53. Finally, E6 is able to activate, independently from p53, the telomerase leading to the immortalization of the infected cell (Figure 10).

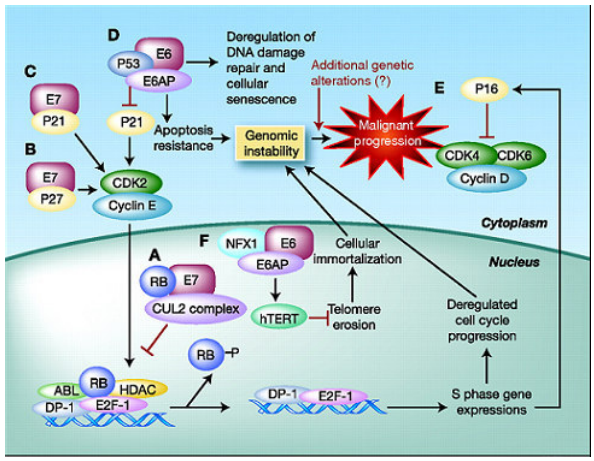

Figure 10. Functions of the E6 / E7 oncoproteins

The transforming capacity of E7 is due to its interaction with members of the pRb tumor suppressor family (p105, p130, p107). The E7 protein of high-risk genotypes binds pRB members with higher affinity than low-risk genotypes (Gage et al., 1990). In a normal cell cycle, pRb is in a hypo-phosphorylated state in the G0 and G1 phases and in this phase, it acts binding and inactivating the transcriptional factor E2F and thus inhibiting the progression of the cell cycle. The E7 protein is able to sequester the hypo-phosphorylated form of pRB, with consequent activation of the E2F target genes, independently of the presence of growth factors such as the Epidermal Growth Factor (EGF) and the Platelet-Derived Growth Factor (PDGF) (Gonzalez et al., 2001; Zhang et al., 2006). Therefore, the action of E7 leads to an uncontrolled proliferation of the infected host cell.

AIM OF THE STUDY

The human oral cavity of healthy subject is strongly colonized by microorganisms, including viruses, bacteria, fungi and protozoa. Many of these are commensal species, which maintains health status when in equilibrium, but can become pathogenetic in response to specific ecological shift in the microbiome, such as poor oral hygiene, immunological disorders and specific genetic components. So far, there have been several studies about the involvement of the bacterial component of the oral cavity in the onset and development of oral diseases, but very few studies concerning oral viroma. In the present study, we have evaluated the prevalence of the DNA viruses mostly involved in the composition of the oral cavity viroma, that are the human Papillomaviruses and Polyomaviruses. The case study comprised both healthy subjects, without or with periodontitis and HIV positive patients. Nucleic acids isolation from saliva, buccal swab and paper points and subsequent Real Time PCR were the employed techniques.

METHODS

4.1 CASE STUDY

The study was carried out on clinical specimens collected from patients referring to the Dental Center of the Galeazzi Orthopedic Institute at Milan and to the Dental School of Temple University at Philadelphia. Saliva and buccal swab and when possible paper point were collected from 20 HIV positive patients (HIV+) without any buccal disease, 39 HIV negative subjects, 9 of which affected with periodontitis (PP). In addition, only buccal swab was collected from 66 HIV negative subjects referring to the Burlo Garofalo Institute at Trieste (Table 5). The local ethics committee approved the study and all patients or patients'parents gave their written informed consent (from the ethics committee of Temple University with the protocol number:24366, from the ethics committee of San Raffaele hospital with the protocol number: HPV-PI e registration number: 81/int/2016).

Table 5. Demographic and clinical data of enrolled patients and controls.

HIV status	Groups	N°	Male (%)	Mean age ± ds
HIV+	**HIV+**	20	13 (65.0%)	54.1 ± 7.0
HIV-	**HS**	96	83 (86.5%)	37.7 ± 12.6
	PP	9	2 (22.2%)	50.3 ± 12.3

HS: Healthy Subjects; **PP**: Subjects affected with periodontitis

As shown in table 6, regarding the group of HIV positive patients, saliva samples and buccal swab samples could be collected for all 20 patients, but not the paper points samples. On the contrary, 39 saliva samples, 105 buccal swab samples and 19 paper points samples were collected from the 105 subjects enrolled in the healthy control group.

Table 6. Type and number of samples collected from enrolled patients and controls.

HIV status	Groups	Saliva	Buccal Swab	Paper Points
HIV+	**HIV+**	20	20	-
HIV-	**HS**	30	96	10
	PP	9	9	9

HS: Healthy Subjects; **PP**: Subjects affected with periodontitis

4.2 BUCCAL SWAB USE AND DNA ISOLATION

Specific buccal swabs were used to collect the oral samples, designed to increase yields and quality of DNA from buccal cells. To efficiently collect buccal cell samples is necessary to insert the swab into the mouth and rub along the entire surface of the tongue for at least one

minute. At this point, the buccal swab is placed in a tube containing a silica gel capsule, which placed in contact with the sample guarantees the long-term stability of the buccal DNA on the head of the swab before arrival in the laboratory. Before proceeding with DNA extraction it is necessary to remove the silica gel capsule from the tube.

The viral DNA was extracted from buccal swab using the commercial kit *Isohelix Buccal-Prep Plus DNA* (Isohelix). Before proceeding with DNA extraction it is necessary to remove the silica gel capsule from the tube, and add 500 µL of BLS solution to the tube containing the buccal swab, seal the tube then vortex. Thus the DNA is stabilized and it is possible either to proceed directly with the extraction or to store it at room temperature for up to a year without risking damaging the sample. Proceeding with extraction, it is necessary to add 20 µL proteinase K solution to the tube containing the buccal swab and BLS solution and briefly vortex. Incubate the tube at 60 ° C in a bath for one hour. Proteinase K is a serinquinase capable of degrading proteins, which having aromatic groups capable of absorbing ultraviolet light as well as nucleic acids, can interfere in reading the concentration of DNA in the spectrophotometer and in subsequent analytical analyzes. At the end of incubation, remove the swab head and add 400 µL BP solution, which consents the precipitation of DNA. Place the tube in a microcentrifuge and spin at maximum speed for 10 minutes. The pellet will contain the DNA. Remove the supernatant carefully, re-suspend the pellet in 50 µL of H_2O and incubate for one hour at room temperature. After the incubation time is complete, re-spin the sample for 15 minutes at maximum speed to remove the insoluble impurities. Transfer the supernatant, containing the DNA, to a new sterile Eppendorf, being careful not to touch the pellet. The viral DNA is then quantified by spectrophotometry and stored at -20 ° C until the subsequent analytical procedures are performed.

4.3 SALIVA COLLECTION AND DNA ISOLATION

For the saliva collection, it was used the *Salivette*® (*Sarstedt*) kit, that contains a cotton swab, which provides an optimal method for hygienic collection of saliva. The swab is removed from the *Salivette®,* placed into the mouth of the patient and chews for about 60 seconds to stimulate the salivation. Then, the swab with the adsorbed saliva is returned to the *Salivette®.* The *Salivette*® is then spinned at 1000 g for 2 minutes, which allows to collect a sample of clear saliva, that can be used for the analysis.

The viral DNA was extracted from saliva using the commercial kit *NucleoSpin RNA Virus* (Macherey-Nagel).

The protocol, based on the principle of chromatography, provides the lysis of the sample under denaturing conditions, followed by a selective adsorption of the DNA to the silica matrix, subsequent washing and final elution. The extraction is performed using 150µl of sample (serum or urine), to which 600µl of RAV1, a lysis buffer and 20µl of proteinase K are added, in order to solubilize the membrane. The sample is then vortexed and subjected to an incubation of 70 ° C for 5 minutes. Subsequently, the precipitation of DNA is obtained by adding 600 µl of ethanol. The solution is loaded onto the spin column and the DNA binds to the silica membrane, while the remaining lysate is removed by centrifugation.

Potential contaminants such as salts, metabolites and soluble macromolecular components of the cell membrane are removed through three serial washes with two specific buffers.

The first wash is carried out by adding 500 µL of RAW buffer, while the last two involve the use of the same RAV3 wash buffer (600µL and 200µL respectively), for the elimination of any ethanol residues and contaminants. The column, at the end of the washings, is incubated at 70 ° C for 1 minute. Following incubation, 50µl of pre-heated RNAse-free water are added directly onto the membrane in order to elute the extracted DNA. The properties of the spin column matrix and the speed of microcentrifugation allow to obtain pure viral DNA in satisfactory quantities for subsequent analyzes. The DNA is then quantified by spectrophotometry and stored at the temperature of -20 ° C until the execution of the subsequent analytical procedures.

4.4 PAPER POINT USE AND DNA ISOLATION

For the sampling of the biofilm present in the subgingival sulcus, the point of paper has been used. The paper points have been inserted in the subgingival sulcus, paying particular attention not to traumatize the junctional epithelium, and remove after 20 seconds. The collected paper points are stored in DNA-free tube with 500 µL di for each patient 6 paper points were collected. Regarding paper point samples, viral DNA extraction was performed using the QIAamp DNA Mini Kit (QIAGEN) commercial kit. The isolation of the genome is based on the property of the DNA to bind to inert supports. These silica supports or filters have hydroxyl groups which selectively bind the negative charges placed on the oxygen atoms of the DNA phosphate groups. They allow, therefore, the selective binding of DNA and the elimination of RNA and proteins by means of a series of washes with appropriate buffers. The DNA bound to the filter can subsequently be eluted by water or a buffer containing Tris-HCl. Up to 200 µl of sample must be used to perform the extraction, to these are added 180 µl of

ATL Buffer, a lysis buffer, and 20 µl of proteinase K. To ensure efficient lysis, it is essential that the sample and Buffer AL are mixed thoroughly to yield a homogeneous solution. The solution thus composed must therefore be incubated at 56°C for 10 min.

At the end of the incubation, 200 µl of 100% ethanol are added to the sample to induce the precipitation of the DNA. The solution obtained is transferred to the QIAamp Mini Spin Column, a column characterized by the presence of a positively charged silica filter, which retains the DNA molecules (negatively charged).

Following the DNA binding to the column two washes are carried out with two different buffers called AW1 and AW2. The first wash is carried out by adding 500 µl of Buffer AW1, which contains high salt concentrations, useful for eliminating the various cellular contaminants; the second washing, instead, is carried out by adding 500 µl of Buffer AW2, to eliminate the residuals of the previous buffer. Finally, we proceed with the elution of genomic DNA using 50µl of water deprived of enzymes with a nuclease action (DNAase free). The viral DNA is then quantified by spectrophotometry and stored at -20 ° C until the subsequent analytical procedures are performed.

4.5 QUANTITATIVE REAL-TIME POLYMERASE CHAIN REACTION

The quantitative Real Time - PCR (Q-PCR) is a specific technique, sensitive and applicable to biological samples of different nature and high number. The Q-PCR monitors the fluorescence emitted during the reaction as an indicator of amplified production during each PCR cycle and, therefore, operates in real time, unlike conventional PCR methods, which determine the final product.

There are two general methods for quantitative analysis of the amplification: fluorescent probes, such as TaqMan probes, and double-strand DNA intercalation agents, such as SYBR green. In our study we use the TaqMan probes, which yield the 5'exonuclease activity of Taq polymerase. They are oligonucleotides 20-30 bases long, which contain a fluorescent marker, called "reporter", bound to the 5 'end, and a fluorescence repressor molecule, called "quencher", linked to the 3' base. TaqMan probes are designed based on the nucleotide sequence of the internal region of the PCR product. When the probe is intact and is excited by a light source, the fluorescence emission by the reporter is suppressed by the quencher, by the fluorescence resonance energy transfer property (FRET, due to the proximity of the two molecules.) When the probe binds to the template and is reached by the DNA polymerase, which is synthesizing the new strand of DNA, is cut off by the 5 'exonuclease activity of the

enzyme. As a consequence, the reporter separates from the quencher and the increase in their distance prevents the energy transfer allowing, thus, the reporter, to emit fluorescence.
The increase in the signal emitted by the fluorescent molecule, which is proportional to the amount of amplified obtained, is read and converted by the instrument into an electrical signal and shown by the software by means of an amplification chart.

To have high standards of specificity and sensitivity, the probe and the primers must have a content of C and G not higher than 80%, because it can interfere with the process of denaturation, annealing, extension and emission of fluorescence. The annealing temperature of the probe must be about 10 ° higher than that of the primers, so that it binds to the template before the primers. Finally, the probe and the primers must be designed in such a way as not to present complementary sequences, to prevent them bind to each other and form probe-primer strands, or to form hairpin-shaped structures called "hairpin", all inside the individual filaments.

Our machine is a 7500 Real-time PCR system (Applied Biosystems), consisting of a thermocycler, a halogen lamp for the excitation of fluorophores, and a CCD camera to capture the emitted fluorescence. The instrument is connected to a computer, supported by a suitable software, able to analyze the data related to the emitted fluorescence, with a wavelength between 500 and 600 nm.

The amplification curve of a PCR product is theoretically exponential, but in reality, after the first phase, it assumes a rectilinear trend that progressively reaches a maximum value, called the plateau phase, to which all the samples tend, regardless of the quantity of Starting DNA due to the exhaustion of PCR reagents.

In the study of a Real Time PCR graph, three basic parameters are defined:

• Baseline region: it is the initial phase of the reaction, in which there are only non-significant variations in the fluorescence, called background noise (background).

• Threshold: is the threshold line, which consists of the fluorescence value above which the signal is considered significant; it is chosen by the operator to intersect the curves of all the samples in the exponential phase.

• Threshold Cycle, specific for each sample, identifies the value of the PCR cycle in which the curve in exponential phase intersects the threshold line. The threshold cycle (Ct = Cycle

threshold) is an important index because there is a linear relation between its value and the initial quantity of the reaction template. The quantification of the viral load of each sample can be made by amplifying serial dilutions of a standard of known DNA concentration, containing the target region to be amplified. This is necessary for the construction of a calibration line, defined as standard curve, with reference to which it will be possible to obtain the viral load values of each sample submitted to the analysis.

4.5.1 Duplex Real Time - PCR for JCPyV and HPyV6

For the amplification and quantification of JCPyV and HPyV6 two sets of primers/probes targeting the T-Ag and the VP1 coding regions, respectively, were used (table 7)

Table 7. Specific sequences of primers and probe of JCPyV and HPyV6 used in the Real Time PCR analysis.

VIRUS	TARGET REGION	PRIMERS /PROBE	POSITION	SEQUENCE
JCPyV	T-Ag	Forward	4299-4321	5'-GAGTGTTGGGATCCTGTGTTTTC-3'
		Reverse	4352-4375	5'-GAGAAGTGGGATGAAGACCTGTTT-3'
		Probe	4323-4350	5'FAM-TCATCACTGGCAAACATTTCTTCATGGC-MGB3'
HPyV6	VP1	Forward	1767-1786	5'-GGCCTGGAAGGGCCTAGTAA -3'
		Reverse	1847-1823	5'-ATTGGCAGCTGTAACTTGTTTTCTG -3'
		Probe	1789-1806	5'JOE-AGAACCAACCATCTGTTG- BHQ1-3'

The reaction mix was prepared as follows (table 8):

Table 8. Reaction mix setup.

COMPONENTS	*FINAL CONCENTRATION*
Master Mix	1X
Forward JCPyV	400 nM
Reverse JCPyV	400 nM
Taqman Probe JCPyV	150 nM
Forward HPyV6	900 nM
Reverse HPyV6	900 nM
Taqman Probe HPyV6	250 nM
DNA sample	≤ 250 ng
H_2O	final volume of 20 µL

4.5.2 Duplex Real Time - PCR for BKPyV and MCPyV

For the amplification and quantification of BKPyV and MCPyV, two sets of primers/probes targeting the VP1 coding regions, were used (Table 9).

Table 9. Specific sequences of primers and probe of BKPyV and MCPyV used in the Real Time PCR analysis.

VIRUS	TARGET REGION	PRIMERS /PROBE	POSITION	SEQUENCE
BKPyV	VP1	Forward	2511-2531	5'-AGTGGATGGGCAGCCTATGTA-3'
		Reverse	2586-2605	5'-TCATATCTGGGTCCCCTGGA -3'
		Probe	2535-2556	5'VIC-TATGGAATCCCAGGTAGAAGA-MGB 3'
MCPyV	VP1	Forward	4053-4072	5'-GAGTGTTGGGATCCTGTGTTTTC-3'
		Reverse	4090-4112	5'-GAGAAGTGGGATGAAGACCTGTTT -3'
		Probe	4074-4089	5-FAM-TCATCACTGGCAAACATTTCTTCATGG C-MGB-3'

The reaction mix was prepared as follows (table 10):

Table 10. Reaction mix setup.

COMPONENTS	*FINAL CONCENTRATION*
Master Mix	1X
Forward BKPyV	200 nM
Reverse BKPyV	400 nM
Taqman Probe BKPyV	150 nM
Forward MCPyV	200 nM
Reverse MCPyV	400 nM
Taqman Probe MCPyV	200 nM
DNA sample	≤ 250 ng
H_2O	final volume of 20 µL

4.5.3 Duplex Real Time - PCR for HPyV7 and HPyV9

For the amplification and quantification of HPyV7 and HPyV9 two sets of primers/probes targeting the VP1 coding regions, were used (Table 11).

Table 11. Specific sequences of primers and probe of BKPyV and MCPyV used in the Real Time PCR analysis.

VIRUS	TARGET REGION	PRIMERS /PROBE	POSITION	SEQUENCE
HPyV7	VP1	Forward	1774-1796	5'-AGGTCAATGAAGCCCTAGAAGGT-3'
		Reverse	1840-1822	5'-TGCTTTCTGAGGGCTTGCA-3'
		Probe	1798-1817	5'-FAM-CAGGCAATACTGATGTAGC-MGB-3'
HPyV9	VP1	Forward	1449-1469	5'-CCCCAAAGAAAAGGCAAGAG -3'
		Reverse	1509-1493	5'-GCGGGTGTTGGACAGGTTT-3'
		Probe	1472-1488	5'-VIC-CGGAGCATGTCCTGTAA-MGB-3'

The reaction mix was prepared as follows (table 12):

Table 12. Reaction mix setup.

COMPONENTS	***FINAL CONCENTRATION***
Master Mix	1X
Forward BKPyV	200 nM
Reverse BKPyV	400 nM
Taqman Probe BKPyV	150 nM
Forward MCPyV	200 nM
Reverse MCPyV	400 nM
Taqman Probe MCPyV	200 nM
DNA sample	≤ 250 ng
H_2O	final volume of 20 µL

For all the HPyVs' Real Time PCR assays performed the cycling conditions were as follow (table 13)

Table 13. Real Time PCR cycler conditions.

STEP	TIME	TEMPERATURE
Uracil-N-glycosylase activity	2 min	50°C
PCR initial activation step	15 min	95°C
Denaturation	15 sec	95°C
Annealing	30 sec	60°C
Number of cycles	40	

4.5.4 Multiplex Real Time - PCR for HPVs

For HPV analysis each DNA were subjected to a quantitative Real Time TaqMan PCR assay targeting seven high risk-HPV genotypes (HPV 16, 18, 31, 33, 45, 51 and 52). No information regarding the primer / probe sequence were available, since they are protected by a manufacturer's patent.

The reaction mix was prepared as follows (table 14):

Table 14. Reaction mix setup.

COMPONENTS	*FINAL CONCENTRATION*
TaqMan Gene Expression Master Mix 2X	1X
HPVs Forward primers	400 nM
HPVs Reverse primers	400 nM
HPVs Taqman Probe	200nM
DNA sample	≤ 250 ng
H_2O	final volume of 20 µL

In each plate negative controls (consisting of the mix with 5µl of H_2O instead of the template) and standards for each of the studied viruses (dilution range: 10^1–10^4 plasmid copies/µl) were added.

The reaction parameters of the quantitative Real Time PCR assays were as follow (table 15)

Table 15. Real Time PCR cycler conditions.

STEP	TIME	TEMPERATURE
Uracil-N-glycosylase activity	2 min	50°C
PCR initial activation step	10 min	95°C
Denaturation	15 sec	95°C
Annealing	30 sec	60°C
Number of cycles	45	

4.5 STATISTICAL ANALYSIS

Comparisons between groups of subjects and the subgroups of the oral specimens were done using the chi-square test or Fisher's exact test. Unpaired t-tests were performed to evaluate the significant differences among the viral loads. Results were considered significant when the p values were less than 0.05.

RESULTS

5.1 QUANTITATIVE REAL-TIME PCR RESULT ON HPyVs

Overall, 20 HIV positive patients and 105 HIV negative controls were included in this study. Demographic data of patients and control subjects is summarized in Table 5.

Table 16 shows the results obtained by quantitative Real Time PCR assays, performed to evaluate the prevalence of the viral genome of 6 HPyVs (JCPyV, BKPyV, MCPyV, HPyV6, HPyV7, HPyV9) in the two groups of patients.

Table 16. Prevalence of HPyVs in HIV + and HIV- group of patients.

	Positive patients / total patients (%)					
Group	**JCPyV**	**BKPyV**	**MCPyV**	**HPyV6**	**HPyV7**	**HPyV9**
HIV+	7/20 * (35.0%)	0/20 (0.0%)	9/20 ** (45.0%)	0/20 (0.0%)	0/20 (0.0%)	0/20 (0.0%)
HIV-	4/105 * (3.8%)	1/105 (1.0%)	25/105 ** (23.8%)	0/105 (0.0%)	0/105 (0.0%)	1/105 (1.0%)

* = $p<0.05$

Prevalence of HPyVs in case and control groups was 60.0% (12/20) and 25.7% (27/105), respectively. Specifically, in the HIV positive group, 7/20 patients (35.0%) were positive for the JCPyV genome and 9/20 patients (45.0%) were positive for the MCPyV genome. Among these patients, 6 out 12 (50.0%) were coinfected by both viruses.

The positive results were distributed as follows, among the healthy subjects: 4/105 (3.8%) were positive for JCPyV, 25/105 (23.8%) were positive for MCPyV, 1/105 (1.0%) was positive for BKPyV and 1/105 (1.0%) was positive for HPyV9. There were two cases of JCPyV and MCPyV concomitant infections, one case of BKPyV and MCPyV concomitant infection and one of HPyV9 and MCPyV. HPyV6 and HPyV7 were not isolated in any samples from either HIV positive and HIV negative subjects.

The association between HIV infection and HPyVs positivity was statistically significant ($p=0.015$), even after adjusting for the presence of periodontitis disease ($p=0.043$). In particular, the different prevalence of JCPyV and MCPyV in the two groups of subjects was statistically significant, with a p value of 0.002 and 0.04 respectively. There was no evidence of differences in the viral load distributions between cases and controls ($p=0.1604$).

Considering HIV negative patients and comparing patients affected with periodontitis (PP) with healthy subjects (HS), the percentages of infections were 11.1% (1/9) and 27.1 (26/96) respectively, with an odds ratio of 0.30 (Fisher exact test, $p=0.684$). Furthermore, within the

control group there is a significant difference between the positivity for JCPyV and MCPyV (p=0.001).

5.1.1 Prevalence of HPyVs in saliva

The subsequent analysis focused on the prevalence of HPyVs in the different types of oral samples (saliva, buccal swab and paper points). For this purpose, table 17 summarized the results in the saliva samples in the two different groups under analysis, while table 18 summarized the mean viral load values of HPyVs.

Table 17. HPyVs detection in saliva samples of patients and control groups.

	Positive saliva samples / total saliva samples (%)					
Group	**JCPyV**	**BKPyV**	**MCPyV**	**HPyV6**	**HPyV7**	**HPyV9**
HIV+	5/20 (25.0%)	0/20 (0.0%)	9/20 (45.0%)	0/20 (0.0%)	0/20 (0.0%)	0/20 (0.0%)
HIV-	4/39 * (13.8%)	0/39 (0.0%)	12/39 * (41.4%)	0/39 (0.0%)	0/39 (0.0%)	0/39 (0.0%)
TOTAL	9/59 ** (15.3%)	0/59 (0.0%)	21/59 ** (35.6%)	0/59 (0.0%)	0/59 (0.0%)	0/59 (0.0%)

* = $p<0.05$

Table 18. Mean viral load of HPyVs in saliva samples of the enrolled patients and controls.

	Mean viral load copies/ml (range)					
Group	**JCPyV**	**BKPyV**	**MCPyV**	**HPyV6**	**HPyV7**	**HPyV9**
HIV+	3,22E+03 (8,84E+03-2,50E+02)	-	1,06E+08 (8,79E+08-5,36E+03)	-	-	-
HIV-	1,53E+04 (4,41E+04-3,29E+02)	-	5,57E+05 (3,90E+06-6,26E+03)	-	-	-

Twelve/20 (60.0%) saliva samples collected from the HIV positive patient were positive for HPyVs; 5/20 (25.0%) saliva samples tested were positive for JCPyV (mean load 3,22E+03 copies/mL; range 8,84E+03-2,50E+02 copies/mL), 9/20 (45.0%) were positive for MCPyV (mean load 1,06E+08 copies/mL; range 8,79E+08-5,36E+03 copies/mL). Among the 39 saliva samples collected from the HIV negative control group, 14/39 (35.9%) were positive for HPyVs, and more specifically 4/39 (10.3%) were positive for JCPyV (mean viral load

1,53E+04 copies/mL; range (4,41E+04-3,29E+02 copies/mL) and 12/39 (30.8%) were positive for MCPyV (mean load 5,57E+05copies/mL; range 3,90E+06-6,26E+03 copies/mL). The difference between the prevalence of HPyVs in the saliva samples between the case and control groups was not statistically significant (p=0.562). On the contrary, overall, MCPyV was much more amplified in all the saliva samples, than JCPyV (p=0.02). This difference is mainly due to the higher prevalence of MCPyV genome, compared to JCPyV genome, in the saliva samples of HIV negative subjects (p=0.04). Considering HIV negative patients and comparing patients affected with periodontitis with healthy subjects, the percentages of infections were 0.0% (0/9) and 46.7% (14/30) respectively, with a p value of 0.015. There was no evidence of differences in the viral load distributions between cases and controls.

5.1.1 Prevalence of HPyVs in buccal swab

Table 19 and 20 summarized the prevalence of HPyVs in the buccal swabs samples and the mean viral load, respectively.

Five/20 (25.0%) buccal swab samples collected from the HIV positive patient group were positive for HPyVs; 4/20 (20.0 %) buccal swab samples were positive for JCPyV (mean load 1,55E+03 copies/mL; range 4,57E+03-3,63E+02 copies/mL), and 1/20 (5.0%) were positive for MCPyV (viral load 2,87E+05 copies/mL). Among the 85 buccal swab samples collected from the control group, 13/85 (15.3%) were positive for HPyVs, and more specifically 13/85 (15.3%) were positive for MCPyV (mean viral load 1,39E+06 copies/mL; range 1,81E+07-3,48E+03 copies/mL) and 1/85 (1.2%) were positive for BKPyV (mean load 5,57E+05copies/mL; range 3,90E+06-6,26E+03 copies/mL).

Table 19. HPyVs detection in buccal swab samples of patients and control groups.

	Positive buccal swab samples / total buccal swab samples (%)					
Group	**JCPyV**	**BKPyV**	**MCPyV**	**HPyV6**	**HPyV7**	**HPyV9**
HIV+	4/20 * (20.0%)	0/20 (0.0%)	1/20 (5.0%)	0/20 (0.0%)	0/20 (0.0%)	0/20 (0.0%)
HIV-	0/85 * (0.0%)	1/85 (1.2%)	13/85 (15.3%)	0/85 (0.0%)	0/85 (0.0%)	0/85 (0.0%)
TOTAL	4/105 ** (3.8%)	1/105 (1.0%)	14/105 ** (13.3%)	0/105 (0.0%)	0/105 (0.0%)	0/105 (0.0%)

* = $p<0.05$

Table 20. Mean viral load of HPyVs in buccal swab samples of the enrolled patients and controls.

	Mean viral load copies/ml (range)					
Group	**JCPyV**	**BKPyV**	**MCPyV**	**HPyV6**	**HPyV7**	**HPyV9**
HIV+	1,55E+03 (4,57E+03-3,63E+02)	-	2,87E+05	-	-	-
HIV-	-	3,84E-01	1,39E+06 (1,81E+07-3,48E+03)	-	-	-

The difference between the prevalence of HPyVs in the buccal swab samples of the case and control groups was not statistically significant (p= 0.327), as there was no evidence of differences in the viral load distributions (p= 0.556), but the positivity of JCPyV genome was significant different among the two groups (p=0.001). Additionally, considering all the analyzed samples of buccal swab, there was a statistical difference in the prevalence of JCPyV and MCPyV (p=0.024). In one HIV positive patients (5.0 %) and in one HIV negative (1.0 %) patients, MCPyV positivity was found in both saliva and buccal swab samples; and in two HIV positive patients (10.0 %) JCPyV positivity was found in both saliva and buccal swab samples.

5.1.1 Prevalence of HPyVs in paper points

Paper points samples were collected only from healthy subjects and the results are reported in tables 21 and 22.

Table 21. HPyV results in paper points samples of patients and control groups.

	Positive paper points samples / total buccal swab samples (%)					
Group	**JCPyV**	**BKPyV**	**MCPyV**	**HPyV6**	**HPyV7**	**HPyV9**
HIV+	-	-	-	-	-	-
HIV-	0/19 (0.0%)	0/19 (0.0%)	3/19 (15.8%)	0/19 (0.0%)	0/19 (0.0%)	1/19 (5.3%)
TOTAL	0/19 (0.0%)	0/19 (0.0%)	3/19 (15.8%)	0/19 (0.0%)	0/19 (0.0%)	1/19 (5.3%)

Table 22. Mean viral load of HPyVs in paper points samples of the enrolled patients and controls.

	Mean viral load copies/ml (range)					
Group	**JCPyV**	**BKPyV**	**MCPyV**	**HPyV6**	**HPyV7**	**HPyV9**
HIV+	-	-	-	-	-	-
HIV-	-	-	2,44E+04 (6,48E+04-4,26E+03)	-	-	2,30E+05

Four/19 (21.0%) paper points samples were positive for HPyVs genome, and the positive results were distributed as follows: 3/19 (15.8%) were positive for MCPyV (mean viral load 2,44E+04 copies/mL; range 6,48E+04-4,26E+03 copies/mL), one of which comes from a patient affected with periodontitis and two from healthy subjects; and 1/19 (5.3%) was positive for HPyV9 (viral load 2,30E+05 copies/mL). In one healthy subject (5.0 %) MCPyV positivity was found in both paper points and buccal swab samples.

5.1 QUANTITATIVE REAL-TIME PCR RESULT ON HPV

The results obtained showed the presence of 3 high risk-HPV genotypes (HPV 16, 51 and 52) in 2/20 (10.0%) HIV positive patients in the saliva samples. No positivity was reported in the control group (Table 23).

Table 23. Prevalence of HPVs in HIV + and HIV- group of patients.

	Positive patients / total patients (%)						
Group	**HPV16**	**HPV18**	**HPV31**	**HPV33**	**HPV45**	**HPV51**	**HPV52**
HIV+	1/20 (5.0%)	0/20 (0.0%)	0/20 (0.0%)	0/20 (0.0%)	0/20 (0.0%)	1/20 (5.0%)	1/20 (5.0%)
HIV-	0/105 (0.0%)	0/105 (0.0%)	0/105 (0.0%)	0/105 (0.0%)	0/105 (0.0%)	0/105 (0.0%)	0/105 (0.0%)

The HPV positivity resulted distributed as follow: co-infection of HPV-51 and 52 in a saliva sample and a single infection for HPV-16 in the other saliva sample. Viral load analysis revealed a viral load of $5,20*10^2$ copies/mL and $6,4*10^1$ copies/mL for HPV-51 and HPV-52 respectively in the first saliva sample and $2,9*10^4$ copies/mL for HPV-16 in the second saliva sample.

CONCLUSIONS

The oral cavity of healthy subjects is colonized by several and different microorganisms, such as viruses, bacteria, fungi and protozoa. Many of these are commensal species, which are essential to maintain a health status when in equilibrium with the environment, but can became pathogenic and capable to eliciting disease when occur environmental changes or shifts in the composition of the oral microbiota (Avila et al., 2015). The oral microbiota is involved in the onset and development of the two most common human oral diseases: dental caries and periodontal disease. Periodontal diseases include a group of chronic inflammatory diseases, that affect the periodontal supporting tissues of teeth and include destructive and nondestructive diseases (Armitage et al., 1999). Periodontitis is a multifactorial inflammatory disease of the periodontium that affects the majority of the adult worldwide (Albandar et al., 2002; Nunn et al., 2003). The main factors responsible for the induction of the inflammatory state are oral microbiota and microbial products. It has been also shown that there are many other both local and systemic cofactors, which are able to increase the inflammatory state or the damaging effects induced by pathogenic microorganisms (Lindhe et al., 1975; Löe et al., 1965). A better understanding of the etiopathogenesis of periodontal diseases seems to be essential to progress in risk assessment, in order to distinguish the factors that actually possess the true effects of risk modification from those that are risk indicators or are simply bystander factors, and to develop therapeutic strategies. Nevertheless, despite there are numerous studies concerning the bacterial communities inhabiting the oral cavity, there are very few studies defining the oral viral community and their role, if any, in the development of oral diseases. Among the viruses, Human herpesviruses (HHVs) are more studied in association with the periodontitis. Human cytomegalovirus (HCMV) and Epsten-Barr virus (EBV) have been proposed as probable risk factor of the aggressive periodontitis (Jakovljevis et al., 2014). Indeed, there is a high prevalence of these viruses, around 52%, in the oral cavity of patients affected with periodontitis compared to their presence in the healthy periodontium, about 8% (Slots et al., 2010). However, as can be seen in tables 1 and 2, there is a large discrepancy in the HHVs prevalence among the studies conducted on both healthy subjects and subjects affected by different degrees of periodontitis. Probably these variances are due primarily to the difference in the type of clinical specimens (saliva, oral biopsies, oral swabs, etc.), in the sampling procedures, as to date guidelines for the collection of the samples do not exist and in the different sensitivity of the techniques.

The limited number of studies conducted to establish a causal or causative role of viral infections in the development of periodontal diseases has provided rather inconclusive results. The only viral family that seems to play a relevant role in the oropharyngeal diseases is so far the one comprising the Human Papillomaviruses (HPVs), that are viruses already associated to different oropharyngeal cancers. Among the more than 100 identified HPV genotypes, 25 of them were detected in the oral cavity. While the prevalence of these viruses in oropharyngeal cancers has increased up to 72% (Mehanna et al., 2013), their prevalence in oral specimens in healthy subjects and their possible role in the onset of oral diseases remain largely unexplored. Together with the *Papillomaviridae* family, another viral family that may be implicated into the periodontitis pathogenesis is the *Polyomaviridae* family. The peculiar characteristics of Human Polyomaviruses (HPyVs), such as their ability to establish latency in the host in different body districts, the recognized etiopathogenic role of some of them in inducing serious diseases in immunocompromised subjects and the recent classification as probable carcinogens, make these viruses excellent candidates as possible factors involved in the pathogenesis of oral diseases. One of the most valid hypothesis to justify a etiopathogenetic role, or more probably co-factorial role, of the viral infection in the periodontal diseases suggests that the establishment of specific pathogens in the oral cavity promotes a chronic inflammatory state, that leads to the development of periodontal pathologies (Horewicz et al., 2010). The persistence of the inflammation of the periodontium and the formation of periodontal pockets contribute to the development of an ideal microenvironment for the persistence of the viruses. This correlation is bi-directional; indeed, the high viral replication in the periodontium contributes to the physio-pathological modifications of the oral cavity, which in turn contributes to the maintenance of oral inflammation and to the progression of the oral pathology.

Given the increasing incidence of oral diseases and the very limited study of viral involvement in these disorders, our study was aimed to give new insights on the possible presence of HPyVs and HPVs in the oral mucosa of both healthy and immunodepressed subjects. We could observe that the prevalence of HPyVs was significantly higher in the group of HIV positive subjects (60.0%) compared to the control group (25.7%). These data are consistent with data reported in previous studies, where the incidence of HPyVs infections was relevant in immunodepressed patients. Nonetheless, oral mucosa infections are characteristic of the HIV diseases, since reduced immunity in these subjects facilitates the

occurrence of viral infections. Among the HPyVs, the most prevalent were MCPyV and JCPyV, while the other HPyVs were absent or amplified in only one subjects.

When the oral specimens were analyzed singularly, it could be observed that 44% (26/59) of the analyzed saliva samples were positive for the presence of at least one HPyV. The frequency detected in our study is in line with the few papers reporting the finding of HPyV DNA in the saliva, that ranges from 0 to 50%. The main difference among the studies is the median, that usually lies between 3% and 4%, much lower than the prevalence found in our study. Interesting MCPyV genome was significantly more present in the saliva than all the other HPyVs. Previously, *Freze Beaz and collegues* detected MCPyV genome in the saliva and in the oral lesions of immunocompetent subjects and transplanted patients. The authors concluded that the predominant detection of MCPyV in the saliva of immunodepressed subjects could have been considered as a consequence of the impairment of the immune system. Additionally, they stated that the presence of the virus in the oral lesions of both immunocompetent and immunosuppressed subjects could suggest the involvement of MCPyV in the onset and development of oral lesions. The data suggests an association between the presence of MCPyV and the oral cavity. *Loyo et al.* described the presence of high titer of MCPyV in the saliva samples of subjects without Merkel Cell Carcinoma (Loyo et al., 2010). On the other hand, there are some studies carried out on healthy subjects and immunocompromised patients that did not report the presence of any HPyVs (Matos et al., 2012; Berger et al., 2006; Sundsfjord et al., 1994). Although different cell types may be collected during sampling, including the lymphocytes in which HPyVs are able to replicate, the viral load found in the tested samples was too high to be due to a random presence of the viruses: the author hypothesis that the oral cavity may be a site of viral replication.

Based on our results, we could conclude that MCPyV may be part of the normal viroma of the oral cavity. Nonetheless, its well-known association with the Merkel Cell carcinoma leads to state that its presence should be monitored, in order to verify whether an association between MCPyV and oral diseases can be rule out.

Regarding the results on the buccal swab samples, the total positivity for the presence of HPyVs was 17% (18/105) and also in this case MCPyV genome was the one detected at the highest percentage (13.3%), with high viral load. Furthermore, a positivity match for MCPyV genome in the saliva sample and in the buccal swab was found for both an HIV positive and a healthy patient. Interestingly, JCPyV was present in 4 HIV+ buccal swabs and in none of the

healthy subjects buccal swabs. Finally, as regard the paper points samples, 21% (4/19) of the analyzed paper point samples were positive for the presence of at least one HPyVs. Also in this case MCPyV was the most evalent, having been found in 3 out of 4 positive samples, and there was a correspondence for a healthy subject between the buccal swab sample and the paper points sample. Unfortunately, no comparison could be made with other results since no paper has been focused on buccal swabs or paper points samples.

Since HPVs infection has been strongly associated to different oropharyngeal cancers and prevalence of them in the oral cavity has not yet been studied, our investigation was extended to this family of viruses to evaluate their possible contribution. Our results showed the presence of three high risk-HPV genotypes (HPV 16, 51 and 52) in 2/20 HIV positive subjects only in the saliva samples. No positivity was reported for any other type of samples and for any healthy subjects.

This study demonstrated the wide presence of MCPyV in oral samples, in both healthy and immunodepressed subjects. There are some limits in this study: a) the limited case study; b) the failure to collect paper points from immunocompromised patients; b) the lack of a group of patients affected by different types of oral pathologies and subjects with a state of immunosuppression of different origins.

However, to our knowledge, this is the first study to examine and compare the presence of HPyVs and HPVs in a broad range of oral sample types. The results here presented represent good basis for better and more thoroughly investigation on the role of viruses, and especially on MCPyV as part of the normal viroma of the oral cavity or as opportunistic agent involved in oral diseases. In the first case, it could be of interest also studying the interaction with other viruses or bacteria in the oral cavity. In the second case, future advances in the prevention of oral manifestations of these viruses can alert clinicians about oral opportunistic diseases and help them to control viral infection more efficiently especially in immunocompromised subjects.

BIBLIOGRAPHY

1. Zarco MF, Vess TJ, Ginsburg GS. The oral microbiome in health and disease and the potential impact on personalized dental medicine. Oral Dis. 2012; 18:109-20.

2. Parahitiyawa NB, Scully C, Leung WK, Yam WC, Jin LJ, Samaranayake LP. Exploring the oral bacterial flora: current status and future directions. Oral Dis. 2010; 16:136-45.

3. Turnbaugh PJ, Ley RE, Hamady M, Fraser-Liggett CM, Knight R, Gordon JI. The human microbiome project: a strategy to understand the microbial components of the human genetic and metabolic landscape and how they contribute to normal physiology and predisposition to disease. Nature. 2007; 449: 804–810.

4. Zaura E, Keijser BJ, Huse SM, Crielaard W. Defining the healthy ‘‘core microbiome’’ of oral microbial communities. BMC Microbiol. 2009; 259: 12.

5. Sonnenburg JL, Fischbach MA. Community health care: therapeutic opportunities in

6. Avila M, Ojcius DM, Yilmaz O. The oral microbiota: living with a permanent guest. DNA Cell Biol. 2009; 28:405-11.

7. Wu RQ, Zhang DF, Tu E, Chen QM, Chen W. The mucosal immune system in the oral cavity-an orchestra of T cell diversity. Int J Oral Sci. 2014;6(3):125-132.

8. Ebersole JL, Dawson D, Emecen-Huja P, et al. The periodontal war: microbes and immunity. Periodontol 2000. 2017;75(1):52-115.

9. Slots J. Periodontitis: facts, fallacies and the future. Periodontol 2000. 2017;75(1):7-23.

10. Albandar JM. Epidemiology and risk factors of periodontal diseases. Dent Clin North Am. 2005;49(3):517-532, v-vi.

11. Paster BJ, Olsen I, Aas JA, Dewhirst FE. The breadth of bacterial diversity in the human periodontal pocket and other oral sites. Periodontol 2000. 2006; 42:80-7.

12. Jakovljevic A, Andric M. Human cytomegalovirus and Epstein-Barr virus in etiopathogenesis of apical periodontitis: a systematic review. J Endod. 2014; 40:6-15.

13. Slots J. Human viruses in periodontitis. Periodontol 2000. 2010; 53:89-110.

14. Ryder MI, Nittayananta W, Coogan M, Greenspan D, Greenspan JS. Periodontal disease in HIV/AIDS. Periodontol 2000. 2012; 60:78-97.

15. Patton LL, Ramirez-Amador V, Anaya-Saavedra G, Nittayananta W, Carrozzo M, Ranganathan K. Urban legends series: oral manifestations of HIV infection. Oral Dis. 2013; 19:533-550.

16. Zhou Y, Gao H, Mihindukulasuriya KA, et al. Biogeography of the ecosystems of the healthy human body. Genome Biol. 2013; 14:R1.

17. Fons MP, Flaitz CM, Moore B, Prabhakar BS, Nichols CM, Albrecht T. Multiple herpesviruses in saliva of HIV-infected individuals. J Am Dent Assoc. 1994; 125:713-9.

18. Grande SR, Imbronito AV, Okuda OS, Lotufo RF, Magalhães MH, Nunes FD. Herpes viruses in periodontal compromised sites: comparison between HIV-positive and -negative patients. J Clin Periodontol. 2008; 35:838-45.

19. Contreras A, Mardirossian A, Slots J. Herpesviruses in HIV-periodontitis. J Clin Periodontol. 2001; 28:96-102.

20. Saygun I, Yapar M, Ozdemir A, Kubar A, Slots J. Human cytomegalovirus and Epstein-Barr virus type 1 in periodontal abscesses. Oral Microbiol Immunol. 2004; 19:83-87.

21. Sanders AE, Patton LL, Webster-Cyriaque J. Periodontitis and oral human papillomavirus. J Am Dent Assoc. 2015; 14 6:715-716.

22. Mehanna H, Beech T, Nicholson T, El-Hariry I, McConkey C, Paleri V, Roberts S. Prevalence of human papillomavirus in oropharyngeal and nonoropharyngeal head and neck cancer--systematic review and meta-analysis of trends by time and region. Head Neck. 2013; 35:747-55.

23. Tominaga S, Fukushima K, Nishizaki K, Watanabe S, Masuda Y, Ogura H. Presence of human papillomavirus type 6f in tonsillar condyloma acuminatum and clinically normal tonsillar mucosa. Jpn J Clin Oncol. 1996; 26:393-7.

24. Kellokoski JK, Syrjänen SM, Chang F, Yliskoski M, Syrjänen KJ. Southern blot hybridization and PCR in detection of oral human papillomavirus (HPV) infections in women with genital HPV infections. J Oral Pathol Med. 1992; 21:459-64.

25. Terai M, Hashimoto K, Yoda K, Sata T. High prevalence of human papillomaviruses in the normal oral cavity of adults. Oral Microbiol Immunol. 1999; 14:201-5.

26. Kreimer AR, Bhatia RK, Messeguer AL, González P, Herrero R, Giuliano AR. Oral human papillomavirus in healthy individuals: a systematic review of the literature. Sex Transm Dis. 2010; 37:386-91.

27. Pullos AN, Castilho RM, Squarize CH. HPV Infection of the Head and Neck Region and Its Stem Cells. J Dent Res. 201; 94:1532-43.

28. Psyrri A, Prezas L, Burtness B. Oropharyngeal cancer. Clin Adv Hematol Oncol. 2008; 6:604-12.

29. Horewicz VV, Feres M, Rapp GE, Yasuda V, Cury PR. Human papillomavirus-16 prevalence in gingival tissue and its association with periodontal destruction: a case-control study. J Periodontol. 2010; 81:562-8.

30. Tezal M. Interaction between Chronic Inflammation and Oral HPV Infection in the Etiology of Head and Neck Cancers. Int J Otolaryngol. 2012; 2012:575242.

31. Hormia M, Willberg J, Ruokonen H, Syrjänen S. Marginal periodontium as a potential reservoir of human papillomavirus in oral mucosa. J Periodontol. 2005; 76:358-63.

32. Hübbers CU, Akgül B. HPV and cancer of the oral cavity. Virulence. 2015; 6:244-8.

33. Tommasino M. The human papillomavirus family and its role in carcinogenesis. Semin Cancer Biol. 201; 26:13-21.

34. Kim RH, Kang MK, Shin KH, Oo ZM, Han T, Baluda MA, Park NH. Bmi-1 cooperates with human papillomavirus type 16 E6 to immortalize normal human oral keratinocytes. Exp Cell Res. 2007; 313:462-72.

35. Cameron JE, Mercante D, O'Brien M, Gaffga AM, Leigh JE, Fidel PL Jr, Hagensee ME. The impact of highly active antiretroviral therapy and immunodeficiency on human papillomavirus infection of the oral cavity of human immunodeficiency virus-seropositive adults. Sex Transm Dis. 2005; 32:703-9.

36. Cameron JE, Hagensee ME. Oral HPV complications in HIV-infected patients. Curr HIV/AIDS Rep. 2008; 5:126-31.

37. Feng H, Shuda M, Chang Y & Moore PS. Clonal Integration of a Polyomavirus in Human Merkel Cell Carcinoma. Science. 2008; 319: 1096–1100.

38. https:

39. Shklar G, Cohen MM. The development of periodontal disease in experimental animals infected with polyoma virus. Periodontics. 1965; 3:281-5.

40. COHEN MM, SHKLAR G. PULPAL PATHOSIS IN MICE INFECTED WITH POLYOMA VIRUS. Oral Surg Oral Med Oral Pathol. 1965; 20:245-51.

41. FLEMING H.S. and SONI N.N. SE POLYOMA VIRUS AND THE PERIODONTIUM. Periodontics. 1964; 115.

42. Robaina TF, Mendes GS, Benati FJ, Pena GA, Silva RC, Montes MA, Janini ME, Câmara FP, Santos N. Shedding of polyomavirus in the saliva of immunocompetent individuals. J Med Virol. 2013; 85:144-8.

43. Robaina TF, Mendes GS, Benati FJ, Pena GA, Silva RC, Montes MA, Otero R, Castro GF, Câmara FP, Santos N. Polyomavirus in saliva of HIV-infected children, Brazil. Emerg Infect Dis. 2013; 19:155-7.

44. Baez CF, Guimarães MA, Martins RA, Zalona AC, Cossatis JJ, Zalis MG, Cavalcanti SM, Varella RB. Detection of Merkel cell polyomavirus in oral samples of renal transplant recipients without Merkel cell carcinoma. J Med Virol. 2013; 85:2016-9.

45. Loyo M, Guerrero-Preston R, Brait M, Hoque MO, Chuang A, Kim MS, Sharma R, Liégeois NJ, Koch WM, Califano JA, Westra WH, Sidransky D. Quantitative detection of Merkel cell virus in human tissues and possible mode of transmission. Int J Cancer. 2010; 126:2991-6.

46. Jeffers LK, Madden V, Webster-Cyriaque J. BK virus has tropism for human salivary gland cells in vitro: implications for transmission. Virology. 2009; 394:183-93.

47. Kutsuna T, Zheng H, Abdel-Aziz HO, Murai Y, Tsuneyama K, Furuta I, Takano Y. High JC virus load in tongue carcinomas may be a risk factor for tongue tumorigenesis. Virchows Arch. 2008; 452:405-10.

48. Polz D, Morshed K, Stec A, Podsiadło Ł, Polz-Dacewicz M. Do polyomavirus hominis strains BK and JC play a role in oral squamous cell carcinoma? Ann Agric Environ Med. 2015; 22:106-9.

49. Polz-Gruszka D, Morshed K, Jarzyński A, Polz-Dacewicz M. Prevalence of Polyoma BK Virus (BKPyV), Epstein-Barr Virus (EBV) and Human Papilloma Virus (HPV) in Oropharyngeal Cancer. Pol J Microbiol. 2015; 64:323-8.

50. Poluschkin L, Rautava J, Turunen A, Wang Y, Hedman K, Syrjänen K, Grenman R, Syrjänen S. Polyomaviruses detectable in head and neck carcinomas. Oncotarget. 2018; 9:22642-22652.

51. EDDY BE, STEWART SE, YOUNG R, MIDER GB. Neoplasms in hamsters induced by mouse tumor agent passed in tissue culture. J Natl Cancer Inst. 1958; 20:747-61.

52. SWEET BH, HILLEMAN MR. The vacuolating virus, S.V. 40. Proc Soc Exp Biol Med. 1960; 105:420-7.

53. Feltkamp MCW, Kazem S, van der Meijden E, Lauber C & Gorbalenya AE. From Stockholm to Malawi: Recent developments in studying human polyomaviruses. Journal of General Virology. 2013; 94:482-96.

54. Mishra N, Pereira M, Rhodes RH, An P, Pipas JM, Jain K, Kapoor A, Briese T, Faust PL, Lipkin WI . Identification of a novel polyomavirus in a pancreatic transplant recipient with retinal blindness and vasculitic myopathy. Journal of Infectious Diseases. 2014; 210:1595-9.

55. Padgett BL, Walker DL, ZuRhein GM, Eckroade RJ, Dessel BH. Cultivation of papova-like virus from human brain with progressive multifocal leucoencephalopathy. Lancet. 1971; 19:1257-60.

56. Gardner SD, Field AM, Coleman DV, Hulme B. New human papovavirus (B.K.) isolated from urine after renal transplantation. Lancet. 1971; 1:1253-57.

57. Allander T, Andreasson K, Gupta S, Bjerkner A, Bogdanovic G, Persson MA, Dalianis T, Ramqvist T, Andersson B. Identification of a third human polyomavirus. J Virol. 2007; 81:4130-6.

58. Gaynor AM, Nissen MD, Whiley DM, Mackay IM, Lambert SB, Wu G, Brennan DC, Storch GA, Sloots TP, Wang D. Identification of a novel polyomavirus from patients with acute respiratory tract infections. PLoS Pathog. 2007; 3:64.

59. Schowalter RM, Pastrana DV, Pumphrey KA, Moyer AL, Buck CB. Merkel cell polyomavirus and two previously unknown polyomaviruses are chronically shed from human skin. Cell Host Microbe. 2010; 7:509-15.

60. van der Meijden E, Janssens RW, Lauber C, Bouwes Bavinck JN, Gorbalenya AE, Feltkamp MC. Discovery of a new human polyomavirus associated with trichodysplasia spinulosa in an immunocompromized patient. PLoS Pathog. 2010; 6:e1001024.

61. Scuda N, Hofmann J, Calvignac-Spencer S, Ruprecht K, Liman P, Kühn J, Hengel H, Ehlers B. A novel human polyomavirus closely related to the african green monkey-derived lymphotropic polyomavirus. J Virol. 2011; 85:4586-90.

62. Siebrasse EA, Reyes A, Lim ES, Zhao G, Mkakosya RS, Manary MJ, Gordon JI, Wang D. Identification of MW polyomavirus, a novel polyomavirus in human stool. J Virol. 2012; 86:10321-6.

63. Buck CB, Phan GQ, Raiji MT, Murphy PM, McDermott DH, McBride AA. Complete genome sequence of a tenth human polyomavirus. J Virol. 2012; 86:10887.

64. Lim ES, Reyes A, Antonio M, Saha D, Ikumapayi UN, Adeyemi M, Stine OC, Skelton R, Brennan DC, Mkakosya RS, Manary MJ, Gordon JI, Wang D. Discovery of STLvpolyomavirus, a polyomavirus of ancestral recombinant origin that encodes a unique T antigen by alternative splicing. Virology. 2013; 436:295-303.

65. Korup S, Rietscher J, Calvignac-Spencer S, Trusch F, Hofmann J, Moens U, Sauer I, Voigt S, Schmuck R, Ehlers B. Identification of a novel human polyomavirus in organs of the gastrointestinal tract. PLoS One. 2013; 8:e58021.

66. Mishra N, Pereira M, Rhodes RH, An P, Pipas JM, Jain K, Kapoor A, Briese T, Faust PL, Lipkin WI. Identification of a novel polyomavirus in a pancreatic transplant recipient with retinal blindness and vasculitic myopathy. J Infect Dis. 2014; 210:1595-9.

67. Liddington RC, Yan Y, Moulai J, Sahli R, Benjamin TL, Harrison SC. Structure of simian virus 40 at 3.8-A resolution. Nature. 1991; 354:278-84.

68. Griffith JP, Griffith DL, Rayment I, Murakami WT, Caspar DL. Inside polyomavirus at 25-A resolution. Nature. 1992; 355:652-4.

69. Louie AJ. The organization of proteins in polyoma and cellular chromatin. Cold Spring Harb Symp Quant Biol. 1975; 39:259-66.

70. Keller W, Müller U, Eicken I, Wendel I, Zentgraf H. Biochemical and ultrastructural analysis of SV40 chromatin. Cold Spring Harb Symp Quant Biol. 1978; 42:227-44.

71. Cole C, Conzen SD, Polyomaviridae: the viruses and their replication. In: Fundamental Virology, 2001. Vol.1, pp. 985-1018, Knipe DM and Howley PM (editors). Lippincott Williams and Wilkins, Philadelphia.

72. Moens U, Rekvig P, Molecular biology of BK virus and clinical and basic aspects of BK virus renal infection. In: Human Polyomaviruses: molecular and clinical perspectives, 2001. Vol. 1, pp. 359-408, Kahlili K and Stoner GL (editors). Wiley-Liss, New York.

73. Brodsky JL, Pipas JM. Polyomavirus T antigens: molecular chaperones for multiprotein complexes. J Virol. 1998; 72:5329-34.

74. An P, Saenz Robles MT, Pipas JM. Large T antigens of polyomaviruses: amazing molecular machines. Annu Rev Microbiol. 2012; 66:213-236.

75. Van Ghelue M, Khan MT, Ehlers B, Moens U. Genome analysis of the new human polyomaviruses. Rev Med Virol. 2012; 22:354-377.

76. Topalis D, Andrei G, Snoeck R. The large tumor antigen: a “Swiss Army knife” protein possessing the functions required for the polyomavirus life cycle. Antiviral Res. 2013; 97:122-136.

77. Kwun HJ, Guastafierro A, Shuda M, et al. The minimum replication origin of Merkel cell polyomavirus has a unique large T-antigen loading architecture and requires small T-antigen expression for optimal replication. J Virol. 2009; 83:12118-12128.

78. Baez CF, Brandão Varella R, Villani S, Delbue S. Human Polyomaviruses: The Battle of Large and Small Tumor Antigens. Virology (Auckl). 2017; 8:1178122X17744785.

79. Whalen KA, de Jesus R, Kean JA, Schaffhausen BS. Genetic analysis of the polyomavirus DnaJ domain. J Virol. 2005; 79:9982-9990.

80. Berjanskii MV, Riley MI, Xie A, Semenchenko V, Folk WR, Van Doren SR. NMR structure of the N-terminal J domain of murine polyomavirus T antigens. Implications for DnaJ-like domains and for mutations of T antigens. J Biol Chem. 2000; 275:36094-36103.

81. Chromy LR, Pipas JM, Garcea RL. Chaperone-mediated in vitro assembly of Polyomavirus capsids. Proc Natl Acad Sci U S A. 2003; 100:10477-10482.

82. Sheng Q, Denis D, Ratnofsky M, Roberts TM, DeCaprio JA, Schaffhausen B. The DnaJ domain of polyomavirus large T antigen is required to regulate Rb family tumor suppressor function. J Virol. 1997; 71:9410-9416.

83. Meinke G, Phelan PJ, Shin J, Gagnon D, Archambault J, Bohm A, Bullock PA. Structural Based Analyses of the JC Virus T-Antigen F258L Mutant Provides Evidence for DNA Dependent Conformational Changes in the C-Termini of Polyomavirus Origin Binding Domains. PLoS Pathog. 2016; 12:e1005362.

84. Lane DP, Crawford LV. T antigen is bound to a host protein in SV40-transformed cells. Nature. 1979; 278:261-3.

85. White EA, Kramer RE, Hwang JH, et al. Papillomavirus E7 oncoproteins share functions with polyomavirus small T antigens. J Virol. 2015; 89:2857-2865.

86. Eash S, Manley K, Gasparovic M, Querbes W, Atwood WJ. The human polyomaviruses. Cell Mol Life Sci. 2006; 63:865-76.

87. Srinivasan A, McClellan AJ, Vartikar J, et al. The amino-terminal transforming region of simian virus 40 large T and small t antigens functions as a J domain. Mol Cell Biol. 1997; 17:4761-4773.

88. Whalen B, Laffin J, Friedrich TD, Lehman JM. SV40 small T antigen enhances progression to >G2 during lytic infection. Exp Cell Res. 1999; 251:121-127.

89. Kolzau T, Hansen RS, Zahra D, Reddel RR, Braithwaite AW. Inhibition of SV40 large T antigen induced apoptosis by small T antigen. Oncogene. 1999; 18:5598-5603.

90. Erickson KD, Bouchet-Marquis C, Heiser K, Szomolanyi-Tsuda E, Mishra R, Lamothe B, Hoenger A, Garcea RL. Virion assembly factories in the nucleus of polyomavirus-infected cells. PLoS Pathog. 2012; 8:e1002630.

91. Gerits N, Moens U. Agnoprotein of mammalian polyomaviruses. Virology. 2012; 432:316-26. Lynch KJ, Frisque RJ. Identification of critical elements within the JC virus DNA replication origin. J Virol. 1990; 64:5812-22.

92. Sock E, Wegner M, Fortunato EA, Grummt F. Large T-antigen and sequences within the regulatory region of JC virus both contribute to the features of JC virus DNA replication. Virology. 1993; 197:537-48.

93. Neu U, Hengel H, Blaum BS, Schowalter RM, Macejak D, Gilbert M, Wakarchuk WW, Imamura A, Ando H, Kiso M, Arnberg N, Garcea RL, Peters T, Buck CB, Stehle T. Structures of Merkel cell polyomavirus VP1 complexes define a sialic acid binding site required for infection. PLoS Pathog. 2012; 8:e1002738.

94. Assetta B, Maginnis MS, Gracia Ahufinger I, Haley SA, Gee GV, Nelson CD, O'Hara BA, Allen Ramdial SA, Atwood WJ. 5-HT2 receptors facilitate JC polyomavirus entry. J Virol. 2013; 87:13490-8.

95. Schowalter RM, Pastrana DV, Buck CB. Glycosaminoglycans and sialylated glycans sequentially facilitate Merkel cell polyomavirus infectious entry. PLoS Pathog. 2011; 7:e1002161.

96. Dugan AS, Eash S, Atwood WJ. An N-linked glycoprotein with alpha(2,3)-linked sialic acid is a receptor for BK virus. J Virol. 2005; 79:14442-5.

97. Eash S, Atwood WJ. Involvement of cytoskeletal components in BK virus infectious entry. J Virol. 2005;79:11734-41.

98. Querbes W, O'Hara BA, Williams G, Atwood WJ. Invasion of host cells by JC virus identifies a novel role for caveolae in endosomal sorting of noncaveolar ligands. J Virol. 2006; 80:9402-13.

99. Di Fiore R, D'Anneo A, Tesoriere G, Vento R. RB1 in cancer: different mechanisms of RB1 inactivation and alterations of pRb pathway in tumorigenesis. J Cell Physiol. 2013; 228:1676-1687.

100. Chinnam M, Goodrich DW. RB1, development, and cancer. Curr Top Dev Biol. 2011; 94:129-169.

101. Bertoli C, Skotheim JM, de Bruin RA. Control of cell cycle transcription during G1 and S phases. Nat Rev Mol Cell Biol. 2013; 14:518-528

102. Stubdal H, Zalvide J, Campbell KS, Schweitzer C, Roberts TM, DeCaprio JA. Inactivation of pRB-related proteins p130 and p107 mediated by the J domain of simian virus 40 large T antigen. Mol Cell Biol. 1997; 17:4979-4990.

103. Brown VD, Gallie BL. The B-domain lysine patch of pRB is required for binding to large T antigen and release of E2F by phosphorylation. Mol Cell Biol. 2002; 22:1390-1401.

104.Sullivan CS, Cantalupo P, Pipas JM. The molecular chaperone activity of simian virus 40 large T antigen is required to disrupt Rb-E2F family complexes by an ATP-dependent mechanism. Mol Cell Biol. 2000; 20:6233-6243.

105.Lin JY, DeCaprio JA. SV40 large T antigen promotes dephosphorylation of p130. J Biol Chem. 2003; 278:46482-46487.

106.Liu J, Zhang C, Hu W, Feng Z. Tumor suppressor p53 and its mutants in cancer metabolism. Cancer Lett. 2015; 356:197-203.

107.Harris, S.L.; Levine, A.J. The p53 pathway: Positive and negative feedback loops. Oncogene. 2005; 24:2899–2908.

108.Lahav G.; Rosenfeld N.; Sigal A.; Geva-Zatorsky N.; Levine A.J.; Elowitz, M.B.; Alon, U. Dynamics of the p53-Mdm2 feedback loop in individual cells. Nat. Genet. 2004; 36:147–150.

109.Brown, C.J.; Lain, S.; Verma, C.S.; Fersht, A.R.; Lane, D.P. Awakening guardian angels: Drugging the p53 pathway. Nat. Rev. Cancer. 2009; 9:862–873.

110.Xiong Y, Hannon GJ, Zhang H, Casso D, Kobayashi R, Beach D. p21 is a universal inhibitor of cyclin kinases. Nature. 1993; 366:701-4.

111.Das D, Wojno K, Imperiale MJ. BK virus as a cofactor in the etiology of prostate cancer in its early stages. J Virol. 2008; 82:2705-14.

112.Russo G, Anzivino E, Fioriti D, Mischitelli M, Bellizzi A, Giordano A, Autran-Gomez A, Di Monaco F, Di Silverio F, Sale P, Di Prospero L, Pietropaolo V. p53 gene mutational rate, Gleason score, and BK virus infection in prostate adenocarcinoma: Is there a correlation? J Med Virol. 2008; 80:2100-7.

113.Bernard HU. Coevolution of papillomaviruses with human populations. Trends Microbiol. 1994; 2:140-3.

114.de Villiers, E. M., C. Fauquet, T. R. Broker, H. U. Bernard, and H. zur Hausen. Classification of papillomaviruses. Virology. 2004; 324:17-27

115.Bernard, H. U., R. D. Burk, Z. Chen, K. van Doorslaer, H. zur Hausen, and E. M. de Villiers. Classification of papillomaviruses (PVs) based on 189 PV types and proposal of taxonomic amendments. Virology. 2010; 401:70-79.

116.Murray PR, B. E., Jorgensen JH, Pfaller MA and Y. RH. Manual of Clinical Microbiology. 2003. Washington.

117.Modis, Y., B. L. Trus, and S. C. Harrison. Atomic model of the papillomavirus capsid. EMBO J. 2002; 21:4754-4762.

118.Narisawa-Saito M, Kiyono T. Basic mechanisms of high-risk human papillomavirus-induced carcinogenesis: roles of E6 and E7 proteins. Cancer Sci. 2007; 98:1505-11.

119.Muñoz, N., X. Castellsagué, A. B. de González, and L. Gissmann. Chapter 1: HPV in the etiology of human cancer. Vaccine 24 Suppl. 2006; 3:S3/1-10.

120.Hughes FJ, Romanos MA. E1 protein of human papillomavirus is a DNA helicase/ATPase. Nucleic Acids Res. 1993;21:5817-23.

121.Spalholz, B. A., P. F. Lambert, C. L. Yee, and P. M. Howley. Bovine papillomavirus transcriptional regulation: localization of the E2-responsive elements of the long control region. J Virol. 1987; 61:2128-2137

122.Mohr IJ, Clark R, Sun S, Androphy EJ, MacPherson P, Botchan MR. Targeting the E1 replication protein to the papillomavirus origin of replication by complex formation with the E2 transactivator. Science. 1990;250:1694-9.

123.Wilson VG, West M, Woytek K, Rangasamy D. Papillomavirus E1 proteins: form, function, and features. Virus Genes. 2002; 24:275-90.

124.Doorbar, J., S. Ely, J. Sterling, C. McLean, and L. Crawford. Specific interaction between HPV-16 E1-E4 and cytokeratins results in collapse of the epithelial cell intermediate filament network. Nature. 1991; 352:824-827.

125.Wilson, R., F. Fehrmann, and L. A. Laimins. Role of the E1--E4 protein in the differentiation-dependent life cycle of human papillomavirus type 31. J Virol. 2005 79:6732-6740.

126.Ashrafi GH, Haghshenas MR, Marchetti B, O'Brien PM, Campo MS. E5 protein of human papillomavirus type 16 selectively downregulates surface HLA class I. Int J Cancer. 2005; 113:276-83.

127.Longworth MS, Laimins LA. Pathogenesis of human papillomaviruses in differentiating epithelia. Microbiol Mol Biol Rev. 2004; 68:362-72.

128.Stanley, M. A., M. R. Pett, and N. Coleman. HPV: from infection to cancer. Biochem Soc Trans. 2007; 35:1456-1460.

129.Giroglou T, Florin L, Schäfer F, Streeck RE, Sapp M. Human papillomavirus infection requires cell surface heparan sulfate. J Virol. 2001; 75:1565-70.

130.Joyce JG, Tung JS, Przysiecki CT, Cook JC, Lehman ED, Sands JA, Jansen KU, Keller PM. The L1 major capsid protein of human papillomavirus type 11 recombinant virus-like particles interacts with heparin and cell-surface glycosaminoglycans on human keratinocytes. J Biol Chem. 1999; 274:5810-22.

131.Culp TD, Christensen ND. Kinetics of in vitro adsorption and entry of papillomavirus virions. Virology. 2004; 319:152-61.

132.Day PM, Lowy DR, Schiller JT. Papillomaviruses infect cells via a clathrin-dependent pathway. Virology. 2003; 307:1-11.

133.Selinka HC, Florin L, Patel HD, Freitag K, Schmidtke M, Makarov VA, Sapp M. Inhibition of transfer to secondary receptors by heparan sulfate-binding drug or antibody induces noninfectious uptake of human papillomavirus. J Virol. 2007; 81:10970-80.

134.You J, Croyle JL, Nishimura A, Ozato K, Howley PM. Interaction of the bovine papillomavirus E2 protein with Brd4 tethers the viral DNA to host mitotic chromosomes. Cell. 2004; 117:349-60.

135.Doorbar J, Foo C, Coleman N, Medcalf L, Hartley O, Prospero T, Napthine S, Sterling J, Winter G, Griffin H. Characterization of events during the late stages of

HPV16 infection in vivo using high-affinity synthetic Fabs to E4. Virology. 1997; 38:40-52.

136. Dürst M, Dzarlieva-Petrusevska RT, Boukamp P, Fusenig NE, Gissmann L. Molecular and cytogenetic analysis of immortalized human primary keratinocytes obtained after transfection with human papillomavirus type 16 DNA. Oncogene. 1987; 1:251-6.

137. Scheffner M, Werness BA, Huibregtse JM, Levine AJ, Howley PM. The E6 oncoprotein encoded by human papillomavirus types 16 and 18 promotes the degradation of p53. Cell. 1990; 63:1129-36.

138. Patel D, Huang SM, Baglia LA, McCance DJ. The E6 protein of human papillomavirus type 16 binds to and inhibits co-activation by CBP and p300. EMBO J. 1999; 18:5061-72.

139. Gage JR, Meyers C, Wettstein FO. The E7 proteins of the nononcogenic human papillomavirus type 6b (HPV-6b) and of the oncogenic HPV-16 differ in retinoblastoma protein binding and other properties. J Virol. 1990; 64:723-30.

140. Gonzalez SL, Stremlau M, He X, Basile JR, Münger K. Degradation of the retinoblastoma tumor suppressor by the human papillomavirus type 16 E7 oncoprotein is important for functional inactivation and is separable from proteasomal degradation of E7. J Virol. 2001; 75:7583-91.

141. Zhang B, Chen W, Roman A. The E7 proteins of low- and high-risk human papillomaviruses share the ability to target the pRB family member p130 for degradation. Proc Natl Acad Sci U S A. 2006; 103:437-42.

142. Armitage GC. Development of a classification system for periodontal diseases and conditions. Ann Periodontol 1999;4(1):1–6.

SCIENTIFIC PUBLICATIONS

Journal of Neuroimmunology 310 (2017) 91–96

Contents lists available at ScienceDirect

Journal of Neuroimmunology

journal homepage: www.elsevier.com/locate/jneuroim

Multiplex array analysis of circulating cytokines and chemokines in natalizumab-treated patients with multiple sclerosis

Sonia Villani[a], Nunzia Zanotta[b], Federico Ambrogi[c], Manola Comar[b,d], Diego Franciotta[e], Maria Dolci[a], Carolina Cason[b], Rosalia Ticozzi[a], Pasquale Ferrante[a], Serena Delbue[a,*]

[a] Department of Biomedical, Surgery and Dental Sciences, University of Milan, Milan, Italy
[b] Institute for Maternal and Child Health—IRCCS "Burlo Garofolo"–Trieste, Trieste, Italy
[c] Department of Clinical Sciences and Community Health, University of Milan, Italy
[d] Medical Science Department, University of Trieste, Trieste, Italy
[e] Laboratory of Neuroimmunology, National Neurological Institute C. Mondino, Pavia, Italy

ARTICLE INFO

Keywords:
JC virus
Cytokines
Natalizumab

ABSTRACT

Natalizumab greatly reduces inflammatory relapses in multiple sclerosis (MS) by blocking the integrin-mediated leukocyte traffic to the brain, but less is known about its effects on the systemic immunity. We measured 48 cytokines/chemokines in sera from 19 natalizumab-treated MS patients. Serum concentrations of both anti-(IL-10, IL1ra) and pro-inflammatory (IL7, IL16) molecules decreased after 21-month treatment, without associations to unbalanced Th2/Th1cytokine ratios, clinical responses, and blood/urine replication of polyomavirus JC (JCPyV). No patient developed the JCPyV-related progressive multifocal leukoencephalopathy (PML), the major risk factor of natalizumab therapy. Our data suggest that natalizumab has marginal impact on the systemic immunity.

1. Introduction

The transmigration of autoreactive-activated T cells from peripheral blood into the central nervous system (CNS) is a crucial step in the initiation and maintenance of brain inflammatory reaction in multiple sclerosis (MS) (Steinman et al., 2002). The α4β1-integrin (VLA-4), expressed on the leukocytes' surface and interacting with the vascular cell adhesion molecule 1 (VCAM-1), is critically involved in this process because it mediates both the adhesion and migration of lymphocytes across the blood-brain barrier (BBB) (Kumar et al., 2005; Kummer and Ginsberg, 2006; Libbey and Fujinami, 2010; Polman et al., 2006; Rose et al., 2002; Sawcer et al., 2011).

Natalizumab is a monoclonal antibody directed against the α4 chain of the VLA-4 and α4β7 integrins and is used as a monotherapy for treating relapsing-remitting MS (RRMS)·(Stuve and Bennett, 2007). Natalizumab substantially reduces the relapse rate and the worsening symptoms, but its use is associated the development of progressive multifocal leukoencephalopathy (PML), a fatal demyelinating disease that occurs due to the lytic replication of the Polyomavirus JC (JCPyV) (Polman et al., 2006).

Chemokines affect the trafficking of leukocytes to the sites of inflammation and have a crucial role in establishing a balance between subpopulations of T helper (Th) cells (Baggiolini, 1998). Th2-related cytokines are associated with inflammatory reduction and improvement of MS symptoms. In contrast, Th1-related cytokines, which are known as pro-inflammatory proteins are increased in brain, cerebrospinal fluid (CSF) and/or blood of MS patients, especially during acute exacerbations (Imitola et al., 2005; Mellergard et al., 2010; Miller et al., 2004; Sharief and Hentges, 1991).

The effects of the cytokine/chemokine levels have been occasionally analyzed, with contrasting results (Khademi et al., 2009; Kivisakk et al., 2009; Mellergard et al., 2010; Ramos-Cejudo et al., 2011). To gain increased insight into the immunomodulating effect of natalizumab systemically, we used a multiplex array to measure the levels of 48 cytokines/chemokines in sera from MS patients treated with natalizumab from 21 months.

2. Materials and methods

2.1. Patients and samples collection

After obtaining signed, informed consent based on the local ethics committee guidelines, 19 patients with RRMS, treated with natalizumab, were enrolled at the "Fondazione Istituto Neurologico C.

* Corresponding author at: Department of Biomedical, Surgical and Dental Sciences, University of Milano, Via Pascal, 36, 20133 Milano, Italy.
E-mail address: serena.delbue@unimi.it (S. Delbue).

http://dx.doi.org/10.1016/j.jneuroim.2017.06.012
Received 21 March 2017; Received in revised form 28 June 2017; Accepted 29 June 2017

Table 1
Demographic, clinical and radiological characteristics in 19 relapsing remitting multiple sclerosis (RRMS) patients receiving Natalizumab.

Demographic, clinical, and radiological characteristics in 19 RRMS patients receiving Natalizumab during 21 months of treatment	
Sex (F/M)	16/3
Age at recruitment (mean ± SD)	34.2 ± 9.8
Disease duration at baseline (mean years ± SD)	10.2 ± 6.2
EDSS at baseline (mean ± SD) (range)	1.3 ± 1.5 (0.0–6.5)
EDSS after 12 months of treatment (mean ± SD) (range)	1.4 ± 1.6 (0.0–6.5)
EDSS after 21 months of treatment (mean ± SD) (range)	1.7 ± 1.7 (0.0–7.0)
Relapsing/non-relapsing patients	5/15
Patients with/without new MRI lesions at the end of treatment	4/15

EDSS = Expanded Disability Status Scale; MRI = Magnetic Resonance Imaging; SD = standard deviation.

Mondino" (Pavia, Italy). Natalizumab was administered intravenously to RRMS patients once every 4 weeks at a dose of 300 mg. Blood, serum and urine samples were collected before the first infusion (T0) and subsequently after 12 (T12) and 21 (T21) months of treatment. At the corresponding time point, Kurtzke's Expanded Disability Status Scale (EDSS) was scored, and Magnetic Resonance Imaging (MRI) scans were performed (Castellazzi et al., 2015).

2.2. Cytokines/chemokines analysis

Quantification of 48-cytokines/chemokines was performed on the serum samples at T0, T12 and T21 using magnetic bead-based multiplex immunoassays (Bio-Plex®) (BIO-RAD Laboratories, Milano, Italy), following the manufacturer's instructions. This procedure uses Luminex Xmap technology with magnetic multi-analyte profiling beads. Briefly, a standard curve was created via dilution of premixed standards to 50,000 pg/mL, followed by series dilution to 8 concentrations. 50 µL of serum (diluted 1:4), and 50 µL of standard curve samples were added to a 96-well filter plate containing anti-cytokine antibody-conjugated beads. After incubation for 30 min at room temperature, followed by washing plate with Bio-Plex Wash Buffer, 25 µL of the antibody-biotin reporter was added and incubated for 30 min shaking at 1100 rpm, and then 50 µL of Streptavidin-PE was added to each well. After incubation of 10 min 125 µL of Bio-Plex assay Buffer was added to plate for reading. The concentration of cytokines was determined by using the Bio-Plex 100 Analyzer (Bio-Rad Laboratories, Hercules, CA) following the manufacturer's instructions. A digital processor managed data output, and the Bio-Plex Manager® software presented the data as median fluorescence intensity (MFI) and concentration (pg/mL) (BIO-RAD Laboratories, Milano, Italy). These assays have a limit of detection of 1–20 pg/mL, depending on the protein target.

Th2/Th1ratio was defined based on the ratio of IL-4, IL-5, IL-6 or IL-10 Th2 related cytokines and pro-inflammatory IFN-ɣ or TNF-α cytokines Th1-related cytokines.

2.3. DNA extraction and JCPyV detection

DNA was isolated from 0.2 mL of blood samples using the QIAampDNA Mini Kit (Qiagen, USA) and 0.15 mL of urine samples with Nucleospin RNA Virus Kit (MachereyNagels, Germany) following the manufacturer's instructions. Quantitative real time PCR (Q-PCR) assay was performed to quantify JCPyV genome using a Taqman chemistry with an Applied Biosystems 7500 Real-Time PCR System (Applied Biosystems, Carlsbad, CA), with specific primers targeting the Large T antigen viral region, following a protocol described previously (Campello et al., 2011; Delbue et al., 2005). Data were expressed as copies/µg of DNA isolated from blood and as copies/mL of urine samples.

2.4. Anti-JCPyV IgG antibodies in serum samples

Serum concentrations of anti-JCPyV IgG were measured using a home-made ELISA previously described, using a GST-JCPyV VP1 protein as the capture antigen (Elia et al., 2016).

2.5. Statistical analysis

The values of the cytokines were analyzed under log transformation considered the skewedness of the distributions. Linear mixed models were used to analyze the change in time of the cytokines with a random intercept for each patient. The same approach was used to compare the values in time of the cytokines of patients with and without JCPyV viruria with an interaction with time of the virus presence. The false discovery rate was used to adjust the *p*-values, considering the multiple testing problem due to the analysis of 48 cytokines. The same analysis strategy was used to evaluate the change over time of the 8 Th2/Th1 ratios. Differences were considered significant at $p < 0.05$ (CI 95%).

3. Results

3.1. Patient characteristics

A total of 19 RRMS patients treated with natalizumab for 21 months was included in the study. Demographic and clinical characteristics are described in Table 1.

3.2. Cytokine/chemokine profile and natalizumab treatment

A panel of 48 soluble immune proteins was measured in the sera for the evaluation of their expression profile in response to natalizumab treatment at T0, T12 and T21. The concentration of the molecules measured as pg/mL, their role and the degree of statistical significance are reported in Table 2. Some of these proteins, including IL-2, IL-15, RANTES, IL-1a, IL-12p40, β-NGF, TNF-β, GM-CSF, MCP-1 and IFN-α, showed a concentration below the detection limit; therefore, they were not considered in the analysis of results. The concentration of seven molecules was significantly increased (Eotaxin) or decreased (IL-1ra, IL-7, IL-10, PDGFbb, IL-16 and HGF) during this time (Table 2 and Fig.1).

Th2/Th1 ratios did not exhibit any differences in the three analyzed time points, except for the IL-10/IFN-ɣ and IL-10/TNF-α ratios (Fig. 2).

3.3. JCPyV DNA detection, seropositivity and natalizumab treatment

JCPyV DNA was not found in any of the blood samples (Data not shown). No significant changes were observed in the urine JCPyV viral load or the levels of serum JCPyV antibodies (Fig. 3).

3.4. Cytokine/chemokine profile and JCPyV detection

The cytokine profiles of patients with JCPyV viruria were compared to those of patients without JCPyV viruria. No significant differences were observed for the considered cytokines (Data not shown).

Table 2
Concentrations of immune mediators in serum of RRMS patients. Data are provided as the means (quartiles) (pg/mL).

Immune effector cells	Immune mediator	Type of mediator	T0	T12	T21	p value
Th1	IFN-γ	Cytokine	59.2 (52.81–64.06)	59.2 (4779.73–6975.63)	55.99 (52.29–63.52)	0.756
	IP-10 (CXCL10)	Chemokine	7061.56 (4970.34–9298.59)	5854.6 (4779.73–6975.63)	6315.67 (4945–9174.54)	0.692
	TNF-α	Cytokine	65.53 (57.92–68.94)	67.23 (57.09–70.65)	66.38 (62.14–71.08)	0.756
	MIG (CXCL9)	Chemokine	374.82 (315.31–515.68)	351.74 (284.82–949.17)	402.24 (293.59–632.20)	0.756
Th2	IL-4	Cytokine	2.06 (1.88–2.43)	2.10 (1.95–2.37)	2.14 (1.84–2.22)	0.756
	IL-5	Cytokine	0.53 (0.52–0.58)	0.53 (0.48–0.58)	0.53 (0.48–0.53)	0.240
	IL-9	Cytokine	14.89 (10.95–23.66)	10.76 (8.94–15.18)	12.25 (7.78–14.51)	0.183
	IL-13	Cytokine	2.21 (1.94–2.95)	2.08 (1.99–2.58)	2.05 (1.83–2.28)	0.494
	Eotaxin (CCL11)	Chemokine	644.54 (409.73–1237.20)	936.6 (523.71–2171.71)	1287.95 (755.12–2129.31)	0.004
Th17	IL-6	Cytokine	9.38 (8.55–10.97)	9.38 (8.30–10.27)	9.58 (8.40–10.47)	0.756
	IL-8 (CXCL8)	Cytokine	16.85 (12.41–24.66)	16.85 (10.88–36.91)	14.92 (10.95–41.79)	0.699
	IL-17	Cytokine	16.77 (12.41–20.04)	13.09 (10.94–19.78)	13.34 (9.79–15.11)	0.146
T reg	IL-10	Cytokine	1.97 (1.61–2.31)	1.70 (1.45–1.91)	1.65 (1.34–1.85)	0.035
B cells	SDF-1α (CXCL12)	Chemokine	38.71 (0.80–62.75)	38.71 (3.96–53.88)	25.87 (0.80–43.98)	0.437
Broad spectrum	IL-7	Cytokine	1.07 (0.96–1.28)	0.98 (0.95–1.15)	0.93 (0.87–10.47)	0.034
	IL-12p70	Cytokine	2.57 (2.01–3.36)	2.57 (1.95–2.97)	1.73 (1.39–3.24)	0.386
	IL-18	Cytokine	53.2 (42.92–63.95)	52.68 (41.96–73.21)	52.68 (41.34–66.33)	0.592
	SCF	Trophic factor	38.19 (24.82–56.04)	31.28 (25.33–46.26)	30.25 (20.98–39.59)	0.768
	SCGF-b	Trophic factor	17,020.42 (6391.02–26,026.38)	13,811.04 (4132–17,700.1)	3265.03 (3138–11,627.08)	0.663
	IL-1β	Cytokine	1.05 (0.98–1.10)	1.06 (1.00–1.21)	1.00 (0.94–1.14)	0.699
	G-CSF	Trophic factor	25.14 (22.42–29.51)	22.42 (19.45–27.60)	21.88 (17.84–25.96)	0.153
Broad spectrum	MIP-1α (CCL3)	Chemokine	3.66 (3.36–4.17)	4.07 (3.37–4.70)	3.53 (3.40–4.03)	0.592
	MIP-1β (CCL4)	Chemokine	67.38 (47.22–99.94)	86.45 (49.86–129.76)	72.48 (49.54–113.04)	0.699
	VEGF	Trophic factor	14.69 (10.36–18.10)	9.29 (6.67–16.72)	8.21 (5.76–12.82)	0.153
	IL-3	Cytokine	4.10 (4.10–6.68)	4.10 (4.10–4.10)	4.10 (4.10–4.10)	0.757
	IL-16	Cytokine	33.33 (16.59–46.43)	21.38 (9.07–41.67)	12.38 (7.56–19.29)	0.041
	CTACK (CCL27)	Chemokine	482.82 (363.93–636.02)	414.88 (364.75–544.42)	419.4 (329.35–490.21)	0.693
	GRO-α (CXCL1)	Chemokine	79.68 (62.17–106.42)	94.07 (75.45–136.63)	71.68 (59.64–108.71)	0.165
	MCP-3	Chemokine	1.12 (1.12–1.81)	1.12 (1.12–1.12)	1.12 (1.12–1.12)	0.756
	M-CSF	Trophic factor	17.63 (15.53–20.24)	15.52(13.59–18.61)	14.07 (12.79–16.33)	0.091
	MIF	Trophic factor	341.60 (300.95–648.75)	533.18 (332.02–713.98)	422.92 (294.96–757.67)	0.735
	TRAIL	Chemokine	27.57 (20.71–41.82)	37.00 (28.74–49.13)	41.81 (24.69–52.82)	0.240
	PDGF bb	Trophic factor	6089.32 (4607.95–7902.88)	5245.34 (3467.16–7184.15)	4160.39 (3228.53–6158.09)	0.023
	IL-2Ra	Cytokine	32.39 (21.78–48.15)	28.74 (24.66–45.06)	29.92 (20.64–38.31)	0.348
	IL-1ra	Cytokine	206.06 (151.70–237.38)	151.69 (115.12–214.33)	124.59 (106.68–173.53)	0.041
	HuLIF	Trophic factor	13.36 (12.40–14.59)	12.40 (10.97–13.85)	12.40 (10.50–13.73)	0.495
	HGF	Trophic factor	590.86 (522.16–665.50)	446.23 (340.90–525.66)	390.50 (289.36–453.85)	0.004
	FGF basic	Trophic factor	5.24 (1.96–10.01)	1.96 (1.96–5.63)	1.96 (1.96–1.96)	0.022

4. Discussion

The beneficial effects of natalizumab in MS patients are associated with the reduction of the inflammatory status in the CNS (Jain et al., 2010; Yednock et al., 1992).

The marked decline of the inflammation intrathecally indicates a decline in the CSF levels of cytokines and chemokines, at both the mRNA and protein levels after one year of treatment (Khademi et al., 2009; Mellergard et al., 2010).

How natalizumab affects the systemic status of inflammation is instead less understood. Khademi and colleagues observed increases in systemic pro-inflammatory cytokine expression (mRNA levels) after 6 and 12 months of treatment. The high levels of pro-inflammatory cytokines in the blood were associated with the lymphocytosis and fatigue, occurring in association with natalizumab treatment (Khademi et al., 2009; Khademi et al., 2008). High numbers of activated T cells expressing pro-inflammatory cytokines in blood have also been observed (Khademi et al., 2009).

Opposite results were reported by Mellergard et al. (2010), who showed a marked decline in circulating plasma GM-CSF, TNFα, IL6 and IL 10 (proteins) after 12 months of treatment. In addition, it has been reported that 20 months of treatment with the antibody did not modify globally the cytokine profile in the blood, although an increase in some pro-inflammatory and anti-inflammatory cytokines has been observed after starting treatment (IFN-γ, IL-4, IL-10, IL-5 and IL-13) and after long-term treatment (IL-1β, IL-2, IL17,IL-5 and IL-13) with natalizumab. In addition, in the same study, the treatment with the antibody did not modify regulatory T cell function. These findings suggested different mechanisms of action of early versus prolonged exposure to Natalizumab on the target immune cells (Ramos-Cejudo et al., 2011).

Our study adds to this debate, given that the sera cytokine/chemokine profiles were defined in 19 patients with clinically defined RRMS before the beginning of natalizumab treatment and after 12 and 21 months. It was not possible to conduct the same analysis on healthy donor subjects in order to obtain data on biological variation and reference range values.

Most of the 48 studied proteins did not exhibit any significant variations during the course of the treatment, except for IL7, IL16, PDGFbb, HGF, IL1ra, and IL10, which decreased over 21 months. The first three listed proteins are pro-inflammatory, produced by Th1 cells, whereas the last three proteins act as anti-inflammatory mediators, secreted by Th2 cells. Despite these variations, the Th2/Th1 ratio was not subjected to any changes at the three analyzed time points, except for the IL-10/IFN-γ and IL-10/TNF-α ratios. Thus, the beneficial effect of natalizumab cannot be associated with a shift in favor of a Th2 anti-inflammatory profile. These data had no clinical counterparts, as they did not correlate with the clinical findings.

As for single cytokines, a significant decrease in IL7, which is a non-redundant cytokine for T-cell development and survival, has been observed. Several reports have indicated that the IL-7 levels increased in MS and experimental allergic encephalomyelitis (EAE) (Chou et al., 1999). IL-7 enhances proliferation and IFN-γ secretion by myelin-activated T cells cultured from both normal controls and MS patients. Consistent with our results, IFN-β1a treatment led to significantly reduced serum IL-7 levels, whereas natalizumab treatment mitigated the serum IL-7 levels (Lundstrom et al., 2014). Analogously to IL-7, IL-16 is

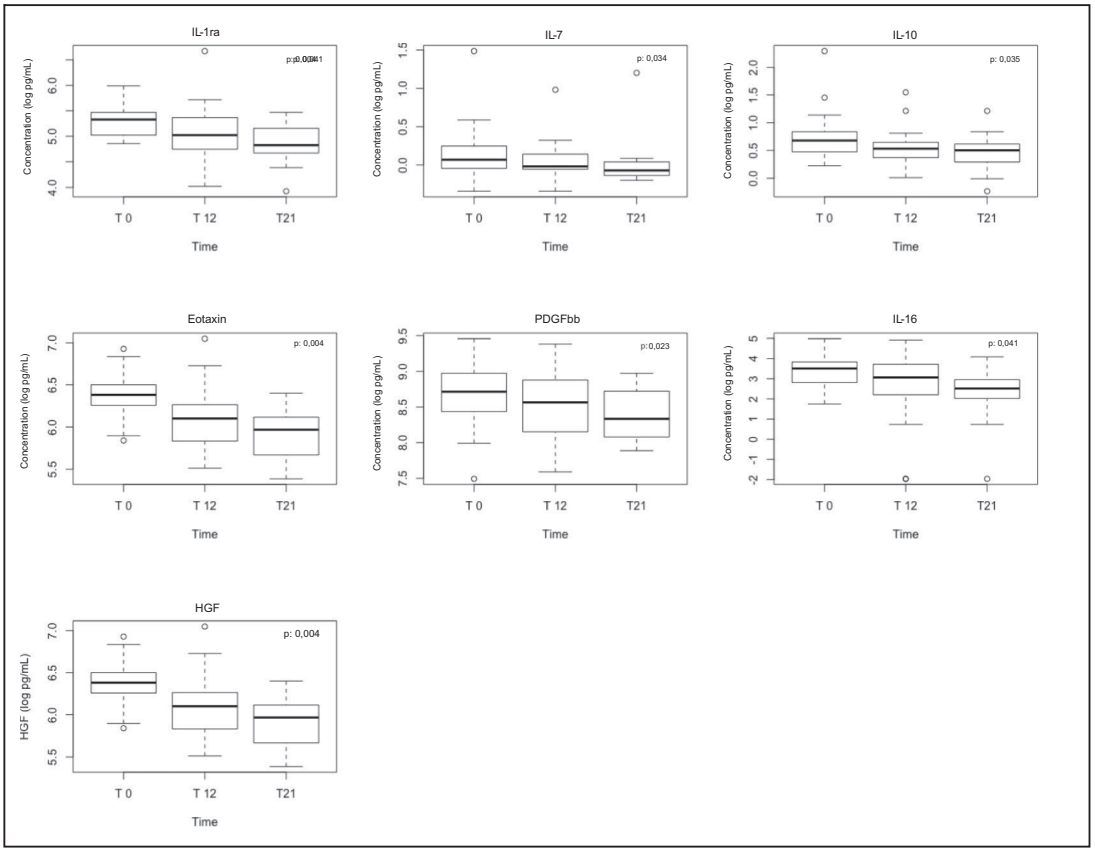

Fig. 1. Serum levels of the seven proteins that were significantly increased (Eotaxin) or decreased (IL-1ra, IL-7, IL-10, PDGFbb, IL-16 and HGF) during the 21 months of natalizumab treatment. The concentrations were measured before starting the treatment (T0), after 12 months (T12) and after 21 months (T21) and are provided as log pg/mL. Data are presented as median and interquartile ranges.

a chemoattractant for $CD4^+$ T lymphocytes, monocytes and eosinophils and is mainly produced by T lymphocytes (Cruikshank et al., 2000); further, $CD4^+$ T-cell infiltration in the CNS correlates with increased IL-16 levels in brain lesions in EAE (Skundric, 2015). The IL-16 concentration in sera from MS patients was increased compared with healthy controls, and the IL-16 serum levels were significantly reduced after two years of IFN-β1a treatment (Nischwitz et al., 2014). In accordance with these previous findings, in our study, 21 months of natalizumab treatment demonstrated the same ability to induce the reduction in IL-16 concentration.

Recent studies have described the anti-inflammatory action of CCL11 (Eotaxin) in a model of experimental autoimmune encephalitis, where the increased concentration of this chemokine was associated with milder disease phenotype, reduced antigenic specific response and a preferential activation of the Th2 immune response (Adzemovic et al., 2012; Tejera-Alhambra et al., 2015). Consistent with this finding, in our study a significant increase in the expression of Eotaxin was observed during the treatment, suggesting that natalizumab might limit the immune and inflammatory processes in MS patients.

Hepatocyte growth factor (HGF) is a pleiotropic protein that modulates immune cell functions and also plays an inhibitory role in the progression of chronic inflammation (Adams et al., 1994). HGF has been found to be increased in CNS diseases, including MS (Tsuboi et al., 2002), but some other studies have found decreased HGF CSF levels in patients with MS or unaltered levels of plasmatic HGF between MS patients and healthy controls(Benkhoucha et al., 2010; Muller et al., 2012). This discrepancy might be attributed to the fact that there is a compartmentalization of the HGF, produced by the lymphocytes present in the CSF, and not in the serum. In line with these last surveys, in our study a significant decrease of HGF concentration in serum of MS patients treated with natalizumab was observed and this finding may be associated with the beneficial effect of natalizumab.

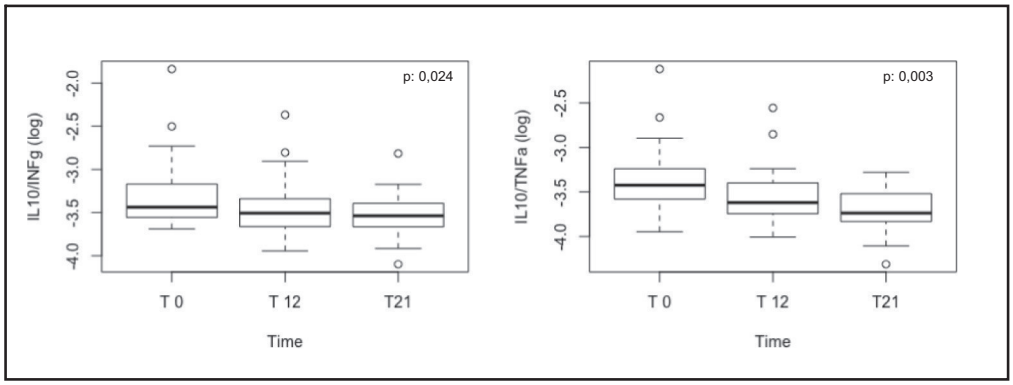

Fig. 2. Th2/Th1 ratios were significantly changed during the time of treatment. Comparative Th2/Th1 ratios considering anti-inflammatory IL-10 cytokine and pro-inflammatory cytokine IFN-γ (A) or TNF-α (B). Box and whiskers plots showing median and interquartile ranges are presented.

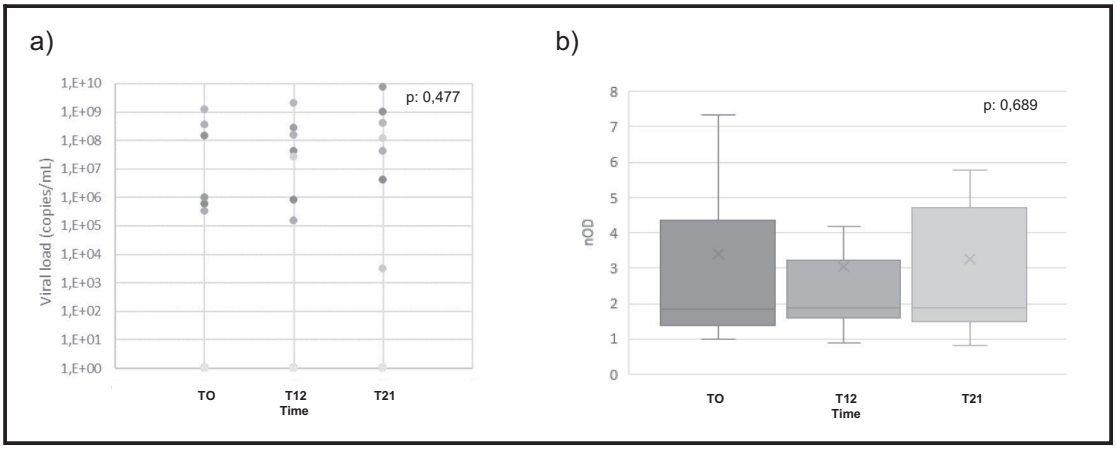

Fig. 3. JCPyV viruria (a) and seroprevalence (b) at T0, T12 and T21. (a) JCPyV viral load in the urine is expressed as viral copies/mL, and data are provided as single measurement and median. (b) JCPyV seroprevalence is expressed as nOD, and box and whiskers plots showing median and interquartile ranges are presented.

Finally, we showed that IL-1ra levels also decreased in the sera of patients during the natalizumab treatment. It has been previously stated that IL-1ra may have a downregulating potential in the disease course of MS, and elevated serum levels in active as well as in stable disease stages have been found compared to controls (Heesen et al., 2000). However, data regarding the role of IL1ra are very poor in literature and it is hard to define the significance of these results.

Besides the effect of natalizumab treatment on the concentration of the circulating cytokines/chemokines, we verified whether the monoclonal antibody affected the replication of JCPyV and/or the IgG response to the virus. However, we could not observe any significant change in the viruria of the patients during the course of treatment, neither in the rate of antibodies directed against JCPyV. This is contrast with some previous published data, that showed increase in JCPyV viruria, seropositivity rate and in the antibodies index in different cohorts of MS patients treated with natalizumab for at least 12 months (Delbue et al., 2015; Outteryck et al., 2014; Raffel et al., 2015). We attributed the discrepancy of these findings to the small sample size analyzed in our study.

5. Conclusions

Long-term treatment of natalizumab was associated with reduced levels of some pro-inflammatory cytokines/chemokines, such as IL-7, IL-16, and with increased levels of Eotaxin. These findings may be related to the beneficial effects associated with natalizumab. However, the treatment did not modify regulatory T cell function or cause a relevant switch in the Th2/Th1 balance, suggesting that natalizumab has marginal impact on the systemic immunity.

Funding

This work was supported by an Italian Minister of the University Grant (PRIN 2010–2011, protocol number 2010PHT9NF 003) to Pasquale Ferrante.

Conflicts of interest

The authors declare that they have no conflicts of interest.

References

Adams, D.H., Harvath, L., Bottaro, D.P., Interrante, R., Catalano, G., Tanaka, Y., et al., 1994. Hepatocyte growth factor and macrophage inflammatory protein 1 beta: structurally distinct cytokines that induce rapid cytoskeletal changes and subset-preferential migration in T cells. Proc. Natl. Acad. Sci. U. S. A. 91, 7144–7148.
Adzemovic, M.Z., Ockinger, J., Zeitelhofer, M., Hochmeister, S., Beyeen, A.D., Paulson, A., et al., 2012. Expression of Ccl11 associates with immune response modulation and protection against neuroinflammation in rats. PLoS One 7, e39794.
Baggiolini, M., 1998. Chemokines and leukocyte traffic. Nature 392, 565–568.
Benkhoucha, M., Santiago-Raber, M.L., Schneiter, G., Chofflon, M., Funakoshi, H., Nakamura, T., et al., 2010. Hepatocyte growth factor inhibits CNS autoimmunity by inducing tolerogenic dendritic cells and CD25 + Foxp3 + regulatory T cells. Proc. Natl. Acad. Sci. U. S. A. 107, 6424–6429.
Campello, C., Comar, M., D'Agaro, P., Minicozzi, A., Rodella, L., Poli, A., 2011. A molecular case-control study of the Merkel cell polyomavirus in colon cancer. J. Med. Virol. 83, 721–724.
Castellazzi, M., Delbue, S., Elia, F., Gastaldi, M., Franciotta, D., Rizzo, R., et al., 2015. Epstein-Barr virus specific antibody response in multiple sclerosis patients during 21 months of natalizumab treatment. Dis. Markers 2015, 901312.
Chou, Y.K., Bourdette, D.N., Barnes, D., Finn, T.P., Murray, S., Unsicker, L., et al., 1999. IL-7 enhances Ag-specific human T cell response by increasing expression of IL-2R alpha and gamma chains. J. Neuroimmunol. 96, 101–111.
Cruikshank, W.W., Kornfeld, H., Center, D.M., 2000. Interleukin-16. J. Leukoc. Biol. 67, 757–766.
Delbue, S., Sotgiu, G., Fumagalli, D., Valli, M., Borghi, E., Mancuso, R., et al., 2005. A case of a progressive multifocal leukoencephalopathy patient with four different JC virus transcriptional control region rearrangements in cerebrospinal fluid, blood, serum, and urine. J. Neuro-Oncol. 11, 51–57.
Delbue, S., Elia, F., Carloni, C., Pecchenini, V., Franciotta, D., Gastaldi, M., et al., 2015. JC virus urinary excretion and seroprevalence in natalizumab-treated multiple sclerosis patients. J. Neuro-Oncol. 21, 645–652.
Elia, F., Villani, S., Ambrogi, F., Signorini, L., Dallari, S., Binda, S., et al., 2016. JC virus infection is acquired very early in life: evidence from a longitudinal serological study. J. Neuro-Oncol.
Heesen, C., Sieverding, F., Buhmann, C., Gbadamosi, J., 2000. IL-1ra serum levels in disease stages of MS—a marker for progression? Acta Neurol. Scand. 101, 95–97.
Imitola, J., Chitnis, T., Khoury, S.J., 2005. Cytokines in multiple sclerosis: from bench to bedside. Pharmacol. Ther. 106, 163–177.
Jain, P., Coisne, C., Enzmann, G., Rottapel, R., Engelhardt, B., 2010. Alpha4beta1 integrin mediates the recruitment of immature dendritic cells across the blood-brain barrier during experimental autoimmune encephalomyelitis. J. Immunol. 184, 7196–7206.
Khademi, M., Stol, D., Olsson, T., Wallstrom, E., 2008. Induction of systemic TNFalpha in natalizumab-treated multiple sclerosis. Eur. J. Neurol. 15, 309–312.
Khademi, M., Bornsen, L., Rafatnia, F., Andersson, M., Brundin, L., Piehl, F., et al., 2009. The effects of natalizumab on inflammatory mediators in multiple sclerosis: prospects for treatment-sensitive biomarkers. Eur. J. Neurol. 16, 528–536.
Kivisakk, P., Healy, B.C., Viglietta, V., Quintana, F.J., Hootstein, M.A., Weiner, H.L., et al., 2009. Natalizumab treatment is associated with peripheral sequestration of proinflammatory T cells. Neurology 72, 1922–1930.
Kumar, V., Abbas, A., Fausto, N., 2005. Robbins and Cotran. Pathologic Basis of Disease, 7th edition. (Unit 1).
Kummer, C., Ginsberg, M.H., 2006. New approaches to blockade of alpha4-integrins, proven therapeutic targets in chronic inflammation. Biochem. Pharmacol. 72, 1460–1468.
Libbey, J.E., Fujinami, R.S., 2010. Potential triggers of MS. Results Probl. Cell Differ. 51, 21–42.
Lundstrom, W., Hermanrud, C., Sjostrand, M., Brauner, S., Wahren-Herlenius, M., Olsson, T., et al., 2014. Interferon beta treatment of multiple sclerosis increases serum interleukin-7. Mult. Scler. 20, 1727–1736.
Mellergard, J., Edstrom, M., Vrethem, M., Ernerudh, J., Dahle, C., 2010. Natalizumab treatment in multiple sclerosis: marked decline of chemokines and cytokines in cerebrospinal fluid. Mult. Scler. 16, 208–217.
Miller, A., Glass-Marmor, L., Abraham, M., Grossman, I., Shapiro, S., Galboiz, Y., 2004. Bio-markers of disease activity and response to therapy in multiple sclerosis. Clin. Neurol. Neurosurg. 106, 249–254.
Muller, A.M., Jun, E., Conlon, H., Sadiq, S.A., 2012. Cerebrospinal hepatocyte growth factor levels correlate negatively with disease activity in multiple sclerosis. J.

Neuroimmunol. 251, 80–86.
Nischwitz, S., Faber, H., Samann, P.G., Domingues, H.S., Krishnamoorthy, G., Knop, M., et al., 2014. Interferon beta-1a reduces increased interleukin-16 levels in multiple sclerosis patients. Acta Neurol. Scand. 130, 46–52.
Outteryck, O., Zephir, H., Salleron, J., Ongagna, J.C., Etxeberria, A., Collongues, N., et al., 2014. JC-virus seroconversion in multiple sclerosis patients receiving natalizumab. Mult. Scler. 20, 822–829.
Polman, C.H., O'Connor, P.W., Havrdova, E., Hutchinson, M., Kappos, L., Miller, D.H., et al., 2006. A randomized, placebo-controlled trial of natalizumab for relapsing multiple sclerosis. N. Engl. J. Med. 354, 899–910.
Raffel, J., Gafson, A.R., Malik, O., Nicholas, R., 2015. Anti-JC virus antibody titres increase over time with natalizumab treatment. Mult. Scler. 21, 1833–1838.
Ramos-Cejudo, J., Oreja-Guevara, C., Stark Aroeira, L., Rodriguez de Antonio, L., Chamorro, B., Diez-Tejedor, E., 2011. Treatment with natalizumab in relapsing-remitting multiple sclerosis patients induces changes in inflammatory mechanism. J. Clin. Immunol. 31, 623–631.
Rose, D.M., Han, J., Ginsberg, M.H., 2002. Alpha4 integrins and the immune response. Immunol. Rev. 186, 118–124.
Sawcer, S., Hellenthal, G., Pirinen, M., Spencer, C.C., Patsopoulos, N.A., Moutsianas, L., et al., 2011. Genetic risk and a primary role for cell-mediated immune mechanisms in multiple sclerosis. Nature 476, 214–219.
Sharief, M.K., Hentges, R., 1991. Association between tumor necrosis factor-alpha and disease progression in patients with multiple sclerosis. N. Engl. J. Med. 325, 467–472.
Skundric, D.S., 2015. Chemotactic signaling and beyond: link between interleukin-16 and axonal degeneration in multiple sclerosis. Neural Regen. Res. 10, 1761–1763.
Steinman, L., Martin, R., Bernard, C., Conlon, P., Oksenberg, J.R., 2002. Multiple sclerosis: deeper understanding of its pathogenesis reveals new targets for therapy. Annu. Rev. Neurosci. 25, 491–505.
Stuve, O., Bennett, J.L., 2007. Pharmacological properties, toxicology and scientific rationale for the use of natalizumab (Tysabri) in inflammatory diseases. CNS Drug Rev. 13, 79–95.
Tejera-Alhambra, M., Casrouge, A., de Andres, C., Seyfferth, A., Ramos-Medina, R., Alonso, B., et al., 2015. Plasma biomarkers discriminate clinical forms of multiple sclerosis. PLoS One 10, e0128952.
Tsuboi, Y., Kakimoto, K., Akatsu, H., Daikuhara, Y., Yamada, T., 2002. Hepatocyte growth factor in cerebrospinal fluid in neurologic disease. Acta Neurol. Scand. 106, 99–103.
Yednock, T.A., Cannon, C., Fritz, L.C., Sanchez-Madrid, F., Steinman, L., Karin, N., 1992. Prevention of experimental autoimmune encephalomyelitis by antibodies against alpha 4 beta 1 integrin. Nature 356, 63–66.

Research Article

For reprint orders, please contact: reprints@futuremedicine.com

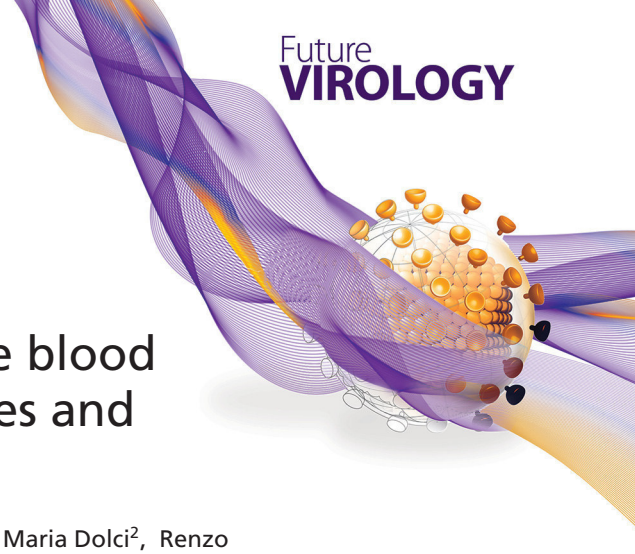

Merkel cell polyomavirus DNA in the blood of patients with neurological diseases and healthy controls

Lucia Signorini[‡,1], Sonia Villani[‡,2], Rosalia Ticozzi[2], Federico Ambrogi[3], Maria Dolci[2], Renzo Boldorini[4], Marco Ciotti[5], Pasquale Ferrante[2] & Serena Delbue[*,2]

[1]Department of Medicine & Surgery, Via Cadore, 48, University of Milano Bicocca, 20900 Monza, Italy

[2]Department of Biomedical, Surgical & Dental Sciences, Via Pascal, 36, University of Milano, 20133 Milano, Italy

[3]Department of Clinical Sciences & Community Health, Medical Statistics, Biometry and Bioinformatics, University of Milan, 20133 Milan, Italy

[4]Unit of Pathology, Department of Health Sciences, University of Eastern Piedmont Novara, Corso Giuseppe Mazzini, 18, 28100 Novara, Italy

[5]Laboratory of Molecular Virology, Polyclinic Tor Vergata Foundation, 00173 Rome, Italy

* Author for correspondence: Tel.: +39 025 031 5070; Fax: +39 025 031 5093; serena.delbue@unimi.it

‡ Authors contributed equally

Aim: Merkel cell polyomavirus (MCPyV) is the etiological agent of Merkel cell carcinoma. Its genome has been detected in anatomic districts from healthy and ill subjects. Data regarding the MCPyV DNAemia in neurological patients are lacking. **Materials & methods:** Blood was obtained from 129 neurological patients and 181 controls (HIV positive or negative). Real-time polymerase chain reaction (Q-PCR) was conducted to quantify MCPyV loads in blood specimens. **Results:** MCPyV DNA was detected in 17.1% of cases and 11.0% of controls in <1% of cells. No association between MCPyV DNA presence and HIV status was observed. **Conclusion:** Blood cells may be a reservoir for MCPyV. The presence of MCPyV genome in blood of healthy subjects might be relevant for transfusion medicine.

First draft submitted: 21 June 2017; Accepted for publication: 1 September 2017; Published online: 27 November 2017

Keywords: blood • Merkel cell polyomavirus • neurological diseases

Merkel cell polyomavirus (MCPyV) was first identified in 2008 in Merkel cell carcinoma (MCC), a rare but aggressive neuroendocrine skin tumor with approximately 80% of cases positive for MCPyV genome [1]. MCPyV has a circular, double-stranded DNA genome of 5387 bp with a genomic organization largely similar to other polyomaviruses. The genome is composed of a noncoding control region, containing the bidirectional origin of replication, separating the early functional and the late structural regions. As for the other members of the *Polymaviridae* family, the primary infection is thought to occur during early childhood, which is generally asymptomatic and is followed by the latent establishment of the virus in the host [2]. Serological tests revealed that MCPyV seroprevalence in the general population ranges from 46 to 88% [2–4]. The epithelial MCPyV tropism supports the theory that the virus could be part of the normal microflora of the human skin [5]. Although MCPyV DNA has been mainly detected in skin tissues, some scientific reports showed the presence of viral sequences also in normal tissues from other anatomic districts including the respiratory tract (nasal swabs and saliva), the oral cavity (tonsil biopsies), the lymphoid tissue, the GI tract (gallbladder, appendix, liver, lung and intestinal tissues), the genital tract (vulva and penis) and the urinary tract, with a relatively low viral load compared with that of the skin samples [1,3–4,6–16]. Recently, at least three independent metagenomics analyses, conducted on several samples, identified sequences belonging to MCPyV in blood products eligible for transfusion and in blood from patients affected with different diseases [17–20]. This finding supports the hypothesis that blood cells might be a reservoir for MCPyV [21], also suggesting other possible viral tropisms and different alternative routes of transmission. However, data regarding the MCPyV DNAemia in neurological patients are still lacking.

Table 1. Sequences of primers and probes used for the quantitative real-time PCR assays to detect and quantify Merkel cell polyomavirus genome and the β-globin gene.

Target	Region	Primer/probe	Position	Sequence
Chromosome 11	β-globin	β-globin-354F	62190–62209†	5′-GTGCACCTGACTCCTGAGGAG-3′
		β-globin-455R	62271–62290†	5′- CCTTGATACCAACCTGCCCAG-3′
		β-globin-402T Probe	62238–62263†	5′JOE-AAGGTGAACGTGGATGAAGTTGGTGG-TAMRA 3′
MCPyV	*VP1* gene	MCPyV Forward	4053–4072‡	5′-TGCCTCCCACATCTGCAAT-3′
		MCPyV Reverse	4090–4112‡	5′-GTGTCTCTGCCAATGCTAAATGA-3′
		MCPyV Probe	4074–4089‡	5′-FAM-TGTCACAGGTAATATC-MGB-3′

†The nucleotide positions are referred to strain U01317.
‡The nucleotide positions are referred to strain EU375803.
MCPyV: Merkel cell polyomavirus.
Data taken from [6,23].

Materials & methods

Subject enrollment & sample collection

Peripheral blood was collected from 129 patients affected with different neurological diseases, either HIV positive or negative, who have been divided into two groups. The first group of HIV negative patients included 71 patients affected with relapsing-remitting multiple sclerosis (RR-MS), including 45 subjects undergoing natalizumab treatment and 26 patients undergoing IFN-β treatment. The second group of HIV positive patients included 41 patients affected with leukoencephalopathies, both JC virus related (progressive multifocal leukoencephalopathy [PML]) and JC virus negative leukoencephalopathies (not determined leukoencephalopathy [NDLE]), and 17 patients with other neurological diseases. The control group was composed of 181 subjects, including 99 HIV negative healthy controls (HC) and 82 HIV positive patients without any neurological signs (NND). Additionally, 16 paraffin-embedded tissues from MCC patients were obtained from the pathology archive of the Ospedale Maggiore della Carità, Novara, Italy, and included in the study as positive controls. After routine blood sample collection at the Neurologico Mondino Hospital and at the Policlinico San Matteo, Pavia, part of the samples was delivered to the Department of Biomedical, Surgical and Dental Sciences, Milan and stored at -80°C until use. This study was approved by the local Ethics Committee and all patients signed a free and informed consent form at the time of sample collection.

DNA extraction from blood & paraffin-embedded tumor tissues

Viral DNA was isolated from 0.2 ml of blood and from the paraffin-embedded tissues using the commercial kits QIAamp DNA Blood Mini Kit (Qiagen, Hilden, Germany) and Qiagen DNeasy FFPE Kit (Qiagen), respectively, in accordance with the manufacturer's instructions. The purity and quantity of DNA were assessed by spectrophotometric analysis according to the 260/280 nm ratio absorbance method.

Quantitative real-time PCR assay

Quantitative real-time PCR assay (Q-PCR) was performed using the Applied Biosystems 7500 Real-Time PCR System (Applied Biosystems, CA, USA) with specific primers and TaqMan probe technology targeting the Viral Protein 1 (VP1) sequence of the MCPyV, as previously described (Table 1) [6]. Q-PCR assay and thermal cycle conditions were performed in accordance with a previously published protocol, and the standard curves were constructed using a tenfold dilution series of a plasmid containing the *VP1* gene of MCPyV (dilution range: 10^8–10^0 copies/µl) [22]. The limit of detection was 10 copies/µl. To determine the percentage of infected cells, a concomitant Q-PCR assay targeting the β-globin gene was performed on the same samples. The β-globin gene was amplified using the primer set and the thermal cycles previously published [23], as reported in Table 1. Negative and positive controls were included in each run. Each sample, standard and control, was tested in duplicate. Results were analyzed by the absolute quantification method and the data were expressed as MCPyV copies per ml/mg of blood/tissue and reported as percentage of infected cells that was calculated as follows: ([viral copies/ml or mg]/[beta-globin copies/2/ml or mg])*100.

Table 2. Sequence of primers for the nested/semi-nested PCRs used for the amplification of two fragments of the LTAg and one fragment of the *VP1* genes.

Region	Outer/inner PCR	Primers	Position†	Sequence	Fragment length	Ref.
LTAg	Outer	LT3FE	571–590	5′-TTGTCTCGCCAGCATTGTAG-3′	280 bp	[1]
		LT3RE	860–879	5′-ATATAGGGGCCTCGTCAACC-3′		
	Inner	LT3FI	741–760	5′-ATCTGCACCTTTTCTAGACTCC-3′	151 bp	
		LT3RE	860–879	5′-ATATAGGGGCCTCGTCAACC-3′		
LTAg	Outer	Tag FwE	1716–1736	5′-GCCTGTGAATTAGGATGTATTTT-3′	477 bp	[12]
		Tag RevE	2210–2198	5′-TGGAAATGACCAGGACAGAAATG-3′		
	Inner	Tag FwI	2010–2033	5′-GCCCATTATCTAGACTTTGCAAA-3′	183 bp	
		Tag RevI	2192–2173	5′-TAGCCAAAAGGAGGTTAGA-3′		
VP1	Outer	VP1 FwE	3174–3194	5′-GGCTTTCTTTTTGAGAGGCCT-3′	440 bp	[12]
		VP1 RevE	3613–3592	5′-TCCTTTGCATAGAGGGCCCACT -3′		
	Inner	VP1 FwI	3276–3297	5′-TTGGGTAAACAGTTTTCTCCTG-3′	240 bp	
		VP1 RevI	3515–3493	5′-AGTAACATTAAAATATCTAGGCA-3′		

†The nucleotide positions are referred to strain EU375803.

Molecular characterization

The strains amplified from the MCC paraffin-embedded tissues were subjected to three different PCRs, for the amplification of two fragments belonging to the LTAg and one to the VP1 regions. The first set of primers, the outer TAg FwE and TAg RvE [12], and the inner TAg FwI and Tag RvI, amplify a 183-bp fragment. The second MCPyV LTAg semi-nested PCR was conducted using the outer primer set LT3FE and LT3RE [1], and the semi-inner pair set, LT3FI and LT3RE, which amplify a fragment of 151 bp. The analysis of the VP1 region was done using a primer set previously described [12], VP1 FwE and VP1 RevE (outer) and VP1 FwI and VP1 RevI (inner), which amplify a 240-bp fragment (Table 2). Each PCR fragment was sent to an external facility for the direct sequencing of both viral strands (Eurofins Genomics, Vimodrone, Italy). Sequence homology searches were performed using a nucleotide BLAST search, database search set 'others', from NCBI site , and, as reference sequence, the MCPyV strain MCC350 (GenBank accession number EU375803) [24].

Statistical analysis

The χ^2 test and the Fisher exact test were used to evaluate the significance of the association between MCPyV infection and neurological disease, and specifically MCPyV infection and MS. Logistic regression was used to evaluate the association between infection, neurological disorders and HIV positivity. $p < 0.05$ was considered significant.

Results

Patient demographic characteristics

Overall, 129 patients and 181 controls were included in this study. Demographic of patients and control subjects is summarized in Table 3.

Merkel cell polyomavirus prevalence in blood samples

MCPyV prevalence and the related mean viral load in the different groups of study are summarized in Table 4. Prevalence in the case and control groups was 17.1% (22/129) and 11.0% (20/181), respectively. Taking into account the subgroups of patients and controls, among the HIV negative neurological patients, overall positivity was 12 out of 71 (16.9%), distributed as follows: 11 out of 45 (24.4%) subjects resulted positive in the RR-MS group of patients undergoing natalizumab treatment, whereas 1 out of 26 (3.8%) subjects was MCPyV positive in the RR-MS group of patients undergoing IFN-β therapy. Regarding the HIV positive group of study, an overall positivity of 10 out of 58 (1.7%) subjects was reported, distributed as follows: 2 out of 17 (11.8%) subjects resulted positive in the PML group, 4 out of 24 (16.7%), and 4 out of 17 (23.5%) subjects were MCPyV DNA positive in the NDLE, and other neurological diseases groups, respectively. Concerning the control groups, the positive results were distributed as follows: 14 out of 82 (17.1%) among the HIV positive NND patients, and 6 out of 99 (6.1%) among the HIV negative subjects.

Table 3. Demographic and clinical data of the enrolled patients and controls.

Groups	n	Female (%)	Mean age ± range	HIV status
Neurological patients				
Relapsing-remitting multiple sclerosis (natalizumab treated)	45	34 (26.4)	40.2 ± 10.5	-
IFN-β treated	26	17 (13.2)	41.9 ± 11.0	-
Progressive multifocal leukoencephalopathy	17	5 (3.9)	41.0 ± 10.2	+
Nondetermined leukoencephalopathy	24	9 (6.9)	44.5 ± 7.5	+
Other neurological diseases	17	6 (4.7)	46.5 ± 8.6	+
Total	129	71 (55.0)	42.3 ± 13.0	
Controls				
Healthy controls	99	53 (53.5)	59.0 ± 19.3	-
Non-neurological diseases HIV+	82	24 (29.3)	44.5 ± 7.5	+
Total	181	77 (42.5)	51.8 ± 12	

Table 4. Prevalence and mean viral load of Merkel cell polyomavirus in the blood of the enrolled patients and controls.

Patients	Treatment	MCPyV+/Tot (%)	Mean viral load copies/ml (range)	Infected cells
Neurological patients				
	Natalizumab treated	11/45 (24.4)†‡	1.5×10^5 (1.2×10^3–1.4×10^6)	0.005
Relapsing remitting MS				
	IFN-β treated	1/26 (3.8)†‡	1.3×10^5	0.003
Progressive multifocal leukoencephalopathy		2/17 (11.8)	6.3×10^3 (1.8×10^2–1.2×10^4)	0.041
Nondetermined leukoencephalopathy		4/24 (16.7)	8.2×10^5 (7.4×10–2.6×10^6)	0.982
Other neurological diseases		4/17 (23.5)	1.3×10^4 (4.4×10–5.0×10^4)	0.064
Total		22/129 (17.1)	2.2×10^5 (7.4×10–2.6×10^6)	0.219
Controls				
Healthy controls		6/99 (6.1)‡	1.5×10^5 (1.2×10^3–1.4×10^6)	0.04
Non-neurological diseases HIV+		14/82 (17.1)	2.3×10^4 (4.9×10–1.6×10^6)	0.14
Total		20/181 (11)	8.6×10^4 (4.9×10–1.6×10^6)	0.09

†$p < 0.05$.
‡$p < 0.005$.
MS: Multiple sclerosis.

Considering HIV negative patients and comparing MS patients with HC, the percentages of infections were 16.9% (12/71) and 6.1% (6/99), respectively, with an odds ratio of 0.30 (Fisher exact test, $p = 0.02$).

The association between HIV infection and virus positivity was not statistically significant ($p = 0.09$) even after adjusting for the presence of neurological disorders ($p = 0.09$).

There was no evidence of differences in the viral load distributions between cases and controls, and the mean percentage of infected cell values in the blood samples of each group resulted lower than 1% without statistically significant differences between the groups, according to the type of pathology.

Merkel cell polyomavirus prevalence in paraffin-embedded tissues

The prevalence in the positive control group of paraffin-embedded MCC tissue samples revealed MCPyV positivity of 10 out of 16 (62.5%; $p < 0.0001$; compared with both the case and control groups). Furthermore, viral load analysis revealed a mean viral load of 5.3×10^3 copies/mg (range: 2.6×10^0–4.1×10^4 copies/mg) with a mean

percentage of infected cells of 57.5%. The amplified and sequenced strains were all defined as MC3350 (data not shown).

Discussion

In the present study, we detected MCPyV DNA in the blood of both neurological patients and controls, without significant differences in the frequency. However, a significant higher frequency was observed in RR-MS patients compared with HC, and among the MS patients, MCPyV was significantly more present in RR-MS patients treated with natalizumab than in RR-MS patients undergoing IFN-β treatment.

To date, no other reports have been published with regard to the presence of MCPyV genome in MS patients. Here, we showed that 24.4% of the RR-MS patients treated with natalizumab had MCPyV in the blood cells. This result is comparable with the presence of the human polyomavirus JC (JCPyV), whose viremia detection varies between 0 and 34.7% in different natalizumab treated cohort of MS patients [2,25–33].

The results of our study indicated an almost null presence of MCPyV DNA in the blood of the RR-MS patients treated with IFN-β, suggesting that IFN-β could have an antiviral effect on MCPyV, as already observed for JCPyV [34–36]. To this regard, it has been shown that Type I IFN-β is able to reduce the large T-antigen expression and this may explain its antiviral effect [37].

Although this is the first report concerning the MCPyV DNAemia in neurological disorders, some other pathologies have been previously studied and MCPyV has been shown to be present in the blood cells of 9.9% of the studied patients with respiratory, cardiovascular or other diseases, such as hypertension, cancer, depression, dementia and rheumatic disease [38]. Moreover, based on the frequent association between human polyomaviruses reactivation after an immune impairment and the development of pathologies, more attention has been given to the possible role of MCPyV in the diseases of the immunocompromised host. A recent study showed the presence of MCPyV DNA in the blood of 17 out of 167 prospectively recruited adult patients undergoing kidney transplantation, but with a very low mean viral load [39]. Furthermore, in a study conducted in the USA in 2012, MCPyV genome was found in the blood of 26% patients with uncharacterized chronic lymphocytic leukemia [40]. To this regard, some reports showed that patients with MCC have an increased risk of developing leukemia and/or lymphoma, proposing a possible MCPyV role in the pathogenesis of those diseases [40–42]. This hypothesis was supported by a recent report by Song and Gyarmati, who were able to amplify the entire genomic sequence of MCPyV in the blood of a patient with acute myeloid leukemia [43].

Interestingly, our results did not indicate any association among the presence of MCPyV DNA in the blood and the HIV infection status of the enrolled patients and controls. Accordingly, Dang and colleagues did not find any associations between MCPyV detection in blood and immunosuppression due to HIV [44]. This is in contrast with the observation that MCC occurs more frequently in HIV positive patients than in immunocompetent hosts [45–49]. Fukumoto and colleagues also reported a significantly higher prevalence of MCPyV DNA in the sera from HIV positive patients than from HIV negative patients, affected with different diseases [50]. However, they observed no differences in the MCPyV load, as we did. On the other hand, and supporting our results, a recent paper reported no differences in the prevalence rate of MCPyV-DNA in the blood of HIV/AIDS, non-AIDS HIV infected and uninfected controls (from 14 to 17%) [51].

Even if the mean viral load was more than 100-fold higher in NDLE patients than in PML patients in our study as expected, the presence of MCPyV genome in all groups of subjects was limited to less than 1% of blood cells, while the virus was shown to infect at least 50% of MCC cells. This finding supports the hypothesis that the blood might represent a reservoir for the virus in its latent state.

Additionally, it is worthy to underline the importance of the presence of the MCPyV genome in the blood of HC. To this regard, Mustafa and colleagues conducted the whole-genome sequencing analysis of 8240 blood DNA samples from healthy subjects without any ascertained infectious disease. The analysis showed the presence of 94 different viruses, including sequences from human DNA viruses, proviruses and RNA viruses in 42% of the study participants, among which 49 individuals resulted positive for MCPyV sequences [18,19]. These data confirmed previously results obtained in another scientific work conducted on 60 buffy coats, obtained from healthy blood donors recruited in Italy. The results indicated that 13 out of 60 samples were positive for MCPyV LTAg sequences with low viral DNA load [19]. However, to give a complete scenario, it is also important to note that Dworkin and colleagues did not detect MCPyV genome in any of the tested normal blood samples [52].

Conclusion & future perspective

It is clear that MCPyV is able to remain in a latent state, even at very low concentration in the blood cells of the host. This is an important issue considering MCPyV can reactivate and is the cause of a severe disease such as MCC. Additionally, and not less important, the presence of viruses in blood products can be relevant for transfusion medicine and it would be worthy to discuss about the opportunity and/or the urgency to add MCPyV to the list of viruses that could be potentially transmitted via blood products [18].

Summary points

- Merkel cell polyomavirus (MCPyV) was first identified in the Merkel cell carcinoma cells.
- MCPyV is a ubiquitous virus, which establishes lifelong latency and can reactivate in immunosuppressed individuals.
- MCPyV genome has been found in the blood cells from healthy subjects and patients affected with different diseases. However, nothing is known about the MCPyV DNA presence in the blood from patients affected with neurological diseases.

Methods

- Peripheral blood was collected from 129 patients with neurological diseases: 71 multiple sclerosis (MS) patients (treated with natalizumab or IFN-β), 41 HIV positive patients with leukoencephalopathies and 17 patients with other neurological diseases. Control group was composed by 181 subjects: 99 healthy subjects and 82 HIV positive patients without any neurological symptoms.
- MCPyV DNAemia was evaluated by means of specific real time polymerase chain reaction (Q-PCR).
- The chi square test and the Fisher exact test were used to evaluate the significance of the association between MCPyV infection and neurological disease, and MCPyV infection and MS. Logistic regression was used to evaluate the association between infection, neurological disorders and HIV positivity.

Results

- MCPyV DNA was detected in the blood of 17.1% of cases and 11.0% of controls.
- MCPyV DNA was detected in very low percentages of cells (<1%) both in the cases and in the controls.
- Higher frequency of MCPyV DNA was found in the blood from relapsing-remitting MS (RR-MS) patients, treated with natalizumab compared with RR-MS patients treated with IFN-β and healthy controls.

Discussion

- This was the first report regarding the presence of MCPyV DNA in blood from patients with neurological diseases.
- The prevalence of MCPyV DNAemia was similar in cases and controls, and HIV infection was not associated with the presence of MCPyV genome.
- The higher presence of MCPyV genome in RR-MS patients treated with natalizumab than in RR-MS patients treated with IFN-β could be due to a strong antiviral effect of the IFN-β.
- Blood cells could be a reservoir for MCPyV, which may be able to reactivate during immunosuppression of the host.
- The presence of MCPyV DNA in blood from healthy controls can be relevant for transfusion medicine.

Acknowledgements

The authors wish to thank all the personnel of the Laboratory of Translational Medicine, University of Milan, Italy.

Financial & competing interests disclosure

This research was supported by the PRIN 2010–2011 grant from the Italian Minister of University to P Ferrante. The authors have no other relevant affiliations or financial involvement with any organization or entity with a financial interest in or financial conflict with the subject matter or materials discussed in the manuscript.

No writing assistance was utilized in the production of this manuscript.

Ethical conduct of research

This study was approved by the local Ethics Committee (protocol 101MS326 – Fondazione Mondino) and all patients signed a free and informed consent form at the time of sample collection.

References

Papers of special note have been highlighted as: • of interest; •• of considerable interest

1. Feng H, Shuda M, Chang Y, Moore PS. Clonal integration of a polyomavirus in human Merkel cell carcinoma. *Science* 319(5866), 1096–1100 (2008).

•• **First paper to describe the finding of an integrated human polyomavirus in human tumor cells and its importance is foremost.**

2. Chen T, Hedman L, Mattila PS *et al.* Serological evidence of Merkel cell polyomavirus primary infections in childhood. *J. Clin. Virol.* 50(2), 125–129 (2011).
3. Schowalter RM, Pastrana DV, Pumphrey KA, Moyer AL, Buck CB. Merkel cell polyomavirus and two previously unknown polyomaviruses are chronically shed from human skin. *Cell Host Microbe* 7(6), 509–515 (2010).
4. Loyo M, Guerrero-Preston R, Brait M *et al.* Quantitative detection of Merkel cell virus in human tissues and possible mode of transmission. *Int. J. Cancer* 126(12), 2991–2996 (2010).
5. Spurgeon ME, Lambert PF. Merkel cell polyomavirus: a newly discovered human virus with oncogenic potential. *Virology* 435(1), 118–130 (2013).
6. Goh S, Lindau C, Tiveljung-Lindell A, Allander T. Merkel cell polyomavirus in respiratory tract secretions. *Emerg. Infect. Dis.* 15(3), 489–491 (2009).
7. Laude HC, Jonchere B, Maubec E *et al.* Distinct Merkel cell polyomavirus molecular features in tumor and nontumor specimens from patients with Merkel cell carcinoma. *PLoS Pathog.* 6(8), e1001076 (2010).
8. Sharp CP, Norja P, Anthony I, Bell JE, Simmonds P. Reactivation and mutation of newly discovered WU, KI and Merkel cell carcinoma polyomaviruses in immunosuppressed individuals. *J. Infect. Dis.* 199(3), 398–404 (2009).
9. Foulongne V, Dereure O, Kluger N, Moles JP, Guillot B, Segondy M. Merkel cell polyomavirus DNA detection in lesional and nonlesional skin from patients with Merkel cell carcinoma or other skin diseases. *Br. J. Dermatol.* 162(1), 59–63 (2010).
10. Foulongne V, Kluger N, Dereure O *et al.* Merkel cell polyomavirus in cutaneous swabs. *Emerg. Infect. Dis.* 16(4), 685–687 (2010).
11. Wieland U, Mauch C, Kreuter A, Krieg T, Pfister H. Merkel cell polyomavirus DNA in persons without Merkel cell carcinoma. *Emerg. Infect. Dis.* 15(9), 1496–1498 (2009).
12. Bofill-Mas S, Rodriguez-Manzano J, Calgua B, Carratala A, Girones R. Newly described human polyomaviruses Merkel cell, KI and WU are present in urban sewage and may represent potential environmental contaminants. *Virol. J.* 7, 141 (2010).
13. Kantola K, Sadeghi M, Lahtinen A *et al.* Merkel cell polyomavirus DNA in tumor-free tonsillar tissues and upper respiratory tract samples: implications for respiratory transmission and latency. *J. Clin. Virol.* 45(4), 292–295 (2009).
14. Campello C, Comar M, D'agaro P, Minicozzi A, Rodella L, Poli A. A molecular case–control study of the Merkel cell polyomavirus in colon cancer. *J. Med. Virol.* 83(4), 721–724 (2011).
15. Babakir-Mina M, Ciccozzi M, Lo Presti A, Greco F, Perno CF, Ciotti M. Identification of Merkel cell polyomavirus in the lower respiratory tract of Italian patients. *J. Med. Virol.* 82(3), 505–509 (2010).
16. Tolstov YL, Pastrana DV, Feng H *et al.* Human Merkel cell polyomavirus infection II. MCV is a common human infection that can be detected by conformational capsid epitope immunoassays. *Int. J. Cancer* 125(6), 1250–1256 (2009).
17. Lau P, Cordey S, Brito F *et al.* Metagenomics analysis of red blood cell and fresh-frozen plasma units. *Transfusion* 57(7), 1787–1800 (2017).
18. Moustafa A, Xie C, Kirkness E *et al.* The blood DNA virome in 8000 humans. *PLoS Pathog.* 13(3), e1006292 (2017).

•• **Metagenomics study on blood, revealing the presence of several viral genomes, probably asbystanders, in the blood cells of healthy subjects**

19. Pancaldi C, Corazzari V, Maniero S *et al.* Merkel cell polyomavirus DNA sequences in the buffy coats of healthy blood donors. *Blood* 117(26), 7099–7101 (2011).
20. Ngoi CN, Siqueira J, Li L *et al.* Corrigendum: the plasma virome of febrile adult Kenyans shows frequent parvovirus B19 infections and a novel arbovirus (Kadipiro virus). *J. Gen. Virol.* 98(3), 517 (2017).
21. Mertz KD, Junt T, Schmid M, Pfaltz M, Kempf W. Inflammatory monocytes are a reservoir for Merkel cell polyomavirus. *J. Invest. Dermatol.* 130(4), 1146–1151 (2010).
22. Signorini L, Belingheri M, Ambrogi F *et al.* High frequency of Merkel cell polyomavirus DNA in the urine of kidney transplant recipients and healthy controls. *J. Clin. Virol.* 61(4), 565–570 (2014).

• **New results about the high urinary excretion of Merkel cell polyomavirus in healthy and immunosuppressed patients, hypothesizing a new site of infection for Merkel cell polyomavirus.**

23. Lo YM, Tein MS, Lau TK *et al.* Quantitative analysis of fetal DNA in maternal plasma and serum: implications for noninvasive prenatal diagnosis. *Am. J. Hum. Genet.* 62(4), 768–775 (1998).
24. NIH. BLAST: Basic Local Alignment Search Tool.http://blast.ncbi.nlm.nih.gov/Blast.cgi
25. Berger JR, Houff SA, Gurwell J, Vega N, Miller CS, Danaher RJ. JC virus antibody status underestimates infection rates. *Ann. Neurol.* 74(1), 84–90 (2013).
26. Jilek S, Jaquiery E, Hirsch HH *et al.* Immune responses to JC virus in patients with multiple sclerosis treated with natalizumab: a cross-sectional and longitudinal study. *Lancet Neurol.* 9(3), 264–272 (2010).

27. Mancuso R, Saresella M, Hernis A *et al.* JC virus detection and JC virus-specific immunity in natalizumab-treated multiple sclerosis patients. *J. Transl. Med.* 10, 248 (2012).
28. Major EO, Frohman E, Douek D. JC viremia in natalizumab-treated patients with multiple sclerosis. *N. Engl. J. Med.* 368(23), 2240–2241 (2013).
29. Rinaldi L, Rinaldi F, Perini P *et al.* No evidence of JC virus reactivation in natalizumab treated multiple sclerosis patients: an 18 month follow-up study. *J. Neurol. Neurosurg. Psychiatry* 81(12), 1345–1350 (2010).
30. Rudick RA, O'connor PW, Polman CH *et al.* Assessment of JC virus DNA in blood and urine from natalizumab-treated patients. *Ann. Neurol.* 68(3), 304–310 (2010).
31. Sadiq SA, Puccio LM, Brydon EW. JCV detection in multiple sclerosis patients treated with natalizumab. *J. Neurol.* 257(6), 954–958 (2010).
32. Warnke C, Adams O, Hartung HP, Kieseier BC. Assessment of JC virus DNA in blood and urine from natalizumab-treated patients. *Ann. Neurol.* 69(1), 215–216 (2011).
33. Chen Y, Bord E, Tompkins T *et al.* Asymptomatic reactivation of JC virus in patients treated with natalizumab. *N. Engl. J. Med.* 361(11), 1067–1074 (2009).
34. Delbue S, Guerini FR, Mancuso R *et al.* JC virus viremia in interferon-beta-treated and untreated Italian multiple sclerosis patients and healthy controls. *J. Neurovirol.* 13(1), 73–77 (2007).
35. Hong J, Tejada-Simon MV, Rivera VM, Zang YC, Zhang JZ. Antiviral properties of interferon beta treatment in patients with multiple sclerosis. *Mult. Scler.* 8(3), 237–242 (2002).
36. Alvarez-Lafuente R, De Las Heras V, Bartolome M, Picazo JJ, Arroyo R. Beta-interferon treatment reduces human herpesvirus-6 viral load in multiple sclerosis relapses but not in remission. *Eur. Neurol.* 52(2), 87–91 (2004).
37. Willmes C, Adam C, Alb M *et al.* Type I and II IFNs inhibit Merkel cell carcinoma via modulation of the Merkel cell polyomavirus T antigens. *Cancer Res.* 72(8), 2120–2128 (2012).
38. Sadeghi M, Aronen M, Chen T *et al.* Merkel cell polyomavirus and trichodysplasia spinulosa-associated polyomavirus DNAs and antibodies in blood among the elderly. *BMC Infect. Dis.* 12, 383 (2012).
39. Bialasiewicz S, Rockett RJ, Barraclough KA *et al.* Detection of recently discovered human polyomaviruses in a longitudinal kidney transplant cohort. *Am. J. Transplant.* 16(9), 2734–2740 (2016).
40. Cimino PJ Jr, Bahler DW, Duncavage EJ. Detection of Merkel cell polyomavirus in chronic lymphocytic leukemia T cells. *Exp. Mol. Pathol.* 94(1), 40–44 (2013).
41. Koljonen V, Kukko H, Pukkala E *et al.* Chronic lymphocytic leukaemia patients have a high risk of Merkel cell polyomavirus DNA-positive Merkel cell carcinoma. *Br. J. Cancer* 101(8), 1444–1447 (2009).
42. Kaae J, Hansen AV, Biggar RJ *et al.* Merkel cell carcinoma: incidence, mortality and risk of other cancers. *J. Natl Cancer Inst.* 102(11), 793–801 (2010).
43. Song Y, Gyarmati P. Identification of Merkel cell polyomavirus from a patient with acute myeloid leukemia. *Genome Announc.* doi:10.1128/genomeA.01241–16 (2017) (Epub ahead of print).
44. Dang X, Bialasiewicz S, Nissen MD, Sloots TP, Koralnik IJ, Tan CS. Infrequent detection of KI, WU and MC polyomaviruses in immunosuppressed individuals with or without progressive multifocal leukoencephalopathy. *PLoS ONE* 6(3), e16736 (2011).
45. Becker JC, Kauczok CS, Ugurel S, Eib S, Brocker EB, Houben R. Merkel cell carcinoma: molecular pathogenesis, clinical features and therapy. *J. Dtsch Dermatol. Ges.* 6(9), 709–719 (2008).
46. Engels EA, Frisch M, Goedert JJ, Biggar RJ, Miller RW. Merkel cell carcinoma and HIV infection. *Lancet* 359(9305), 497–498 (2002).
47. Pulitzer MP, Amin BD, Busam KJ. Merkel cell carcinoma: review. *Adv. Anat. Pathol.* 16(3), 135–144 (2009).
48. Izikson L, Nornhold E, Iyer JG, Nghiem P, Zeitouni NC. Merkel cell carcinoma associated with HIV: review of 14 patients. *Aids* 25(1), 119–121 (2011).
49. Wieland U, Silling S, Scola N *et al.* Merkel cell polyomavirus infection in HIV-positive men. *Arch. Dermatol.* 147(4), 401–406 (2011).
50. Fukumoto H, Sato Y, Hasegawa H, Katano H. Frequent detection of Merkel cell polyomavirus DNA in sera of HIV-1-positive patients. *Virol. J.* 10, 84 (2013).
51. Vahabpour R, Nasimi M, Naderi N *et al.* Merkel cell polyomavirus IgG antibody levels are associated with progression to AIDS among HIV-infected individuals. *Arch. Virol.* 162(4), 963–969 (2017).
52. Dworkin AM, Tseng SY, Allain DC, Iwenofu OH, Peters SB, Toland AE. Merkel cell polyomavirus in cutaneous squamous cell carcinoma of immunocompetent individuals. *J. Invest. Dermatol.* 129(12), 2868–2874 (2009).

In press.

Characterization of an *in vitro* model to study the possible role of polyomavirus BK in prostate cancer

Running title: BK polyomavirus and prostate cancer

Sonia Villani[1*], Nicoletta Gagliano[2*], Patrizia Procacci[2], Patrizia Sartori[2], Manola Comar[3,4], Maurizio Provenzano[5], Evaldo Favi[6], Mariano Ferraresso[6], Pasquale Ferrante[1], Serena Delbue [1#]

[1]Department of Biomedical, Surgical and Dental Sciences, Università degli Studi di Milano, Italy

[2]Department of Biomedical Sciences for Health, Università degli Studi di Milano, Italy

[3]Institute for Maternal and Child Health - IRCCS "Burlo Garofolo," Trieste, Italy

[4]Department of Medical Sciences, University of Trieste, Trieste, Italy,

[5]Oncology Research Unit, Department of Urology and Division of Surgical Research, University and University Hospital of Zurich, CH-8091 Zurich, Switzerland

[6]Renal Transplantation Unit, Fondazione IRCCS Ca' Granda - Ospedale Maggiore Policlinico, Milan, Italy

***** S. Villani and N. Gagliano should be considered joint first author

Acknowledgement

The study was supported by the Italian Ministry of University – PRIN 2015 to Pasquale Ferrante; contract grant number 2015w729wh. We thank Dott. Vincenzo Conte for skilful technical assistance in the EM, and Miss. Rosalia Ticozzi for technical help. The authors declare that they have no actual or potential competing financial interests.

#Corresponding Author:

Serena Delbue, PhD

Department of Biomedical, Surgical and Dental Sciences

Via Pascal, 36 - 20133 Milano – Italy, University of Milan

tel. 0250315070, serena.delbue@unimi.it

Abstract

Prostate cancer (PCa) is one of the most common male neoplasms in the Western world. Various risk factors exist that may lead to carcinogenesis, including exposure to infectious agents such as the polyomavirus BK (BKPyV), which infects the human renourinary tract, establishes latency, and encodes oncoproteins.

Previous studies have suggested that BKPyV plays a role in PCa pathogenesis. However, the unspecific tropism of BKPyV and the lack of *in vitro* models of BKPyV-infected prostate cells cast doubt on this hypothesis.

The aim of the present study was to determine whether BKPyV could a) infect normal and/or tumoral epithelial prostate cells, and b) affect their phenotype. Normal epithelial prostate RWPE-1 cells and PCa PC-3 cells were infected with BKPyV for 21 days. Cell proliferation, cytokine production, adhesion, invasion ability, and epithelial-to-mesenchymal transition (EMT) markers were analyzed.

Our results show that a) RWPE-1 and PC-3 cells are both infectable with BKPyV, b) cell proliferation and TNF-α production were increased in BKPyV -infected RWPE-1, but not in PC-3 cells, c) adhesion to matrigel and invasion abilities were elevated in BKPyV-infected RWPE-1 cells, d) loss of E-cadherin and expression of vimentin occurred in both uninfected and infected RWPE-1 cells. In conclusion, BKPyV may change some features of the normal prostate cells, but is not needed for maintaining the transformed phenotype in the PCa cells The fact that RWPE-1 cells exhibit some phenotype modifications related to EMT represents a limit of this *in vitro* model.

Key words: Prostate Cancer, Polyomavirus, in vitro model, cytokine production

Introduction

Prostate cancer (PCa) is the most common malignant neoplasm in men and the second leading cause of cancer-related death in the Western world (NCI-NIH, 2018). In addition to several risk factors that play a role in PCa development, infectious agents such as the human polyomavirus BK (BKPyV) should be considered in PCa studies. BKPyV has been categorized by the International Agency for Research on Cancer as "possibly" carcinogenic to humans due to evidence of carcinogenic activity *in vitro* in cell lines and *in vivo* in animals (Bouvard et al., 2012). Additionally, the potential association between BKPyV and PCa is supported by previous studies, indicating that BKPyV infection is significantly more prevalent in cancer tissues than in control tissues, and that there is a significant association between viral expression and cancer (Delbue et al., 2014). Unfortunately, the unspecific tropism of BKPyV and the lack of *in vitro* models of BKPyV infection in prostate cells cast doubt on this hypothesis.

The "phenotypic switch" that changes the phenotype of a cell from epithelial-to-mesenchymal, also referred to as the epithelial-to-mesenchymal transition (EMT) process, plays a pivotal role in PCa progression, because it causes tumor cells to become invasive and able to metastasize to distant organs. The main characteristics of the EMT phenotype are loss of cell-cell adhesion and epithelial polarity markers (due to downregulation of E-cadherin), cytoskeleton reorganization (via expression of vimentin and α-smooth muscle actin), abnormal motile properties, and secretion of matrix metalloproteinases (MMPs) (Thiery, 2002).

The main goal of the present study was to determine whether BKPyV could infect normal and/or neoplastic prostate epithelial cells and, if so, whether this could affect cell morphology, proliferation, and adhesive properties, focusing also on EMT markers. For this

purpose, we used the normal human prostate epithelial cell line RWPE-1 and the human PCa cell line PC-3.

Materials and methods

Cell cultures

The RWPE-1 (ATCC® CRL-11609) cell line was established from the epithelial cells of the peripheral zone of a normal adult human prostate, transfected with a single copy of human papillomavirus 18 (HPV-18). RWPE-1 cells were grown in a keratinocyte serum-free medium (K-SFM; GIBCO/Invitrogen, Karlsruhe, Germany) supplemented with 50 µg/mL recombinant human epidermal growth factor (rhEGF; GIBCO/Invitrogen, Karlsruhe, Germany), 5 ng/mL bovine pituitary extract (BPE; GIBCO/Invitrogen, Karlsruhe, Germany), and antibiotics (2.5 µg/mL Fungizone™; GIBCO/Invitrogen, Karlsruhe, Germany) (50 U/mL penicillin; 50 µg/mL streptomycin; Euroclone, Italy). The human PCa cell line PC-3 (ATCC® CRL-1435) was derived from the grade IV prostate adenocarcinoma metastasis of a 62-year-old Caucasian patient. PC-3 cells were grown and subcultured in nutrient mixture Ham's F-12 Coon's modification medium with L-glutamine (Sigma-Aldrich, Germany) containing 10% v/v fetal bovine serum and antibiotics (50 U/mL penicillin; 50µg/mL streptomycin; Euroclone, Italy). All cells were maintained in an incubator at 37 °C in a 5% CO_2 humidified atmosphere.

BKPyV infection

Cells were infected using 10^8 virions ($4*10^6$ virus copies/mL) of BKPyV archetype (WW) strain stock, that was purchased at ATCC® (VR-837). The day before infection, $2*10^6$ cells were plated in a T75 flask. On day 0, the cells (which reached 70% confluence) were washed twice with Dulbecco's phosphate-buffered saline w/o calcium and magnesium (DPBS; Euroclone, Italy) and then the virus stock, diluted with specific serum-free culture medium,

was added to the flask. The cells were held at 37 °C for 90 min. Then, the inoculum was removed, the cells were washed with DPBS in order to eliminate the unbound virus, and the complete medium was added. The uninfected control was created following the same procedure as for the infected cells but without the addition of the virus.

Infected and uninfected cells were continuously cultured with complete medium and were split every three days up to 21 days. For each splitting, aliquots of cells and cell culture supernatants were collected. Virions were precipitated from the culture medium using PEG-it Virus Precipitation Solution (PEG) (System Biosciences, USA) and then treated with DNase I; briefly, one part cold PEG (4 °C) was added to every four parts culture medium, refrigerated overnight, then processed according to the manufacturer's protocol. Supernatants were diluted 1:1 with nuclease-free water and treated with 5 U DNase I (5 U/µl) (AppliChem, Germany) or mock-treated with water. After 1 h at 37 °C, the enzyme was heat- inactivated at 99 °C for 10 min (Kantola et al., 2009).

BKPyV DNA isolation and quantitative real-time PCR

Viral DNA was isolated from the encapsidated virions and from the cell pellet using a Nucleospin RNA kit (Macherey-Nagel, Germany) and a QIAamp DNA blood mini kit (Qiagen, USA) according to the manufacturer's instructions. Titration and evaluation of extracellular and intracellular viral loads were carried out by BKPyV-specific quantitative real-time PCR (Q-PCR).

BKPyV Q-PCR assays were performed using a TaqMan chemistry with an Applied Biosystems 7500 Real-Time PCR System (Applied Biosystems, Carlsbad, CA), targeting the highly-conserved VP1 region and following a protocol previously described by Delbue and colleagues (Kantola et al., 2009). A standard curve for quantification of the BKPyV viral load was obtained after serial dilution of the plasmid pBKPyV Dunlop with a dilution range between 10^0 and 10^8 plasmid copies/µL. Negative controls were included in each run and for

each sample. Standards and controls were tested in triplicate. Data are expressed as viral copies/mL.

Cell proliferation assay

The viability of infected and uninfected cells was measured by 3-[4,5-dimethylthiazol-2-yl]-2,5-diphenyltetrazolium bromide (MTT) assay. BKPyV-infected and uninfected cells were seeded in 96-well plates ($5*10^4$ cells per well) and cultured in complete medium at 37 °C and 5% CO_2 for 24 hours, 48 hours, 72 hours, and 6 days. At each point in time, cells were washed with DPBS, and after adding 100 µL MTT (Sigma-Aldrich, Germany), were left for 3 hours at 37 °C in the dark. Following incubation, the plate was centrifuged at 1200 rpm for 10 min and then the medium was removed. To dissolve formazan product crystals, dimethyl sulfoxide (DMSO; Sigma-Aldrich, Germany) was added to each well and the plate was shaken for 10 min in the dark. Absorbance was measured using a BioTek Synergy™ 4 Hybrid Microplate Reader (Biotek, USA) at 550 nm. The background, read at 650 nm, was removed. Three replicates were made for each group. Cell viability was calculated as follows:

$$\text{Cell viability \%} = \frac{(\text{Absorbance of sample - Absorbance of blank})}{\text{Absorbance of negative control}} \times 100$$

Cytokine, chemokine, and growth factor analysis

Quantification of 48 different cytokines, chemokines, and growth factors (pro-human cytokine 27-Plex M50-0KCAF0Y and 21-Plex MF0-005KMII, Bio-Rad, Hercules, CA) was performed on the culture media of both BKPyV-infected and uninfected RWPE-1 and PC-3 cell lines when cells were split, by magnetic bead-based multiplex immunoassay (Bio-Plex®) (BIO-RAD Laboratories, Milano, Italy), following the manufacturer's instructions. Specifically, we determined the presence and concentration of IL 1α-β-ra-2-2Ra-3-4-5-6-7-8-

9-10-12p40 and p70-13-15-16-17-18, eotaxin, basic FGF, G-CSF, GM-CSF, IFN-γ, IP10, MCP1-α, MCP1-β, PDGFBB, RANTES, TNF-α, VEGF, CTACK, GRO-α, HGF, IFN-α2, LIF, MCP-3, M-CSF, MIF, MIG, β-NGF, SCF, SCGF-β, SDF1-α, TNF-β, TRAIL, ICAM1, and VCAM1. For data acquisition and output, we used the Bio-Plex 200 reader and a digital processor. The Bio-Plex Manager® software presented data as median fluorescence intensity (MFI) and concentration (pg/mL) (BIO-RAD Laboratories, Milano, Italy), as described previously (Campisciano et al., 2018).

Matrigel cell adhesion

96-well plates were coated with 200 μL/cm^2 Cultrex® Basement Membrane Extract without phenol red (BME, PathClear®), a soluble form of basement membrane whose major components include laminin, collagen IV, entactin, and heparan sulfate proteoglycan. The plates were incubated at 37 °C for 30 min to allow polymerization of the matrix and the wells were washed with 1% bovine serum albumin in DPBS to block unspecified cell adhesion. Subsequently, infected and uninfected RWPE-1 and PC-3 cells were seeded at 5*10^4 cells per well and cultured in their specific complete media at 37 °C and 5% CO_2 for 60 min. A plastic plate was used as background control. To remove cells that did not adhere to the matrix, the wells were washed with specific cell-type media. The remaining adherent cells were fixed with 1% glutaraldehyde and counted microscopically. The mean cellular adhesion rate (adherent cells in coated wells - adherent cells in uncoated wells) was calculated from three different observation fields using a phase-contrast microscope. The invasive characteristics of both cell lines were evaluated at days 4, 8, 15, and 21 post-infection, and compared with those of uninfected cells.

Immunofluorescence for EMT marker analysis

RWPE-1 and PC-3 cells were cultured on 12-mm diameter round coverslips in 24-well culture plates. Cells were washed in DPBS, fixed in 4% paraformaldehyde in DPBS

containing 2% sucrose for 10 min at room temperature, post-fixed in 70% ethanol, and stored at -20 °C until use. Cells were then washed in DPBS three times and incubated for 1 hour at room temperature with the primary antibodies anti-E-cadherin (1:2500, Becton Dickinson), anti-N-cadherin (1:200, Santa Cruz), anti-vimentin (1:200, Novocastra), and anti-αSMA (1:400, Sigma-Aldrich). Secondary antibodies conjugated with Alexa 488 (1:500, Molecular Probes, Invitrogen) were applied in DPBS for 1 h at room temperature in the dark. Negative controls were incubated in the same way, omitting the primary antibody. Finally, cells on coverslips were incubated for 15 min with DAPI (1:100.000, Sigma-Aldrich) and mounted onto glass slides using Mowiol. The cells were photographed using a digital camera connected to a Nikon Eclipse microscope.

SDS-zymography for invasive potential analysis

Culture media were mixed 3:1 with sample buffer containing 10% SDS. Samples (10 µg total protein per sample) were run under non-reducing conditions without heat denaturation on 10% polyacrylamide gel (SDS-PAGE) co-polymerized with 1 mg/mL type I gelatin at 4 °C. After SDS-PAGE, the gels were washed twice in 2.5% Triton X-100 for 30 min each and incubated overnight in a substrate buffer at 37 °C (Tris-HCl 50 mM, $CaCl_2$ 5 mM, NaN_3 0.02%, pH 7.5). After staining the gels with Coomassie Brilliant Blue R-250, MMP gelatinolytic activity was detected as clear bands on a blue background, quantified by densitometric scanning (UVBand, Eppendorf, Italy).

Tissue inhibitor of metalloproteinase-2 real-time PCR

Tissue inhibitor of metalloproteinase-2 (TIMP-2) gene expression was analyzed by real-time PCR. Total RNA was isolated by a modified version of the acid guanidinium thiocyanate-phenol-chloroform method (Tri-Reagent, Sigma, Italy). 1 µg total RNA was reverse-transcribed in 20 µL (final volume) reaction mix (Biorad, Segrate-Milan, Italy). TIMP-2 mRNA levels were assessed and glyceraldehyde 3-phosphate dehydrogenase (GAPDH) was

used as an endogenous control to normalize differences in the amount of total RNA in each sample. The primer sequence was sense CCCTTCATTGACCTCAACTACATG, antisense TGGGATTTCCATTGATGACAAGC for GAPDH and sense TGGAAACGACATTTATGGCAACCC, antisense CTCCAACGTCCAGCGAGACC for TIMP-2.

Amplification reactions were conducted in a 96-well plate in a final volume of 20 μL per well. Each well contained 10 μL 1X SYBR Green Supermix (BioRad, Italy), 2 μL template, and 300 pmol of each primer. Each sample was analyzed in triplicate in a Bioer LineGene 9600. The cycle threshold was determined and gene expression levels relative to that of GAPDH were calculated.

Electronic microscopy for morphological analysis

RWPE-1 cells, grown at confluence, were harvested at 250 g for 5 min at room temperature. The culture medium was removed and replaced with a solution containing 2% freshly prepared paraformaldehyde and 2% glutaraldehyde in 0.1 M sodium cacodylate buffer (pH 7.4). After fixation for 2–4 h at 4 °C, cells were centrifuged and rinsed twice in cacodylate buffer for 20 min, post-fixed in 1% osmium tetroxide in the same buffer at 0 °C for 30 min, washed in distilled water, and *en bloc* stained with 2% aqueous uranyl acetate. After dehydration in a graded acetone series, samples were embedded in Epon-Araldite resin. Ultrathin sections (70–100 nm) were cut on a Leica Supernova ultramicrotome and stained with Reynolds' lead citrate. Transmission electron microscopy was performed with a Zeiss EM10 electron microscope.

Statistical analysis

All experiments were performed three to six times. Statistical significance was assessed using the Wilcoxon-Mann-Whitney U test. Differences were considered statistically significant at p

< 0.05. Linear regression was performed for analyzing changes in cytokine concentration over time.

Results

BKPyV infection

RWPE-1 and PC-3 cell lines were infected *in vitro* with a BKPyV archetype strain, and viral extracellular and intracellular DNA was quantified by specific Q-PCR at different time points postinfection. Both normal and cancerous epithelial prostate cell lines were found to be infectable with BKPyV, although a different time course of infection was observed in each cell line. Infection peaked on day 3 p.i. in RWPE-1 cells, with an extracellular viral load of $4.0*10^6$ copies/mL and an intracellular viral load of $2.3*10^6$ copies/mL. Viral replication was observed until day 14 p.i. (culture medium: undetectable; cell pellet: $7.7*10^2$ copies/mL) (Figure 1A). In the PC-3 cell line, infection peaked on day 10 p.i., and the virus remained productive over 21 days p.i. with a mean extracellular viral load of $6.9*10^5$ copies/mL (range: $8.7*10^3$–$2.6*10^6$ copies/mL) and an intracellular viral load of $1.7*10^6$ copies/mL (range: $2.4*10^5$–$3.9*10^6$ copies/mL) (Figure 1B). Uninfected RWPE-1 and PC-3 did not harbour BKPyV genome or other DNA virus genomes, besides HPV-18, used for the immortalization of the RWPE-1 (data not shown).

BKPyV infection affects RWPE-1 cell proliferation

To evaluate the effect of BKPyV infection on the growth rate of RWPE-1 and PC-3 cells, an MTT assay was performed on infected and uninfected cells. Infected cell viability was normalized to the viability of uninfected cells. Infected RWPE-1 cells showed a higher rate of proliferation compared to uninfected cells (range +25%/+58%, $p < 0.05$) (Figure 2A), whereas infected PC-3 cells displayed a significantly lower rate of proliferation than uninfected cells (range: -37%/-73%, $p < 0.05$) (Figure 2B).

BKPyV infection induces significant expression of inflammatory factors and activators in RWPE-1 cells

A panel of 48 cytokines and chemokines in the culture supernatants of infected and uninfected RWPE-1 and PC-3 cells was analyzed at seven time points p.i (24 and 48 hours; 3, 7, 12, 17, and 21 days). The concentration of three factors involved in the tumor inflammatory microenvironment (IL-18, TNF-α, and MCP1) increased significantly in the supernatant of RWPE-1 infected cells compared to mock-infected counterparts (linear trend estimation: $R2 \geq 0.6$, $p \leq 0.04$; Figure 3A, B, and C). In particular, the concentration of the proinflammatory cytokine TNF-α in the supernatant of the RWPE-1 infected cells showed a linear increase from 1.13 pg/mL at hour 24 to 6.86 pg/mL on day 21 ($R^2 = 0.9$, $p < 0.0001$), which was much greater than the increase seen in uninfected cells (on average 1.58 ± 0.18 pg/ml from 24 hours to 21 days). Among factors showing downregulation, the concentration of IL-3, a strong inducer of the active immune response, decreased significantly in the supernatant of infected RWPE-1 cells from 34.10 pg/ml at hour 24 to 6.58 pg/ml on day 21, unlike in their uninfected counterparts (4.77 to 48.05 pg/ml). The linear trend for IL-3 shows the significant impact of BKPyV infection on constitutive cytokine expression ($R^2 = 0.56$, $p < 0.05$) (Figure 3D). No significant linear trends were observed in the levels of cytokine/chemokine production between infected and uninfected PC-3 cells (table 1).

Matrigel adhesion assay

To investigate the effect of BKPyV infection on the invasive behavior of RWPE-1 and PC-3 cells, both cell lines were seeded on BME, which mimics the extracellular matrix, and the binding rate of infected cells per mm^2 was calculated. Results were normalized to the binding rate of uninfected cells. Both infected cell lines showed a higher binding rate compared to their mock treated counterparts. Specifically, the rate was between +17% and +1570% for RWPE-1 cells and between +9% and +811% for PC-3 cells (Figure 4, panels A and B).

EMT marker analysis

EMT marker expression was assessed by immunofluorescence in both infected and uninfected RWPE-1 cells. At all time points, uninfected RWPE-1 cells exhibited low or undetectable levels of E-cadherin. Notably, immunoreactivity was observed mostly in the cytoplasm and not at cell boundaries, where functional adherens junctions are located in normal differentiated epithelial cells. Infected RWPE-1 cells showed a similar pattern of E-cadherin expression. N-cadherin expression was almost undetectable, with scattered positive cells in both infected and uninfected RWPE-1 cells. Vimentin was expressed at similar levels in infected and uninfected RWPE-1 cells (Figure 5, panel A).

To better understand the effect of BKPyV on normal epithelial cells and to further investigate its possible involvement in PCa oncogenesis, the expression of EMT markers was analyzed in PC-3 cells before and after BKPyV infection. As expected, E-cadherin was almost completely undetectable in both infected and uninfected PC-3 cells at all time points. N-cadherin and vimentin expression were similarly expressed in control and BKPyV-infected PC-3 cells (Figure 5, panel B).

Invasive potential

To assess the invasive potential of infected and uninfected RWPE-1 and PC-3 cells, MMP-2 and MMP-9 gelatinolytic activity in cell supernatants was assessed by SDS-zymography. Densitometric scanning of lytic bands on zymograms revealed that MMP-2 and MMP-9 were similarly expressed in uninfected and infected RWPE-1 cells up to day 3. However, at all subsequent time points, MMP-2 and MMP-9 were strongly induced in BKPyV-infected cells compared to uninfected cells (Figure 7, panel A and B).

Densitometric analysis of lytic bands also showed that the activity of MMP-2 and MMP-9 in PC-3 cells were differently affected by BKPyV infection in a time-dependent manner that could not be properly defined (data not shown). To elucidate whether the invasive potential

of PC-3 cells was influenced by BKPyV infection, we analyzed the expression of TIMP-2, a natural inhibitor of MMP-2, and described MMP-2 and MMP-9 activity in relation to TIMP-2 expression. The MMP-2:TIMP-2 ratio was strongly increased by BKPyV from day 3 to day 14, and thereafter, was similar to that in control cells. A comparable pattern was observed in the MMP-9:TIMP-2 ratio (Figure 7, panel C).

Morphological analysis by electron microscopy

The morphology and ultrastructure of infected and uninfected RWPE-1 cells at different time points were analyzed by electron microscopy. For each pellet, 120 cells were photographed and evaluated to observe the presence of any viral particles. Both uninfected and infected cells showed similar morphologies (Figure 8, panel a) and contained a high number of viral particles (Figure 8, panel b). Surprisingly, viral particles were observed in both infected and uninfected RWPE-1 cells, although BKPyV DNA was undetectable by Q-PCR.

Discussion

BKPyV is a member of the *Polyomaviridae* family with very well-known *in vitro* oncogenic properties, mainly resulting from the production of large T antigen protein, which is able to induce cell transformation (Tognon et al., 2003). Based on serological and molecular studies, it has been suggested that BKPyV may be involved in the etiology and/or development of PCa (Delbue et al., 2014; Keller et al., 2015a). In addition, a study carried out on a large cohort of PCa patients revealed a statistically strong association between IgG response against LTag and the risk of PCa progression (Keller et al., 2015b). However, it remains uncertain whether BKPyV infection is the causative agent in PCa or is an epiphenomenon. Additionally, the lack of an *in vitro* model of BKPyV-infected epithelial prostate cells represents a major limit in this field.

Thus, in the present study, we infected prostate cells with BKPyV with the aim of establishing and characterizing an *in vitro* model to obtain innovative insight into the relationship between viral activity and possible phenotypic changes.

We demonstrated for the first time that both the normal epithelial prostate cell line RWPE-1 and the PCa cell line PC-3 are infectable with BKPyV. The outcomes of the infection vary between the two cell lines, being lost from RWPE-1 by day 14 p.i., but persisting in PC-3 up to three weeks p.i. The dramatic falling off of BKPyV copy number over two weeks in RWPE-1 lead to hypothesize that normal prostate cells are subjected to an abortive infection. On the contrary, PC-3 cells appear to maintain a steady state of BKPyV genome copies over time, so it is possible that a persistent infection was established. Unfortunately, the expression of either early or late viral proteins could not be assessed, and this represents a major limit of the study. Further study should be conducted in order to verify whether an abortive infection of the RWPE-1 cells could lead to viral DNA integration, protein expression limited to the T Antigens and possible cellular transformation.

Additionally, our findings were not comparable with other studies, since all the previous experiments concerning BKPyV infection *in vitro* have been performed in human or monkey kidney cells, lung fibroblasts, or epithelial cells from salivary glands (Acott et al., 2006; Jeffers-Francis et al., 2015; Li et al., 2013). Despite its low level of replication, BKPyV seems to contribute to alter some of the properties of normal prostate cells, such as their rate of proliferation and the production of some factors which may be involved in malignant transformation.

TNF-α is a pleiotropic cytokine that can induce cancer cell death, but may also favour cell proliferation under certain specific conditions (Tse et al., 2012). In addition, TNF-α orchestrates the expression of inflammatory cytokines involved in the development of castrate-resistant PCa, such as IL-6 (Nguyen et al., 2014). It was recently demonstrated that

the release of TNF-α in the microenvironment of PCa tumors leads to the expression of factors responsible for the progression of this malignancy (Banzola et al., 2018) .

It has been shown that TNF-α produced by PCa cells is able to activate neutrophils and macrophages and induce the synthesis of other proinflammatory cytokines (Sharma et al., 2014). In mice models with chemically-induced PCa, TNF-α has been shown to promote cell proliferation and survival (Galheigo et al., 2016). Interestingly, TNF-α had a strong growth-stimulating effect on simian polyomavirus 40-transformed keratinocytes (Kobayashi et al., 1999), and a similar effect on BKPyV-infected prostate cells can be hypothesized, upon synergic stimulation of proliferation with viral LTag.

The combinatory upregulation of TNF-α, IL-18, and MPC-1 upon BKPyV infection might contribute to the promotion of prostatic cells toward a cancerous phenotype (Ito et al., 2015; Palma et al., 2013). In addition, the role of IL-18 as a potent inducer of IFN-γ, which is in turn the main inducer of IDO, suggests a relevant role of BKPyV in PCa development and progression (Feder-Mengus et al., 2008). Finally, the inhibition of IL-3 production should help BKPyV evade the host innate immune response (Broughton et al., 2012).

On the contrary, PC-3 cells showed a decrease in their rate of proliferation, probably due to the cytopathic effect, and stable expression levels of TNF-α after BKPyV infection. Vaughan and colleagues also observed that TNF-α increased glycolysis, ATP production, and lactate export in RWPE-1 cells, but not in PC-3 cells (Vaughan et al., 2013).

The binding of BKPyV-infected RWPE-1 and PC-3 cells to the extracellular matrix was evaluated in the present study, because direct interaction with the extracellular matrix may lead to transendothelial invasion. Higher adhesion to the Matrigel has been observed in BKPyV-infected cells relative to uninfected cells, even without a specific trend over time. Higher levels and activity of MMP-2 and MMP-9 in BKPyV-infected RWPE-1 showed that the virus elicited an invasive phenotype in normal cells. Increased expression of MMP-2 and,

consequently, strong invasive behavior of the cells has previously been described in a transgenic mouse model with polyomavirus-induced osteosarcoma (Velupillai et al., 2010). The same phenomenon was observed during the progression of mammary carcinomas in a polyomavirus middle T oncogene mouse model, where MMP-13 was strongly upregulated concurrently with the transition to invasive and metastatic carcinomas (Nielsen et al., 2008). Very recently, the induction of several MMPs has been described in an *in vitro* model of Merkel cell carcinoma induced by Merkel cell polyomavirus; the authors hypothesized that dysregulated MMP gene expression may contribute to virus-induced oncogenesis (Liu et al., 2016). Both the enhanced cell adhesion to the extracellular matrix and the increased activity of MMP-2 and MMP-9 have been observed even after clearance of the BKPyV genome from the RWPE-1 cells. This finding may confirm the fact that the viral DNA is not retained in transformed cells and tumor samples, resembling the well-known hit-and-run model of viral tumorigenesis (Delbue et al., 2017).

The increased levels and activity of MMPs induced by BKPyV in PC-3 cells suggests that the virus was effective in adding invasive potential to already established invasive properties. This effect is evident until 14 days p.i. and is lost thereafter, suggesting that its activity could play a major role in the early phases of oncogenesis, but is then stabilized.

Although all the above evidence could reasonably lead to the hypothesis that BKPyV catalyses some changes in RWPE-1 cells, we observed an unexpected result regarding EMT markers and the EMT-related phenotype. Uninfected RWPE-1 cells are normal epithelial cells, but our data shows that they do not present a clear epithelial phenotype; E-cadherin downregulation and cytoplasmic localization was detected in most cells, and vimentin expression was observed in both control and BKPyV-infected cells, thus suggesting that uninfected cells underwent EMT. This finding was consistent with the morphological results in the same cells as described by Tamand colleagues. (Tam et al., 2017). To better understand

this unexpected result, we analyzed RWPE-1 cells with an electron microscope. Small viral particles were detected not only in BKPyV-infected cells, but also in normal, uninfected RWPE-1 prostate cells, although BKPyV viral DNA was undetectable by Q-PCR, suggesting that these viral particles were a result of HPV-18 used for RWPE-1 immortalization.

It is likely that RWPE-1 cells, which have been immortalized with a defective HPV-18 genome, are still able to produce viral capsid proteins (known as L1), which spontaneously self-assemble into a structure closely mimicking the natural surface of native papillomavirus virions (Buck et al., 2013). The concomitant presence of these pseudovirions and the observation of an EMT-related phenotype in uninfected RWPE-1 cells strongly suggests that RWPE-1 cells do not retain a normal epithelial morphology (Bello et al., 1997) and may not serve as a model of normal epithelial prostate cells, even if they are widely used in research (Deng et al., 2017; Souza et al., 2018). BKPyV-infected and uninfected RWPE-1 cells exhibit a similar EMT phenotype, suggesting that uninfected cells do not retain normal epithelial characteristics and thus their use as a model of normal epithelial prostate cells may be limited. However, under our experimental conditions, we were able to demonstrate that BKPyV infection induced increased gelatinolytic activity in RWPE-1 cells, allowing us to detect the effect of BKPyV in inducing the invasive properties of infected cells, consistent with their malignant transformation. Previous reports have described aberrant expression of E-cadherin and vimentin in normal prostate tissues (Figiel et al., 2017; Rubin et al., 2001), strongly indicating that further research is necessary to understand whether the EMT morphological features of untreated RWPE-1 cells are induced by HPV and validate the use of these cells as an experimental model for normal prostate epithelial cells.

As expected, PC-3 carcinoma cells were characterized by an EMT phenotype and no additional morphological modifications were induced by BKPyV infection. In contrast, BKPyV infection increased their invasive potential.

Considered as a whole, our results show that a) normal epithelial prostate RWPE-1 cells and PC-3 cells are infectable with BKPyV, but the outcomes of infection vary, b) cell proliferation and TNF-α production were increased by BKPyV in RWPE-1 cells, but not in PC-3 cells, c) adhesion to Matrigel and invasion potential, observed as MMP-2 and MMP-9 activities, were increased upon BKPyV infection of RWPE-1 cells, d) both mock treated and BKPyV-infected RWPE-1 cells exhibit loss of E-cadherin and expression of vimentin.

In conclusion, we hypothesize that BKPyV may establish an abortive infection in normal epithelial prostate cells and change some phenotypic features, such as the proliferation, adhesion and invasive potential, but then it is not needed for maintaining the transformed phenotype of prostate tumor cells. However, the fact that mock treated RWPE-1 cells exhibit some phenotype modifications related to EMT represents a limit of this *in vitro* model. Therefore, further research is required to verify the transformation of the cells and the possible integration of the viral genome and thus to confirm or to deny the usefulness of these cells as an experimental model of normal prostate epithelial cells.

.

Table 1: Cytokine and chemokine concentration trends in BKPyV-infected RWPE-1 and PC-3 cells

Cytokine/chemokine	*Linear trend estimation*,***	
	RWPE-1	**PC-3**
IL-18	**R^2 0.69; p=0.02**	R^2 0.89; p=0.09
TNF-α	**R^2 0.85; p<0.01**	R^2 0.61; p=0.80
MCP1	**R^2 0.59; p=0.04**	R^2 0.86; p=0.17
IL-15	R^2 0.24; p=0.26	n.a.
IL-2	R^2 0.4; p=0.12	R^2 0.13; p=0.26
IL-6	R^2 0.03; p=0.71	R^2 0.80; p=0.42
IL-9	R^2 0.07; p=0.55	R^2 0.20; p=0.07
GM-CSF	R^2 0.3; p=0.1	R^2 0.39; p=0.4
FGF-basic	R^2 0.21; p=0.29	R^2 0.99; p=0.12
MIP-1a	R^2 0.26; p=0.24	R^2 0.59; p=0.06
MIP-1b	R^2 0.04; p=0.95	R^2 0.01; p=0.60
IL-3	**R^2 0.56; p=0.05**	R^2 0.96; p=0.36
M-CSF	R^2 0.03; p=0.70	R^2 0.74; p=0.66
SDF-1	R^2 0.29; p=0.20	R^2 0.89; p=0.64

**compared to uninfected RWPE-1 cells*

***from 1 to 21 days p.i.*

References

Acott PD, O'Regan PA, Lee SH, Crocker JF. 2006. Utilization of vero cells for primary and chronic BK virus infection. Transplant Proc 38(10):3502-3505.

Banzola I, Mengus C, Wyler S, Hudolin T, Manzella G, Chiarugi A, Boldorini R, Sais G, Schmidli TS, Chiffi G, Bachmann A, Sulser T, Spagnoli GC, Provenzano M. 2018. Expression of indoleamine 2,3-dioxygenase induced by IFN-γ and TNF-α as potential biomarker of prostate cancer progression. Frontiers in Immunology 9(MAY).

Bello D, Webber MM, Kleinman HK, Wartinger DD, Rhim JS. 1997. Androgen responsive adult human prostatic epithelial cell lines immortalized by human papillomavirus 18. Carcinogenesis 18(6):1215-1223.

Bouvard V, Baan RA, Grosse Y, Lauby-Secretan B, El Ghissassi F, Benbrahim-Tallaa L, Guha N, Straif K. 2012. Carcinogenicity of malaria and of some polyomaviruses. Lancet Oncol 13(4):339-340.

Broughton SE, Dhagat U, Hercus TR, Nero TL, Grimbaldeston MA, Bonder CS, Lopez AF, Parker MW. 2012. The GM-CSF/IL-3/IL-5 cytokine receptor family: from ligand recognition to initiation of signaling. Immunol Rev 250(1):277-302.

Buck CB, Day PM, Trus BL. 2013. The papillomavirus major capsid protein L1. Virology 445(1-2):169-174.

Campisciano G, Zanotta N, Licastro D, De Seta F, Comar M. 2018. In vivo microbiome and associated immune markers: New insights into the pathogenesis of vaginal dysbiosis. Sci Rep 8(1):2307.

Delbue S, Comar M, Ferrante P. 2017. Review on the role of the human Polyomavirus JC in the development of tumors. Infect Agent Cancer 12:10.

Delbue S, Ferrante P, Provenzano M. 2014. Polyomavirus BK and prostate cancer: an unworthy scientific effort? Oncoscience 1(4):296-303.

Deng G, Zheng X, Jiang P, Chen K, Wang X, Jiang K, Zhang W, Tu L, Yan D, Ma L, Ma S. 2017. Notch1 suppresses prostate cancer cell invasion via the metastasis-associated 1-KiSS-1 metastasis-suppressor pathway. Oncol Lett 14(4):4477-4482.

Feder-Mengus C, Wyler S, Hudolin T, Ruszat R, Bubendorf L, Chiarugi A, Pittelli M, Weber WP, Bachmann A, Gasser TC, Sulser T, Heberer M, Spagnoli GC, Provenzano M. 2008. High expression of indoleamine 2,3-dioxygenase gene in prostate cancer. Eur J Cancer 44(15):2266-2275.

Figiel S, Vasseur C, Bruyere F, Rozet F, Maheo K, Fromont G. 2017. Clinical significance of epithelial-mesenchymal transition markers in prostate cancer. Hum Pathol 61:26-32.

Galheigo MR, Cruz AR, Cabral Á, Faria PR, Cordeiro RS, Silva MJ, Tomiosso TC, Gonçalves BF, Pinto-Fochi ME, Taboga SR, Góes RM, Ribeiro DL. 2016. Role of the TNF-α receptor type 1 on prostate carcinogenesis in knockout mice. Prostate 76(10):917-926.

Ito Y, Ishiguro H, Kobayashi N, Hasumi H, Watanabe M, Yao M, Uemura H. 2015. Adipocyte-derived monocyte chemotactic protein-1 (MCP-1) promotes prostate cancer progression through the induction of MMP-2 activity. Prostate 75(10):1009-1019.

Jeffers-Francis LK, Burger-Calderon R, Webster-Cyriaque J. 2015. Effect of Leflunomide, Cidofovir and Ciprofloxacin on replication of BKPyV in a salivary gland in vitro culture system. Antiviral Res 118:46-55.

Kantola K, Sadeghi M, Lahtinen A, Koskenvuo M, Aaltonen LM, Mottonen M, Rahiala J, Saarinen-Pihkala U, Riikonen P, Jartti T, Ruuskanen O, Soderlund-Venermo M, Hedman K. 2009. Merkel cell polyomavirus DNA in tumor-free tonsillar tissues and upper respiratory tract samples: implications for respiratory transmission and latency. J Clin Virol 45(4):292-295.

Keller EX, Delbue S, Tognon M, Provenzano M. 2015a. Polyomavirus BK and prostate cancer: a complex interaction of potential clinical relevance. Rev Med Virol 25(6):366-378.

Keller XE, Kardas P, Acevedo C, Sais G, Poyet C, Banzola I, Mortezavi A, Seifert B, Sulser T, Hirsch HH, Provenzano M. 2015b. Antibody response to BK polyomavirus as a prognostic biomarker and potential therapeutic target in prostate cancer. Oncotarget 6(8):6459-6469.

Kobayashi T, Okumura H, Hashimoto K, Asada H, Yoshikawa K. 1999. Growth-stimulating effects of tumor necrosis factor-alpha on simian virus 40-transformed human keratinocytes is linked to phosphorylation of retinoblastoma protein. J Dermatol Sci 22(1):38-44.

Li R, Sharma BN, Linder S, Gutteberg TJ, Hirsch HH, Rinaldo CH. 2013. Characteristics of polyomavirus BK (BKPyV) infection in primary human urothelial cells. Virology 440(1):41-50.

Liu W, Yang R, Payne AS, Schowalter RM, Spurgeon ME, Lambert PF, Xu X, Buck CB, You J. 2016. Identifying the Target Cells and Mechanisms of Merkel Cell Polyomavirus Infection. Cell Host Microbe 19(6):775-787.

NCI-NIH. 2018. Cancer Stat Facts https://seer.cancer.gov/statfacts/html/prost.html.

Nguyen DP, Li J, Tewari AK. 2014. Inflammation and prostate cancer: the role of interleukin 6 (IL-6). BJU Int 113(6):986-992.

Nielsen BS, Egeblad M, Rank F, Askautrud HA, Pennington CJ, Pedersen TX, Christensen IJ, Edwards DR, Werb Z, Lund LR. 2008. Matrix metalloproteinase 13 is induced in fibroblasts in polyomavirus middle T antigen-driven mammary carcinoma without influencing tumor progression. PLoS One 3(8):e2959.

Palma G, Barbieri A, Bimonte S, Palla M, Zappavigna S, Caraglia M, Ascierto PA, Ciliberto G, Arra C. 2013. Interleukin 18: friend or foe in cancer. Biochim Biophys Acta 1836(2):296-303.

Rubin MA, Mucci NR, Figurski J, Fecko A, Pienta KJ, Day ML. 2001. E-cadherin expression in prostate cancer: a broad survey using high-density tissue microarray technology. Hum Pathol 32(7):690-697.

Sharma J, Gray KP, Harshman LC, Evan C, Nakabayashi M, Fichorova R, Rider J, Mucci L, Kantoff PW, Sweeney CJ. 2014. Elevated IL-8, TNF-α, and MCP-1 in men with metastatic prostate cancer starting androgen-deprivation therapy (ADT) are associated with shorter time to castration-resistance and overall survival. Prostate 74(8):820-828.

Souza AG, B Silva IB, Campos-Fernández E, Marangoni K, F Bastos VA, Alves PT, Goulart LR, Alonso-Goulart V. 2018. Extracellular vesicles as drivers of epithelial-mesenchymal transition and carcinogenic characteristics in normal prostate cells. Mol Carcinog 57(4):503-511.

Tam KJ, Hui DHF, Lee WW, Dong M, Tombe T, Jiao IZF, Khosravi S, Takeuchi A, Peacock JW, Ivanova L, Moskalev I, Gleave ME, Buttyan R, Cox ME, Ong CJ. 2017. Semaphorin 3 C drives epithelial-to-mesenchymal transition, invasiveness, and stem-like characteristics in prostate cells. Sci Rep 7(1):11501.

Thiery JP. 2002. Epithelial-mesenchymal transitions in tumour progression. Nat Rev Cancer 2(6):442-454.

Tognon M, Corallini A, Martini F, Negrini M, Barbanti-Brodano G. 2003. Oncogenic transformation by BK virus and association with human tumors. Oncogene 22(33):5192-5200.

Tse BW, Scott KF, Russell PJ. 2012. Paradoxical roles of tumour necrosis factor-alpha in prostate cancer biology. Prostate Cancer 2012:128965.

Vaughan RA, Garcia-Smith R, Trujillo KA, Bisoffi M. 2013. Tumor necrosis factor alpha increases aerobic glycolysis and reduces oxidative metabolism in prostate epithelial cells. Prostate 73(14):1538-1546.

Velupillai P, Sung CK, Tian Y, Dahl J, Carroll J, Bronson R, Benjamin T. 2010. Polyoma virus-induced osteosarcomas in inbred strains of mice: host determinants of metastasis. PLoS Pathog 6(1):e1000733.

Figure captions

Figure 1: Titration of BKPyV load, expressed as copies/mL, in RWPE-1 and PC-3 culture media and cell pellets, at every analyzed time points, from day 3 to day 21 p.i..

Figure 2: Effect of BKPyV infection on the growth rate of RWPE-1 and PC-3 cells measured by the MTT assay. Data are expressed as percentage of the cell viability, compared to the uninfected cells (100%).

Figure 3: Concentration of four most significant cytokines (A: IL-18; B: TNF-α; C: MCP1; and D: IL-3), measured in the culture medium of the infected and uninfected RWPE-1 cells, at every analyzed time points, from day 1 to day 21 p.i. Data are expressed as pg/mL and as percentage of increase. Linear trend estimation is indicated for every cytokines.

Figure 4: Panel A and B represent the percentage of adhesion rate to the extracellular matrix of the BKPyV infected RWPE-1 and PC-3, respectively, at different time points, from 4 to 21 days p.i.. Adhesion capacity is depicted as percentage of cell adhesion/square millimeter (mean± SD), compared to uninfected cells (100%).

Figure 5: a) Representative micrographs at the fluorescence microscope showing the expression epithelial and mesenchymal markers in control and BKPyV-infected RWPE-1 cells 7 days p.i. (original magnification 60x). b) Representative micrographs at the fluorescence microscope showing the expression epithelial and mesenchymal markers in control and BKPyV-infected PC-3 cells 21 days p.i. (original magnification 60x).

Figure 6: A) Representative gelatin zymogram and bar graphs showing MMP-2 (B) and MMP-9 (C) activity in supernatants of cultured control and BKPyV-infected RWPE-1 cells. Data are expressed as mean ± SD. Representative gelatin zymogram and bar graphs showing MMP-/TIMP-2 (D) ratio and MMP-9/TIMP-2 ratio (E) activity in supernatants of cultured control and BKPyV-infected PC3 cells. Data are expressed as mean ± SD.

Figure 7: A) Transmission electron micrographs of RWPE-1 non infected (a) and BKPyV-infected-RWPE-1 (b) cells at 3 days showing a similar morphology. Scale bars = 0,5 μm. Boxed areas show at higher magnification the viral particles present in both experimental conditions. Scale bars = 200 nm. B) Transmission electron micrographs of RWPE-1 non infected (c) and BKPyV-infected-RWPE-1 (d) cells at 10 days p.i. containing viral particles (some indicated by white arrows). Scale bars = 0,5 μm. A viral particle from each experimental condition is shown at higher magnification in boxed areas. Scale bars = 120 nm.